TESLA - COLLABORATION

Transparencies from the

Coupler Workshop at DESY, April 26 - 27, 1999

Editor: D. Proch

DESY

May 1999, TESLA 99-10

Input Coupler Workshop at DESY, April 26-27, 1999

INPUT COUPLER WORKSHOP - AGENDA

Monday, April 26

MORNING SESSION - ONGOING EXPERIMENTS WITH INPUT COUPLERS

10:00 - 10:10 Welcome, Introduction
10:10 - 10:50 A new matched window-waveguide to coax transition assembly - P. Leqercq, LAL
10:50 - 11:30 Detailed analysis of lambda/2 window - Low level measurements of TW window - C. Travier, Saclay
11:30 - 12:00 Coffee
12:00 - 13:00 Ti coating of ceramics - J. Lorkiewicz, DESY

AFTERNOON SESSION - RF CONDITIONING: EXPERIENCE, UNDERSTANDING - REPORTS AND DISCUSSION

14:00 - 14:45 Conditioning experiment - C. Travier, S. Chel, Saclay
14:45 - 15:30 Reports about conditioning experience with the latest module 3 couplers - W.-D. Moeller, DESY
15:30 - 16:00 Coffee
16:00 - 17:00 Open discussion:
- Some speculation about physics of RF conditioning,
- Where is all that H coming from when training a coupler,
- Best procedure for cleaning and baking of coupler parts.

Tuesday, April 27

MORNING SESSION - INPUT COUPLERS FOR SUPERSTRUCTURE

09:00 - 10:00 Spec. for TESLA couplers/RF specification (Power, Q_{ext}, coupling) - J. Sekutowicz, R. Brinkmann, S. Simrock, DESY
10:00 - 10:45 Status of waveguide coupler development for superstructure - M. Dohlus, DESY
10:45 - 11:30 Status of coaxial coupler development for superstructure - B. Dwersteg, DESY
11:30 - 12:00 Coffee
12:00 - 13:00 Calculation of coupling elements of coaxial and waveguide input couplers for superstructure - A. Zavadtsev, DESY

AFTERNOON SESSION, starting at 14:00
Data bank for ceramics
Space for new contributions
Coordination of future development
AOB
Conclusion

D. Proch 05.05.99

Summary
Input Coupler Workshop
26. - 27.04.99, DESY

This is the second input coupler workshop jointly organized by Saclay/DESY (the first was held in autumn 1998) in order to

- organize exchange of experience in the field of input coupler developments for TESLA,
- stimulate discussion among experts,
- coordinate future work in different labs.

As one can see in the agenda, there were three main topics:

I Reports about ongoing experiments with input couplers,
II Reports and discussions about the nature of RF-processing,
III Specification and design work for superstructure couplers.

I Reports about ongoing experiments with input couplers

a) A new design of a matched waveguide to coax transition has been developed at Saclay. The main advantage is the missing "door-knob" piece which results in a simple mechanical layout. Matching is established with two steps reduced height insertion in the rectangular waveguide section. First low power bench measurements are planned for this summer.

b) Detailed high power measurements with a $\lambda/2$ coaxial window were reported from Saclay. This window has been tested up to 1 MW under warm (300 K) and cold (80 K) conditions. In addition a scan with DC-bias of the inner conductor was carried out under high power RF conditions. For comparison with the calculated multipacting behaviour with DC-bias a more detailed MP-map from the Helsinki group is needed. The available MP chart covers the range up to 5 MW and does not display all details in the lower (< 1 MW) power regime. The measured high power results prove that this window can carry up to 1 MW of RF power. Main draw back is an enhanced RF loss in the thick ceramic and a geometry position of the window with direct sight to the beam line. In the case of the CEBAF window severe charging of the ceramic by field emission electron is observed. On the other hand the coax window can be placed much further away from the beam line so that might not be so dangerous. It was reported that the coax window was covered during RF processing with a complete reflection layer (it was due to a misfunction of the interlock which ignored an excessive increase of the vacuum pressure). Astonishingly, this layer could be removed by furthe conditioning. Additional high power tests are planned with two more windows with different Ti coatings.

c) Ti-coating (sputtering) is done by SICN company for the Saclay windows and by TiN (sublimation from heated Ti under ammonia pressure, 2E-4 mbar) for some DESY windows. The DESY apparatus had to be established in short time in order to coat the rectangular waveguide window for the module III couplers. Both methods seem to work, but further systematic correlation of coating procedure and RF behaviour are necessary for optimization of the coating process.

II Reports and discussions about the nature of RF-processing

Understanding of RF conditioning was a major aim of this meeting. During RF conditioning the following phenomena are generally observed:

1 increase of vacuum pressure. Both, "static" increase as well as fast "bursts" are detected,
2 detection of electron current at coaxial probes,
3 detection of light (by photo multipliers looking through a small window).

High power RF operation at "bad" vacuum pressure ($p \geq 10E\text{-}5$ mbar) clearly will initiate glow discharge. In several cases sputtering of the surface occured. Coating of Cu surface with steel as well as "Decoating" of the thin Cu layer has been observed. Pre-baking (300 °C) of the coupler parts and in situ bake out (200 °C) of the completely assembled coupler test stand could reduce the amount of time needed for RF conditioning (see Möller's talk). The differential mass spectrum taken before and during RF conditioning uncovered that the dominant residual gases during conditioning are H_2 (mass 2), CO (mass 28) and CO_2 (mass 44). The same mass spectrum is observed in vacuum chambers in circular acceleration. Here the mechanism of gas desorption is understood by release of phsysorped gas by bombardment of photo-electrons being created by γ-radiation of the circular beam. Therefore the working hypothesis of RF conditioning is, that "low energy" electrons ($50 < eV < 500$) from the multipacting process initiate desorption of physisorbed gases. This understanding results in some consequences:

1 Bake out is needed but not sufficient for severe cut down of the time needed for conditioning.
2 Material and treatment for vacuum chambers of synchrotron light sources have undergone extensive investigations to reduce out-gassing effects. These works will be carefully scanned (B. Aune at Saclay) for possible application to coupler parts.
3 Degassing effects as well as contaminations of the Al_2O_3 material are not well understood. Here C. Pagani (INFN) offered help in analyzing window material. Furthermore a collection of relevant Al_2O_3 investigations will be collected at DESY. Please send papers, reports to K. Lando (e-mail attachment, fax, mail) for establishing a data bank.
4 Technical procedures for RF conditioning will be investigated to operate at high gas desorption rates (for fast cleaning) but to avoid glow discharge (e.g. very short but very high RF power pulses but adequate pumping time between pulses).
5 Increase the pumping speed at coupler ports.
6 Apply "inner" pumping by coating coupler parts with a thin film of NEG (non evaporating getter) pumping surface. This development has already been started (Ch. Benvenuti, CERN and D. Proch, DESY) and will be reported at the next coupler workshop.

III Specification and design work for superstructure couplers

a) The specification for the superstructure is clearly described in Sekutowicz's contribution. In summary: 1 MW is needed per input coupler per 4 subunits (each 7 cells) to satisfy beam loading and Lorentz force detuning and regulation reserve. A possible energy up-grade of TESLA will double the power per coupler up to 2 MW. In both cases the optimum Q_{ext} value is 2 x 10E6. It was concluded that no need of variable coupling adjustment is needed. Fine adjustment will be done by external stub tuners, but at the cost of enhanced standing wave voltage in the coupler. The voltage enhancement scales with the square root of the transformation ratio for Q_{ext}.

b) The design effort for a high power superstructure input coupler was reported. The coaxial version is a larger diameter coupler of type III. The diameter increase is chosen for shifting multipacting levels up (they scale by $(f \times d)^4$, f: frequency, d: distance between inner and outer coax). This version is matched RF-wise and seems to fit into the cryostat. As next step a low power model is planned.

c) The rectangular waveguide design has converted into an elliptical version. Shielding the window against the beam is accomplished by two baffle barriers at the cold end. The cold part (including cold window) is matched RF wise. Some mechanical constrains (transitions between Nb and stub) are not yet solved. The heat load to 2 K, 4 K and 80 K is comparable to the coax design.

Action points

- coordinate review of material investigations of vacuum chamber for synchrotron light sources, possible application to coupler fabrication/treatment; coordinator: B. Aune
- coordinate investigations of Al_2O_3 material (bulk properties, surface contaminations, ...); coordinator: C. Pagani
- collect material of earlier investigations with Al_2O_3 for RF windows; coordinator: D. Proch

Next meeting

First week in December (second choice: last week in November)

P Lepercq

NEW MATCHED WINDOW COAXIAL TO WAVEGUIDE TRANSITION

Simplified transition

Polarisable transition

SIMPLIFIED TRANSITION

Goal : integration of the « hot » ceramic window in the design of a simplified transition with

-transition working under neutral gaz pressure
-large mechanical tolerances } Low cost

-low dielectric losses in the ceramic window

-low electric field in the transition

Solution : 1/ unmatched straight coaxial to waveguide transition

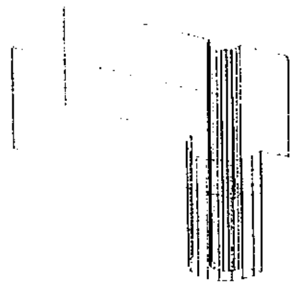

simple structure

easy to realize

2/ unmatched cylindrical window

thickness of the ceramic can be adjust to minimize the dielectric losses

3/ matching is realised with reduced heigth waveguide

STRUCTURE OF THE TRANSITION

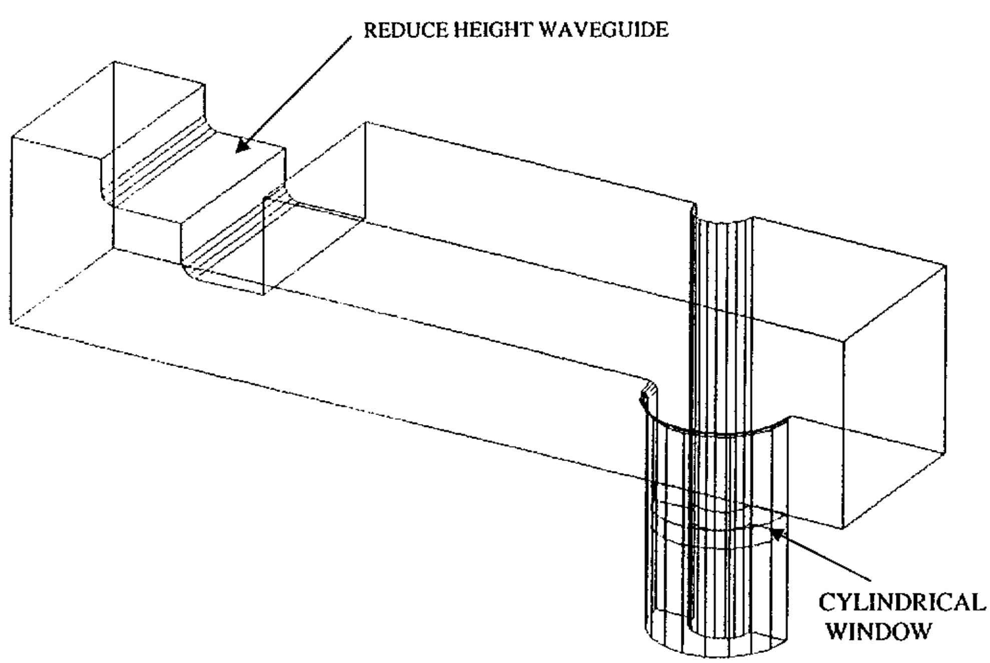

OPTIMIZATION WITH HFSS
DIMENSIONS

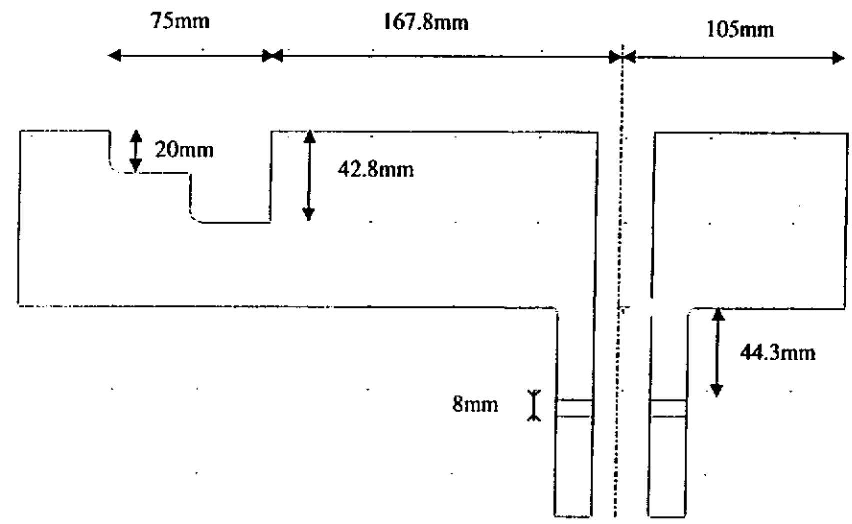

OPTIMIZATION WITH HFSS
SCATTERING PARAMETER

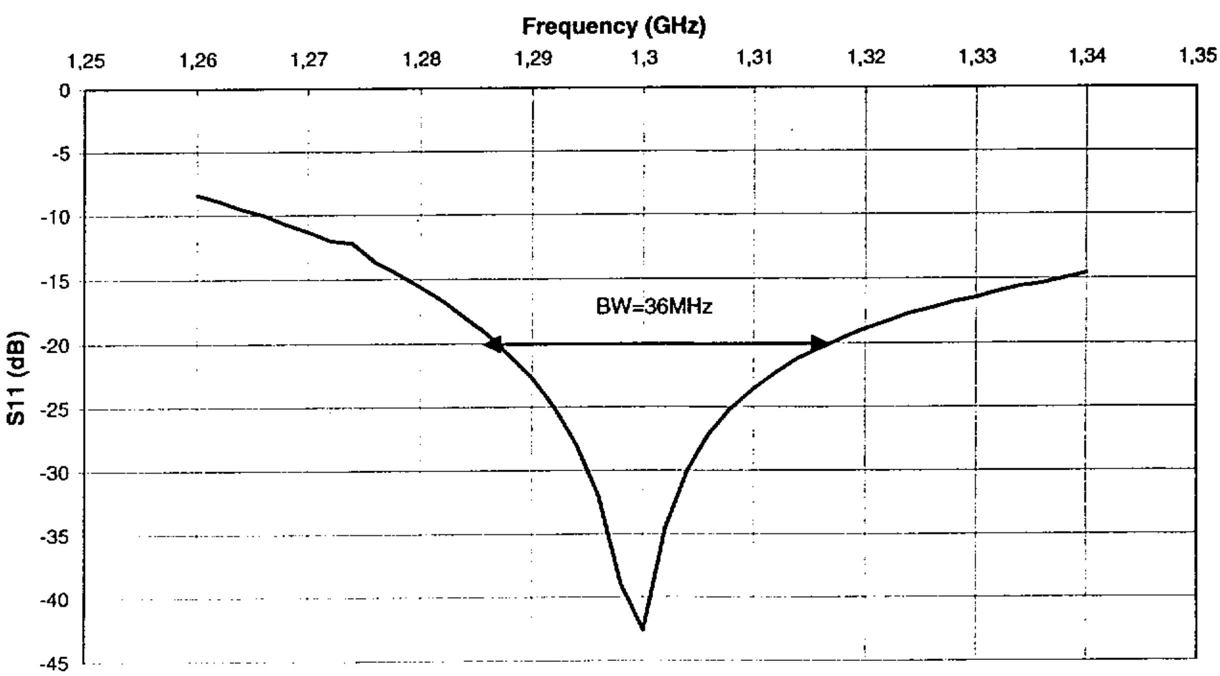

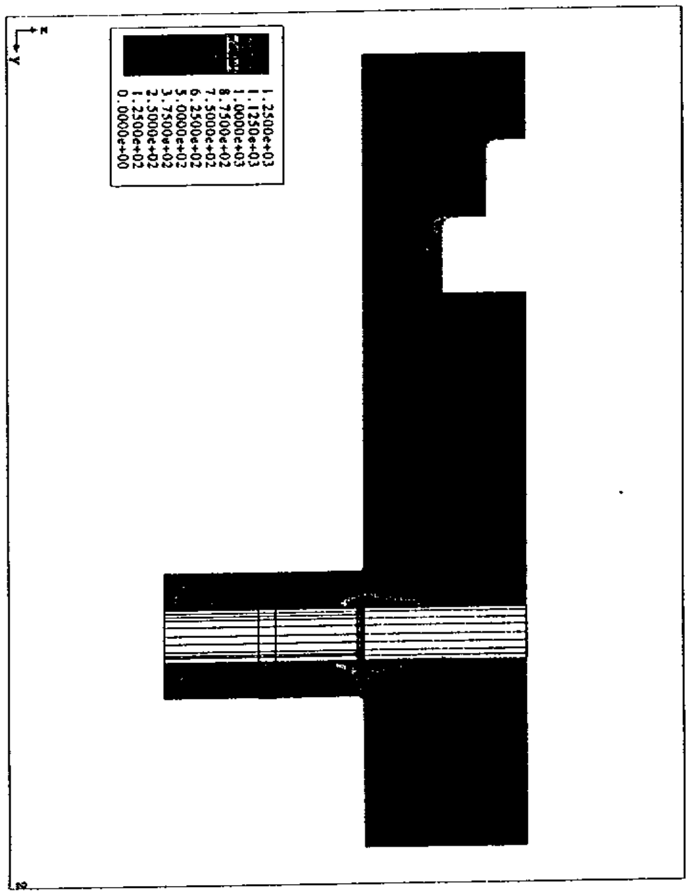

EFFECT OF SHIFT IN DIMENSIONS

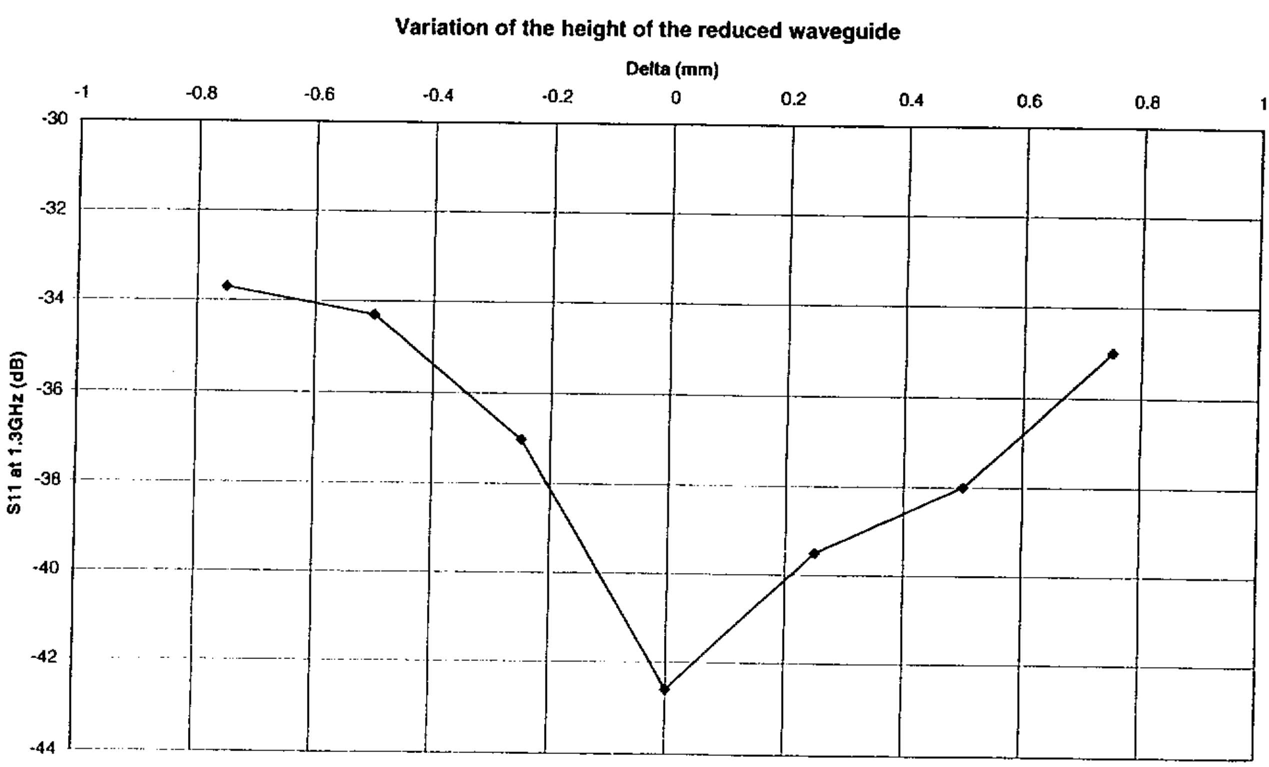

EFFECT OF SHIFT IN DIMENSIONS

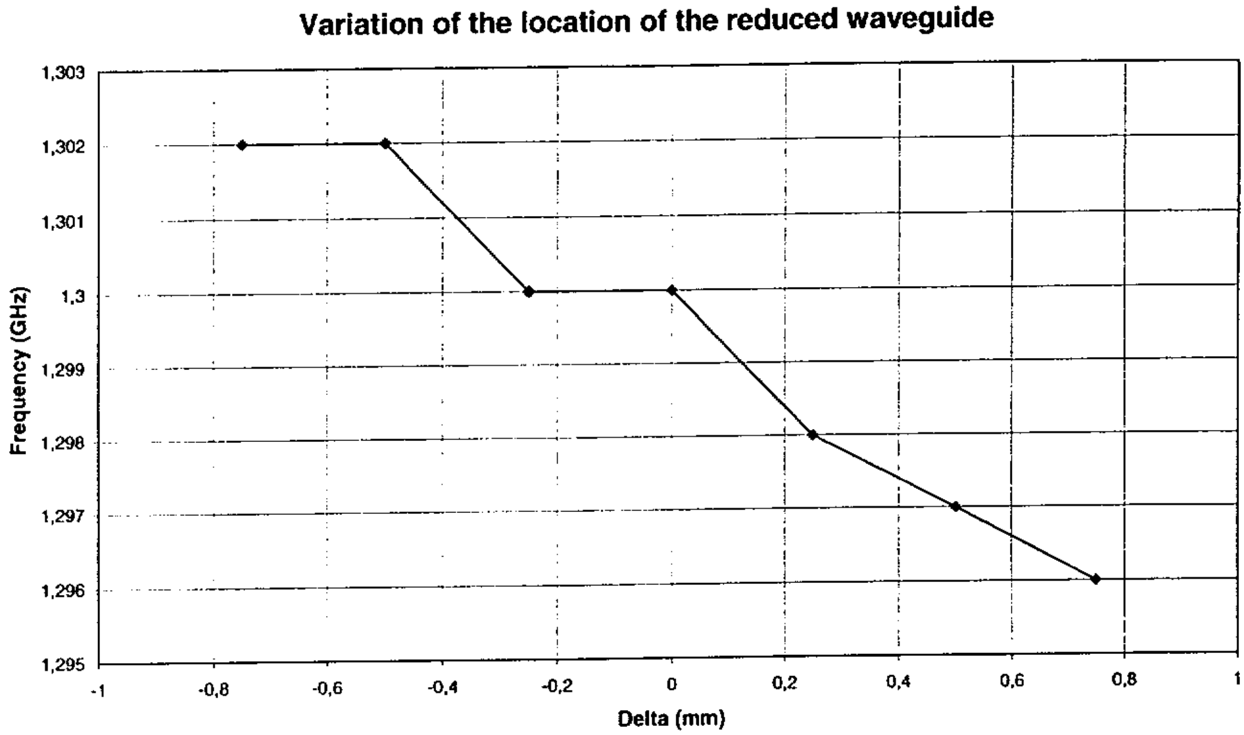

EFFECT OF SHIFT IN DIMENSIONS

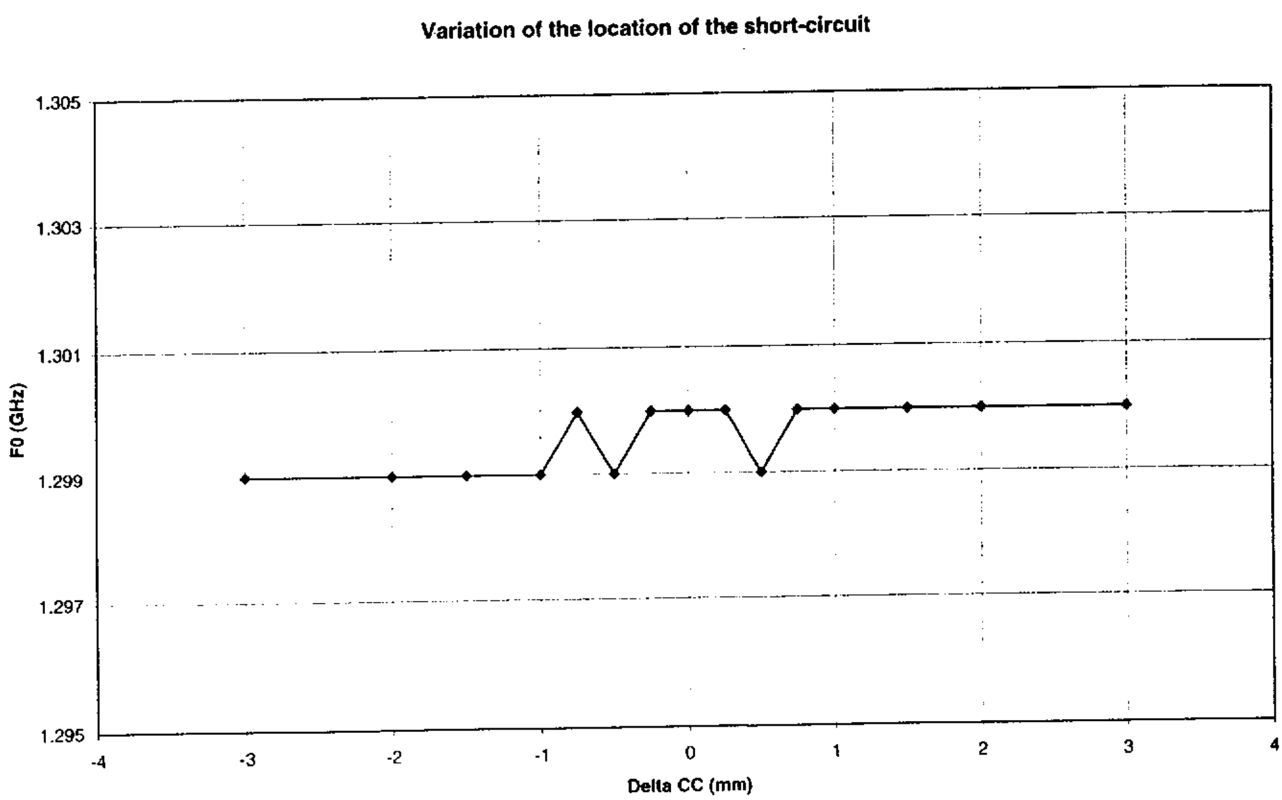

8

POLARISABLE TRANSITION

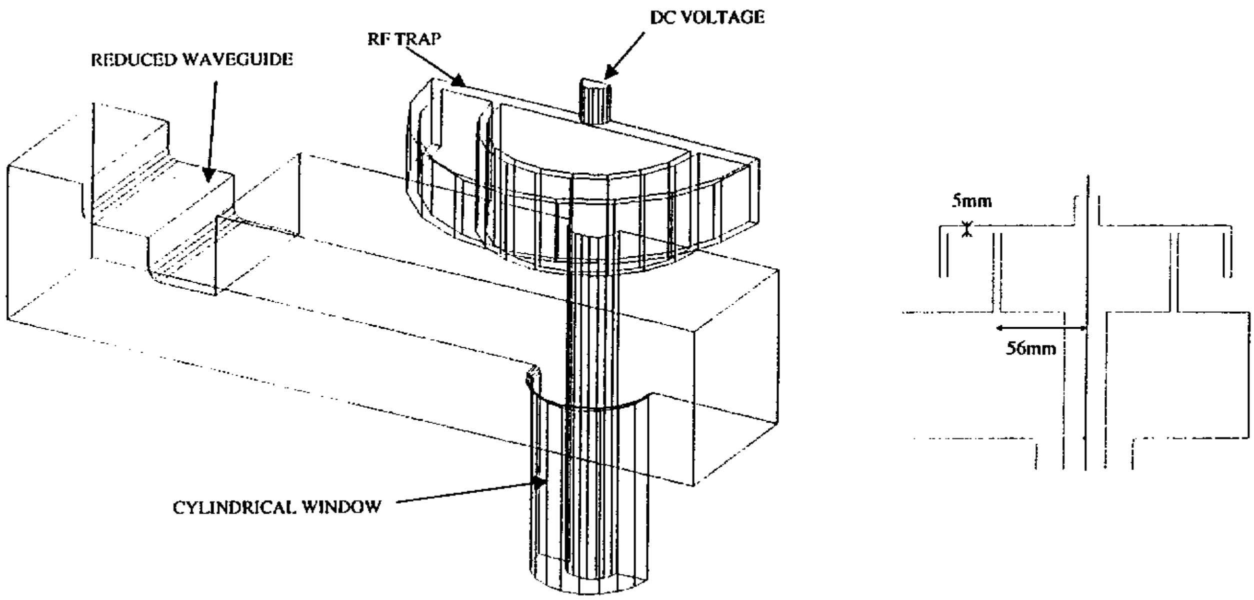

POLARISABLE TRANSITION
OPTIMIZATION WITH HFSS

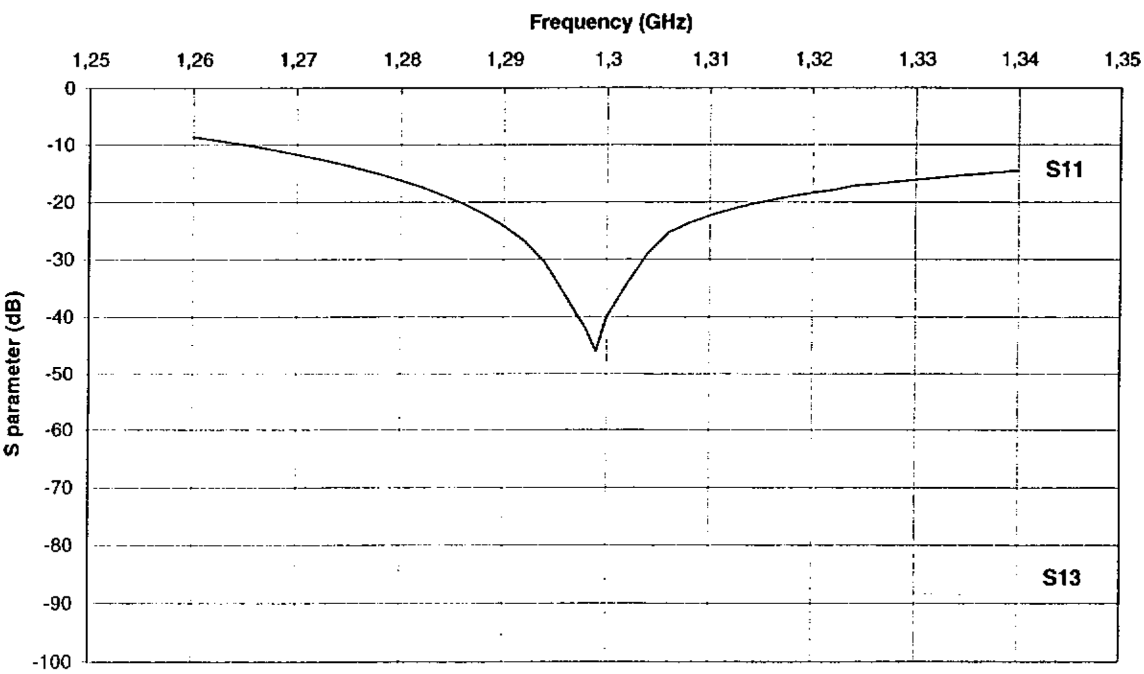

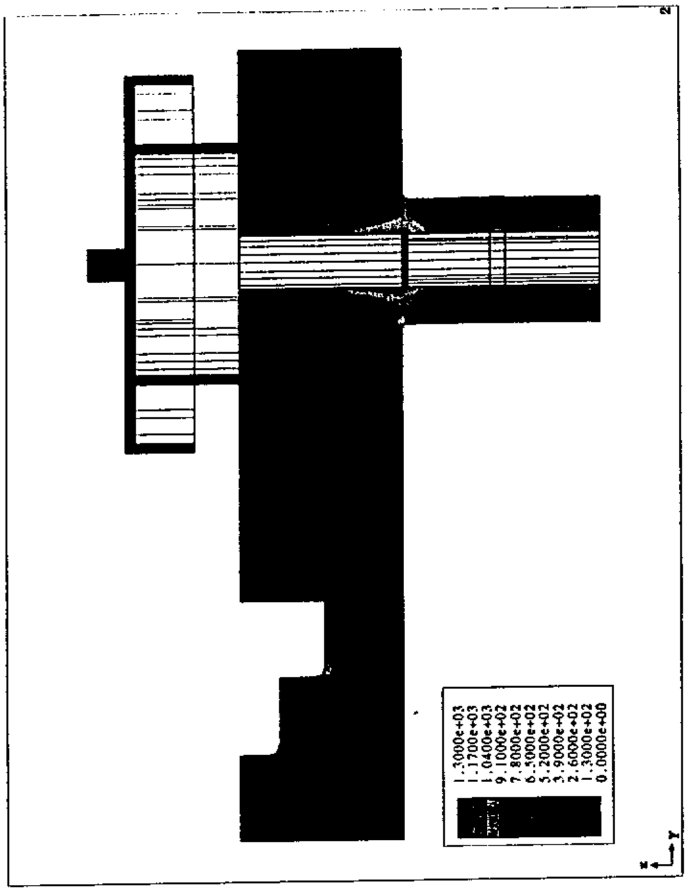
1.3000e+03
1.1700e+03
1.0400e+03
9.1000e+02
7.8000e+02
6.5000e+02
5.2000e+02
3.9000e+02
2.6000e+02
1.3000e+02
0.0000e+00

Coupler workshop, DESY, April 26-27, 1999.

$\lambda/2$ WINDOW EXPERIMENT ANALYSIS

TRAVELLING WAVE WINDOW LOW LEVEL MEASUREMENT

C. TRAVIER

CEA Saclay

11

List of tested components

Waveguide to coax transition

tested 04/1997	• 4 stubs transition (Φ40)	OK 1 MW
tested 04/1997	• doorknob transition	OK 1 MW
tested 11/1997	• antenna transition	OK 1 MW
tested 12/1998	• polarized doorknob transition	not OK 1MW
to be fabricated	• new transition with window	

Windows

tested 03/1997	• THOMSON waveguide window	OK 1 MW
tested 07/1997	• FERMI conical coax window	OK 1 MW @300K
tested 08/1998	• first $\lambda/2$ coax window	OK 1 MW @300K-80 K
to be tested	• second $\lambda/2$ coax window	
to be tested 05/99	• 2 travelling wave coax windows	

Other components

tested 05/1997	• ϕ60-ϕ40 taper	not OK multipactor for P<500 kW
tested 08/1998	• coax bellows	not OK
to be tested	• $\lambda/2$ RF trap	
to be fabricated	• ϕ60-ϕ40 step transition	

$\lambda/2$ window

Advantages

- easiest concept
- low cost
- robustness
- E field parallel to ceramic
  ➡ no multipactor

Drawbacks

- maximum field at brazing point
- high dielectric losses
- direct view of cavity electrons

12

Fabricated by SICN

ceramic: Wesgo Al300 + TiN coating
inner conductor: copper
outer conductor: kovar + copper coated SS

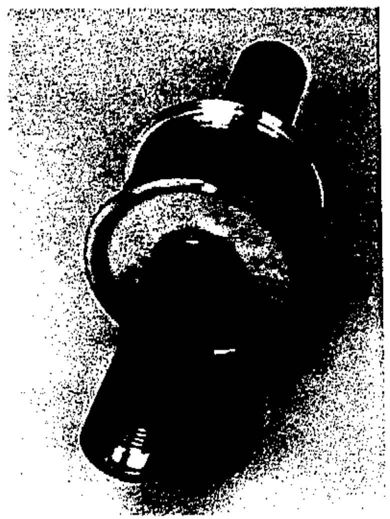

$\lambda/2$ window experiment

Dates	Temperature (K)	SW /TW	Number pulses	Comment
10/08/98 25/09/98	300	SW	338,000	Conditionning
25/09/98 28/09/98	300	TW	28,000	Conditionning
28/09/98 09/10/98	300	SW 1MW	97,000	Losses measurements
12/10/98 15/10/98	80	SW	20,000	Conditionning
15/10/98 06/11/98	80	TW	160,000	Conditioning and losses measurements
06/11/98 19/11/98	300	TW	120,000	
19/11/98 26/11/98	300	SW	62,000	
30/11/98 16/12/98	300	SW	75,000	With polarisation
16/12/98 08/01/99	300	TW	87,000	With polarisation

Nearly 1.000.000 pulses

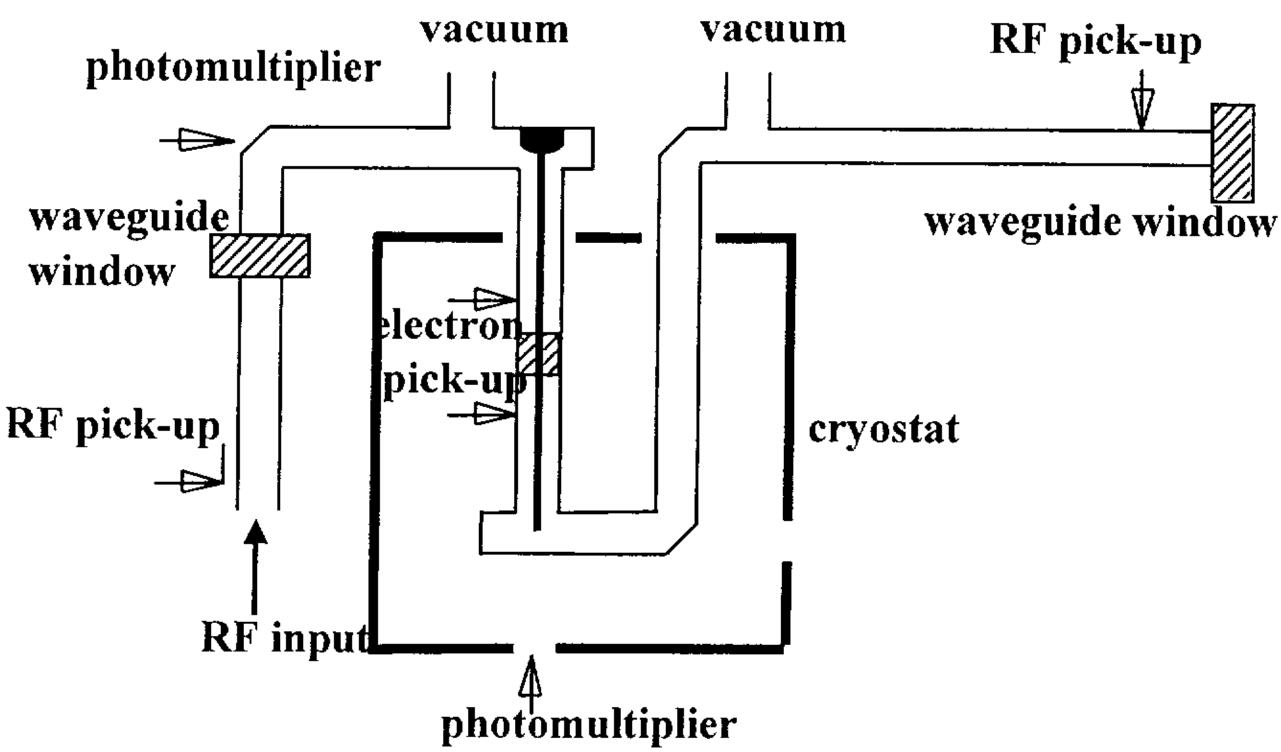

Coupler test stand

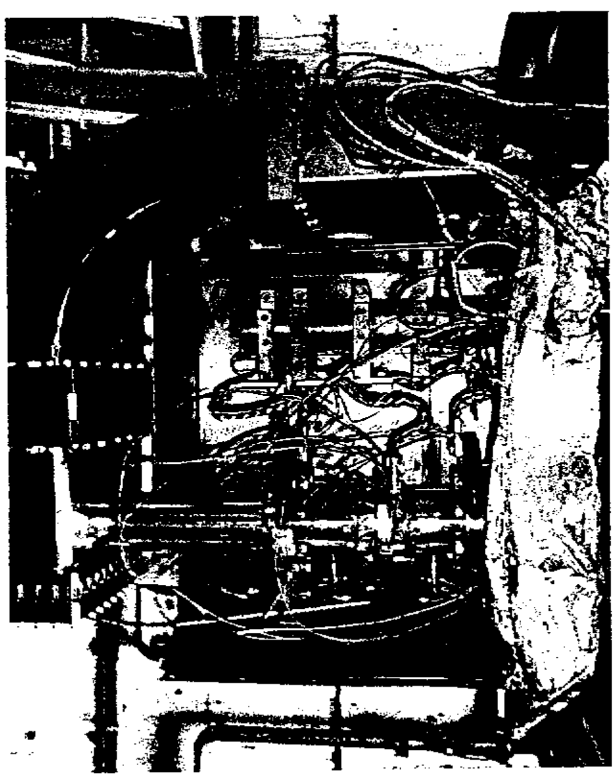

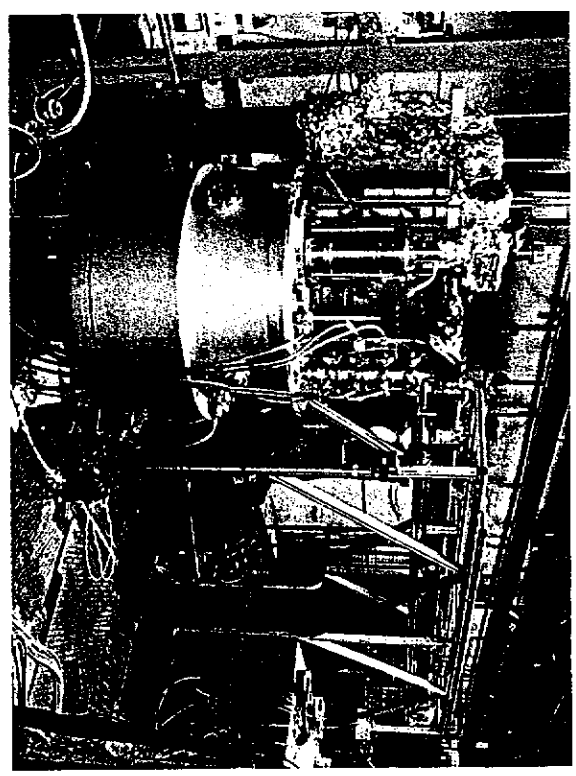

½ window history.
1,000,000 pulses

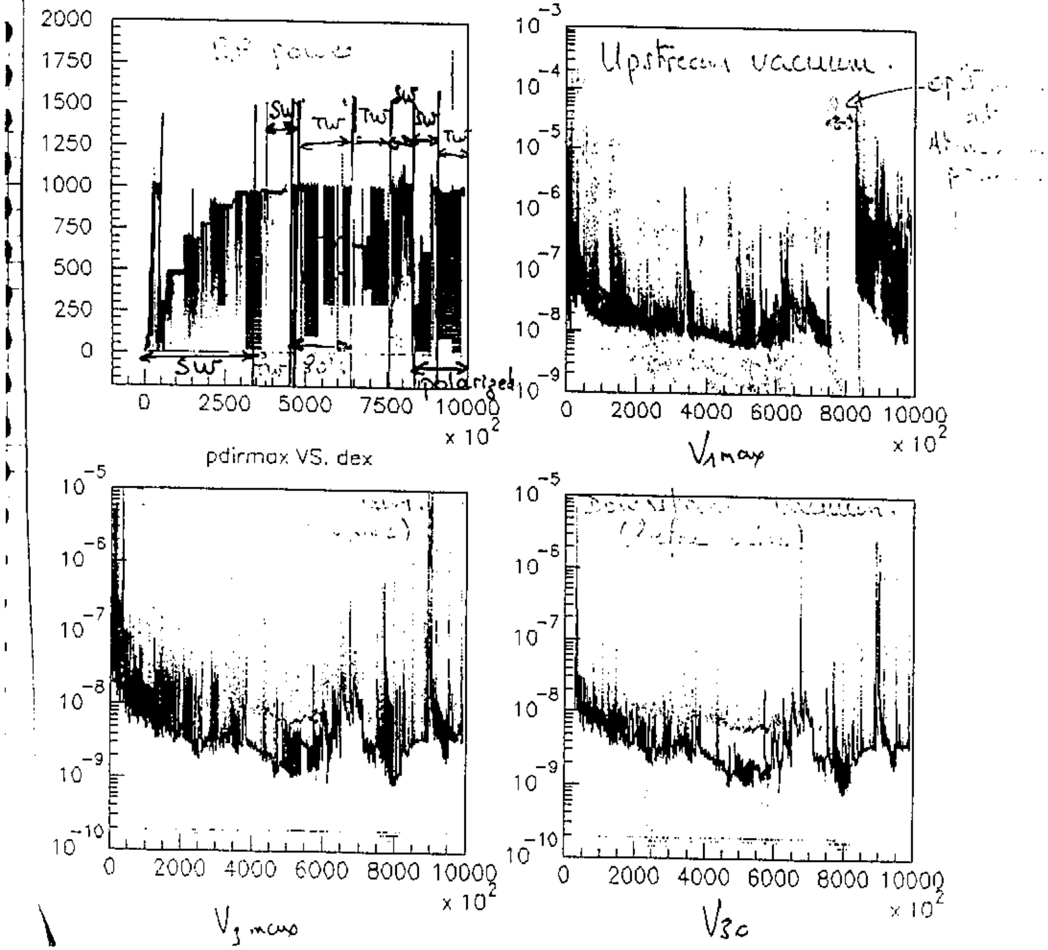

½ window history.

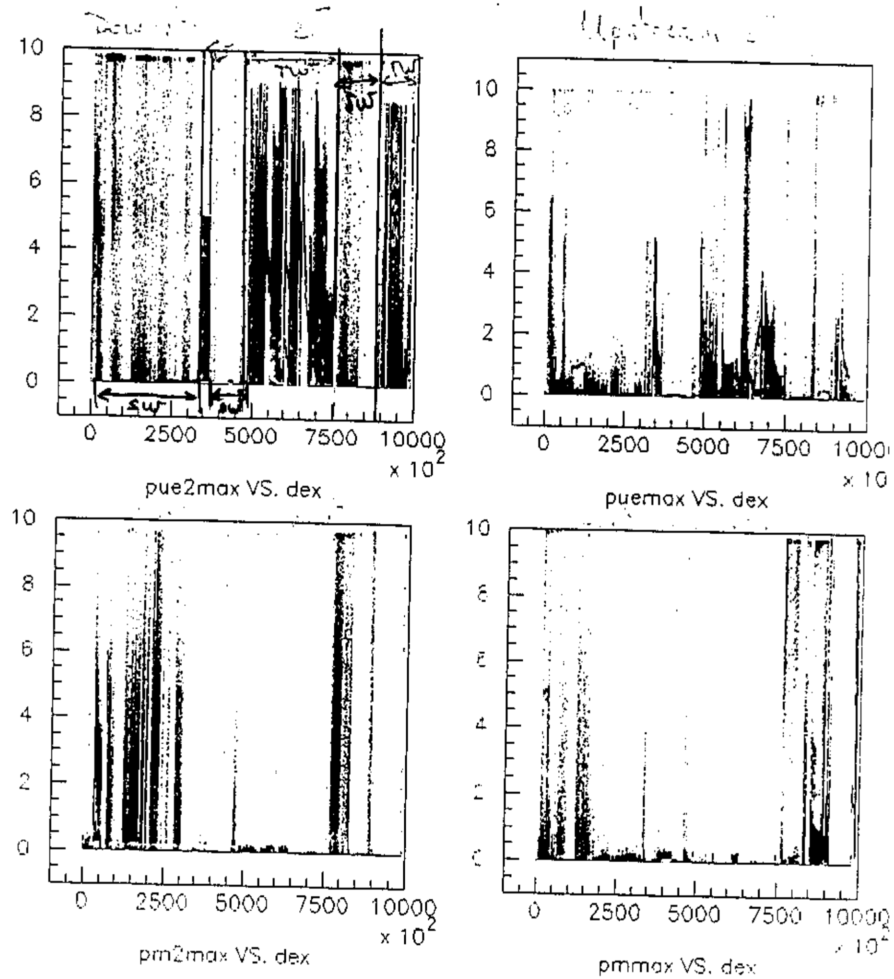

SW
300 k.

λ/2 WINDOW DRAMATIC WEEK-END

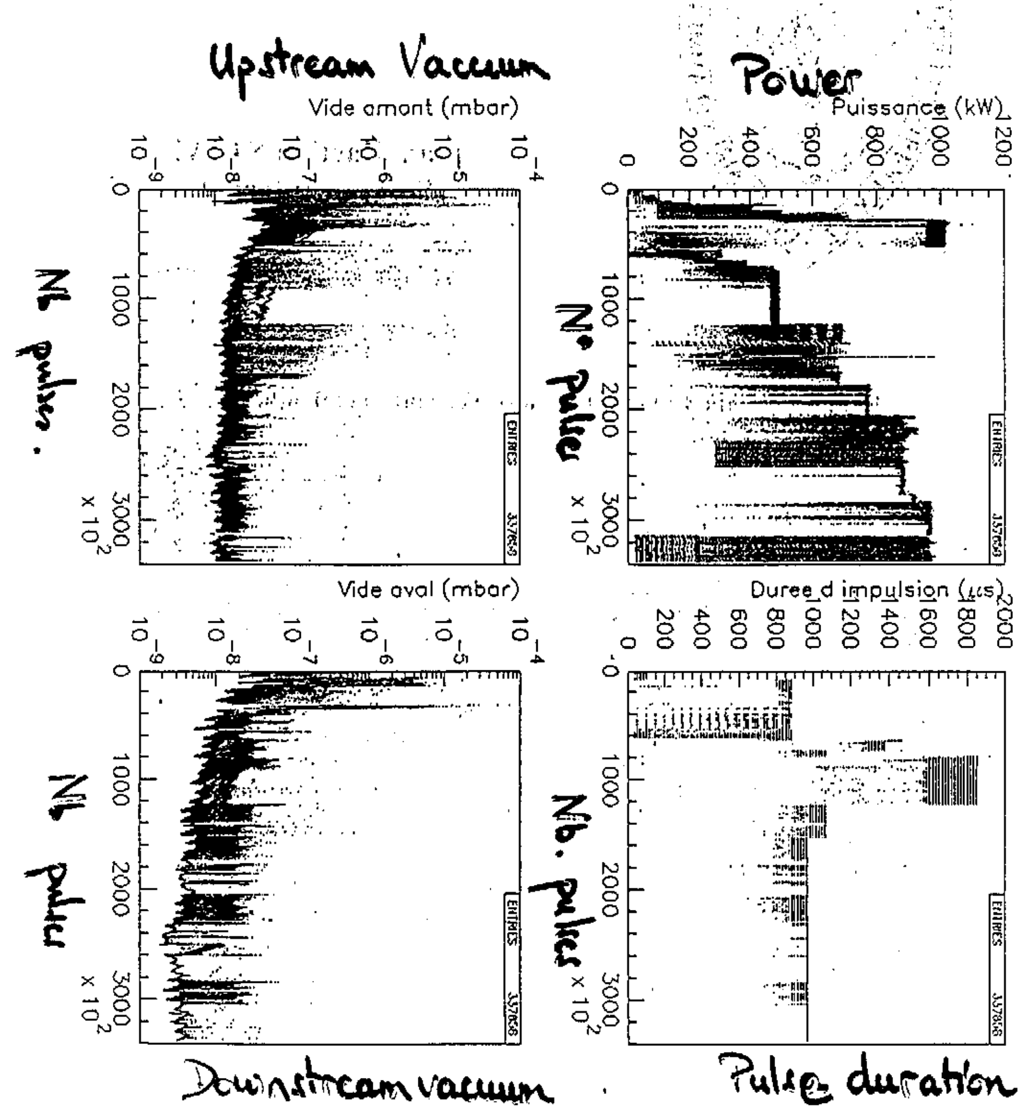

After λ/2 window was dismounted we observed that on the downstream side:

- ceramic was coated with grey layer
- inner and outer conductor were also coated.
- coating on ceramic presented many white spots (silver?)
- the brazing region was much darker and turned green after a few days (Copper).

15

Something happened during August 15-16 Week-end. while running @ 1 MW. A "bug" in the control software prevented the power to be reduced.

- The first conditioning took 30,000 pulses to reach 1 MW:
  - upstream vacuum : 4.10^-8 mbar
  - upstream e⁻ : < 0,5 V
  - downstream vacuum : 2.10^-8 mbar
  - downstream e⁻ : < 0,5 V

- After this bad WE, it took 250,000 pulses to reach 1 MW

A zoom on sad event.

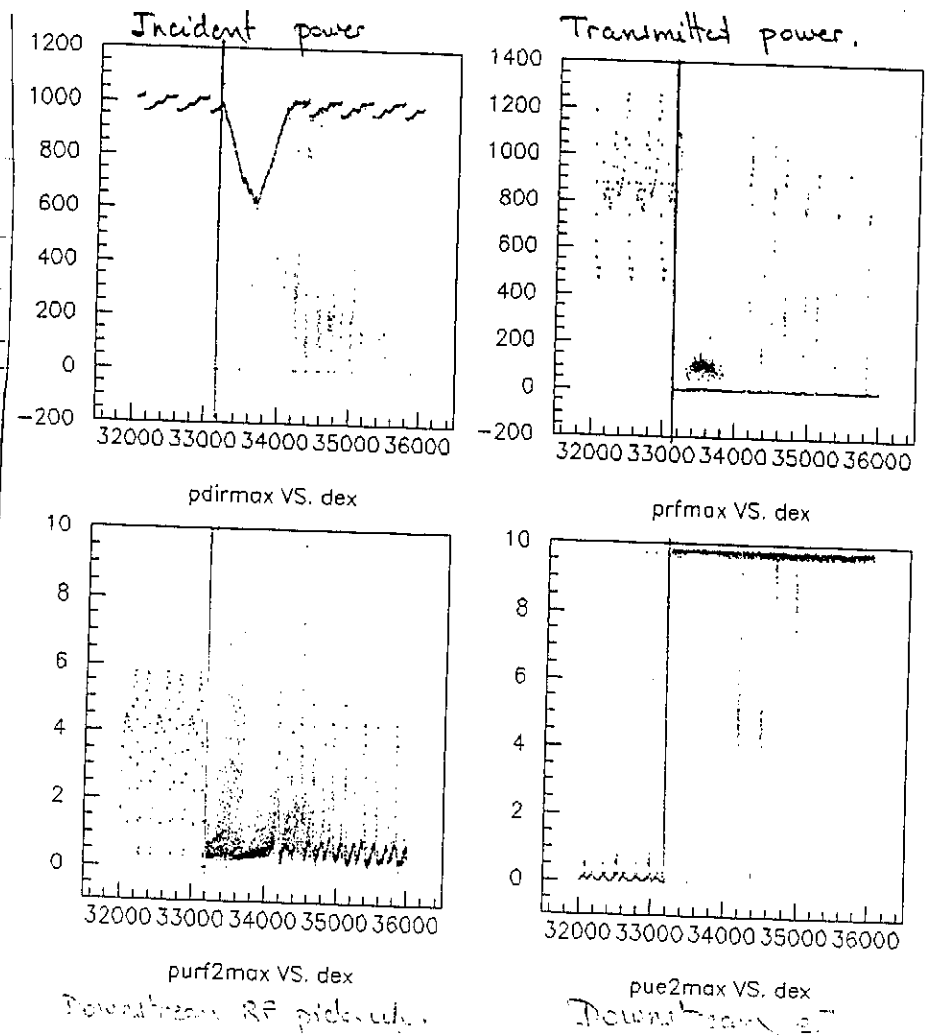

The power is fully reflected near the downstream side of the window.

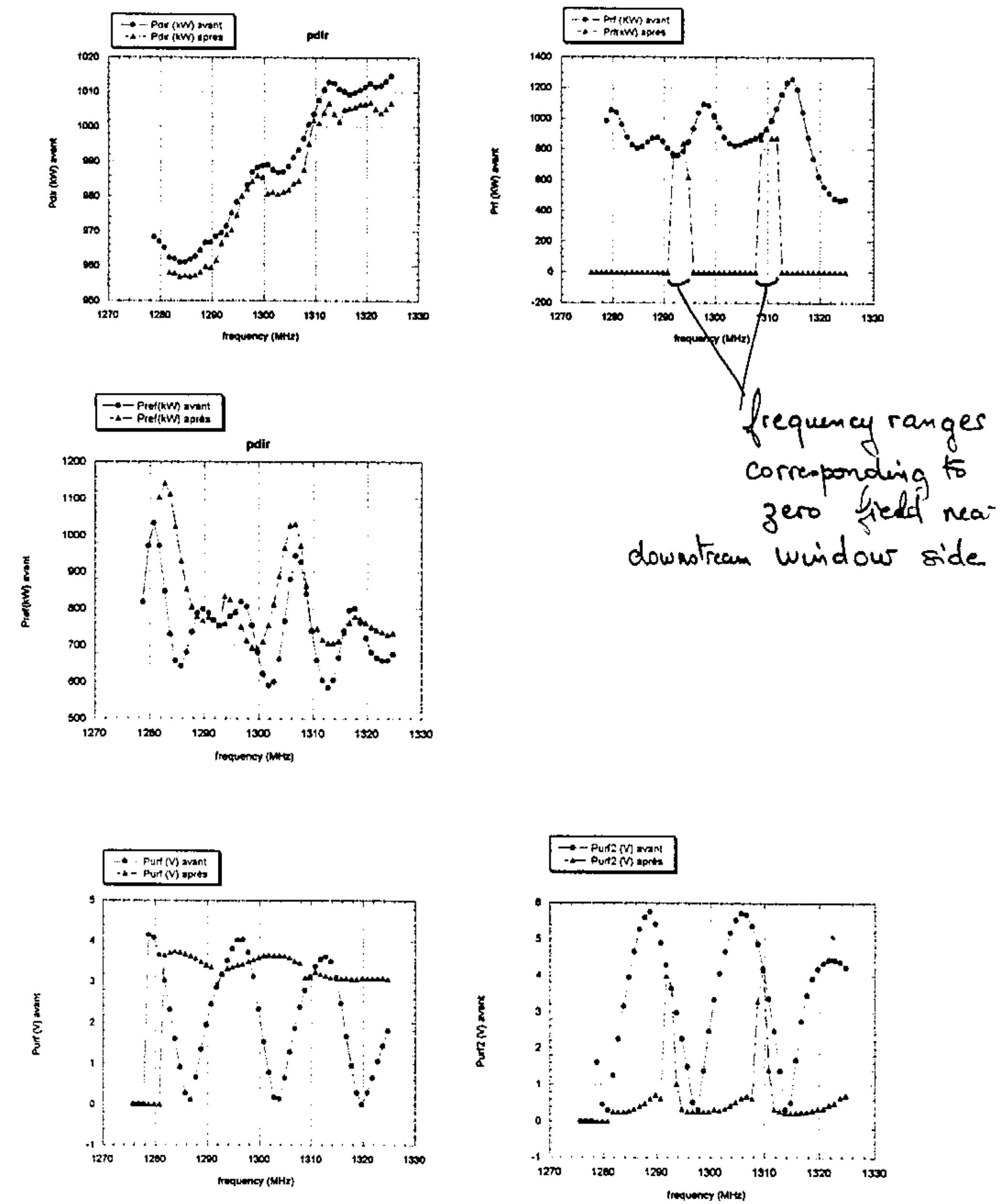

upstream light signal ~ Power ~~no more multipacting~~ Same behaviour as warm case

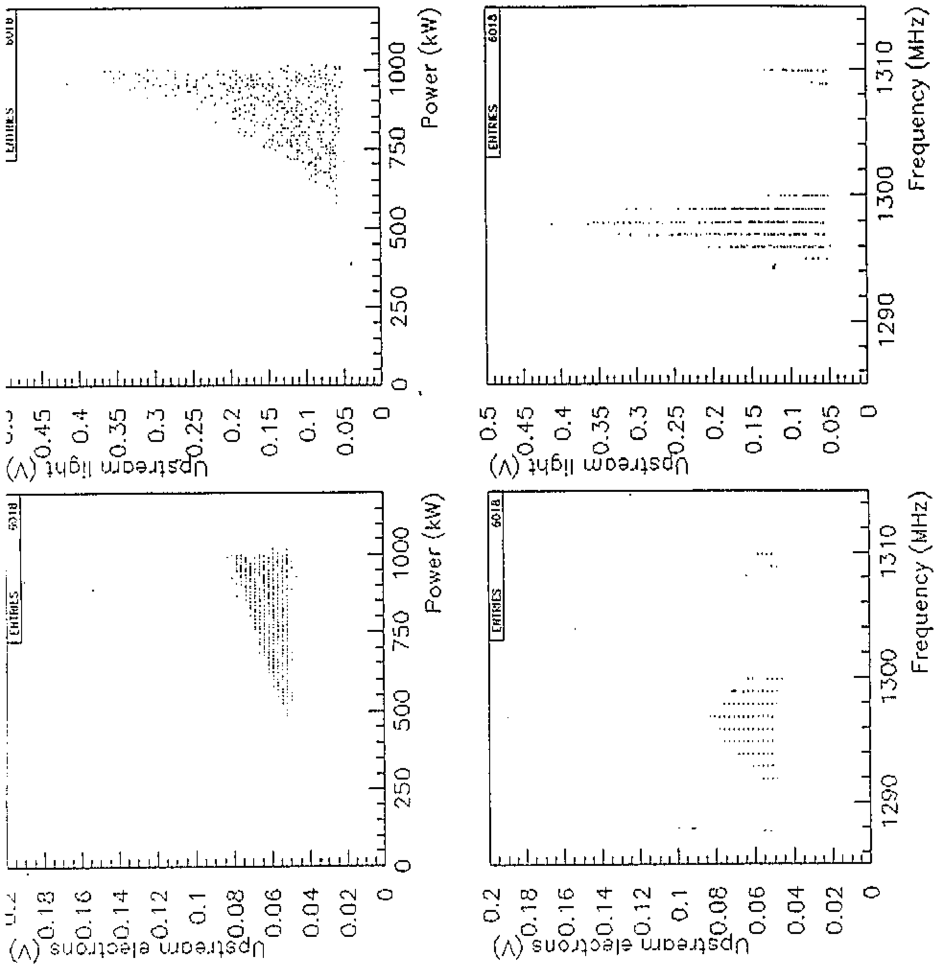

upstream electrons no more multipacting only remains signal ~ Power

~~upstream~~ light

Downstream side.

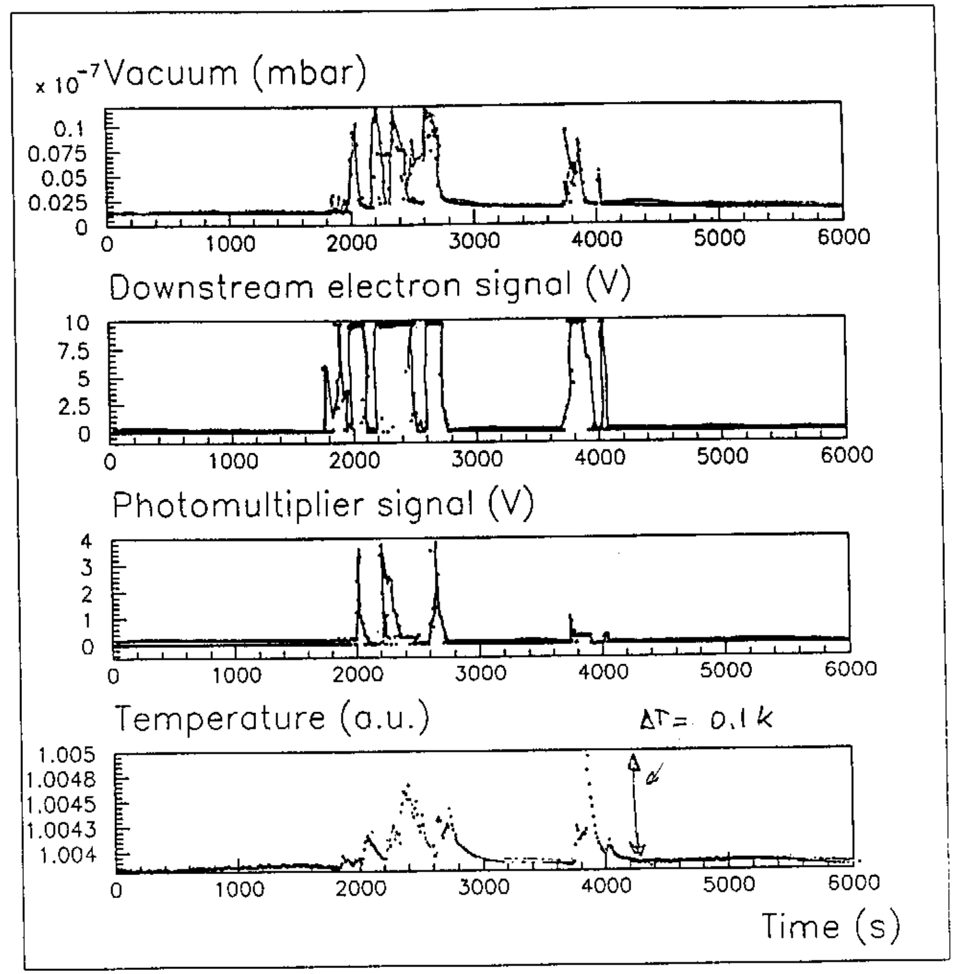

Figure 1: An example of multipactor behaviour at 1 MW (standing wave conditions) @ 1299 MHz. @ 80k.

TW
300k

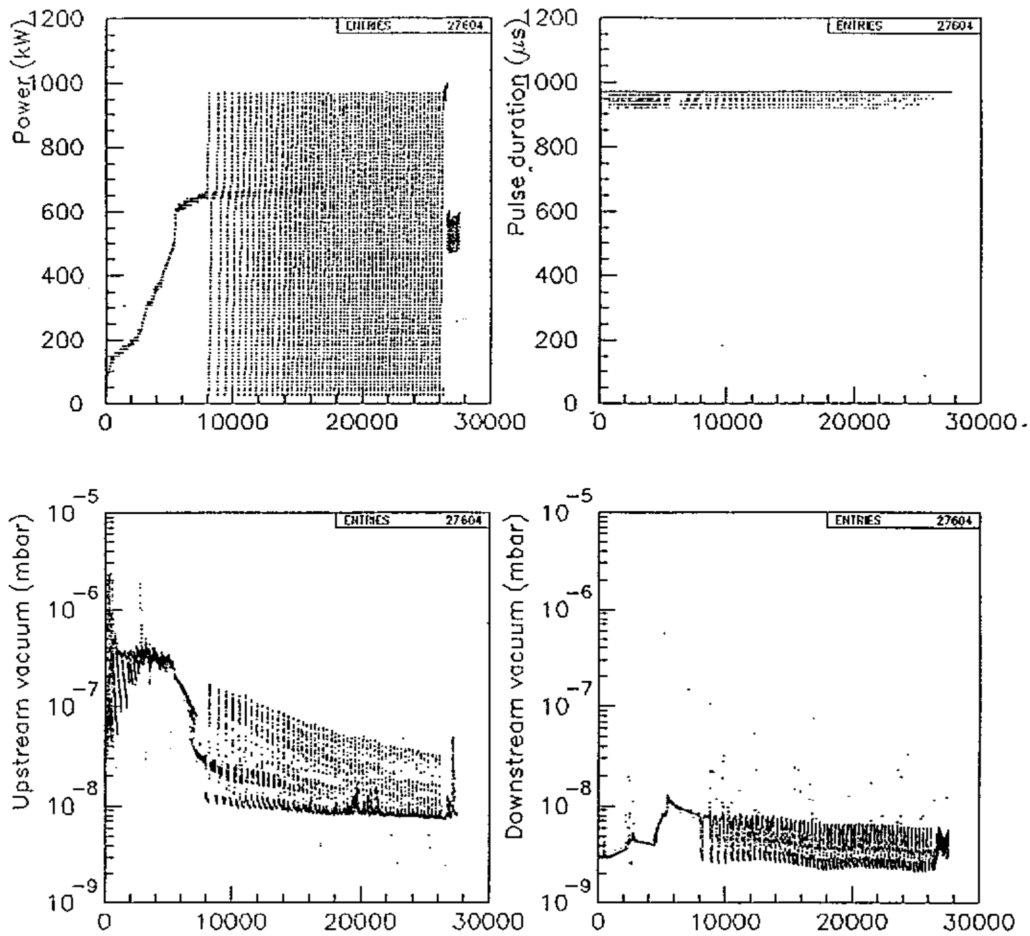

ENTRIES 27604
Power (kW)
0
200
400
600
800
1000
1200
0
10000
20000
30000
ENTRIES 27604
Pulse duration (μs)
ENTRIES 27604
Upstream vacuum (mbar)
ENTRIES 27604
Downstream vacuum (mbar)
10^{-5}
10^{-6}
10^{-7}
10^{-8}
10^{-9}

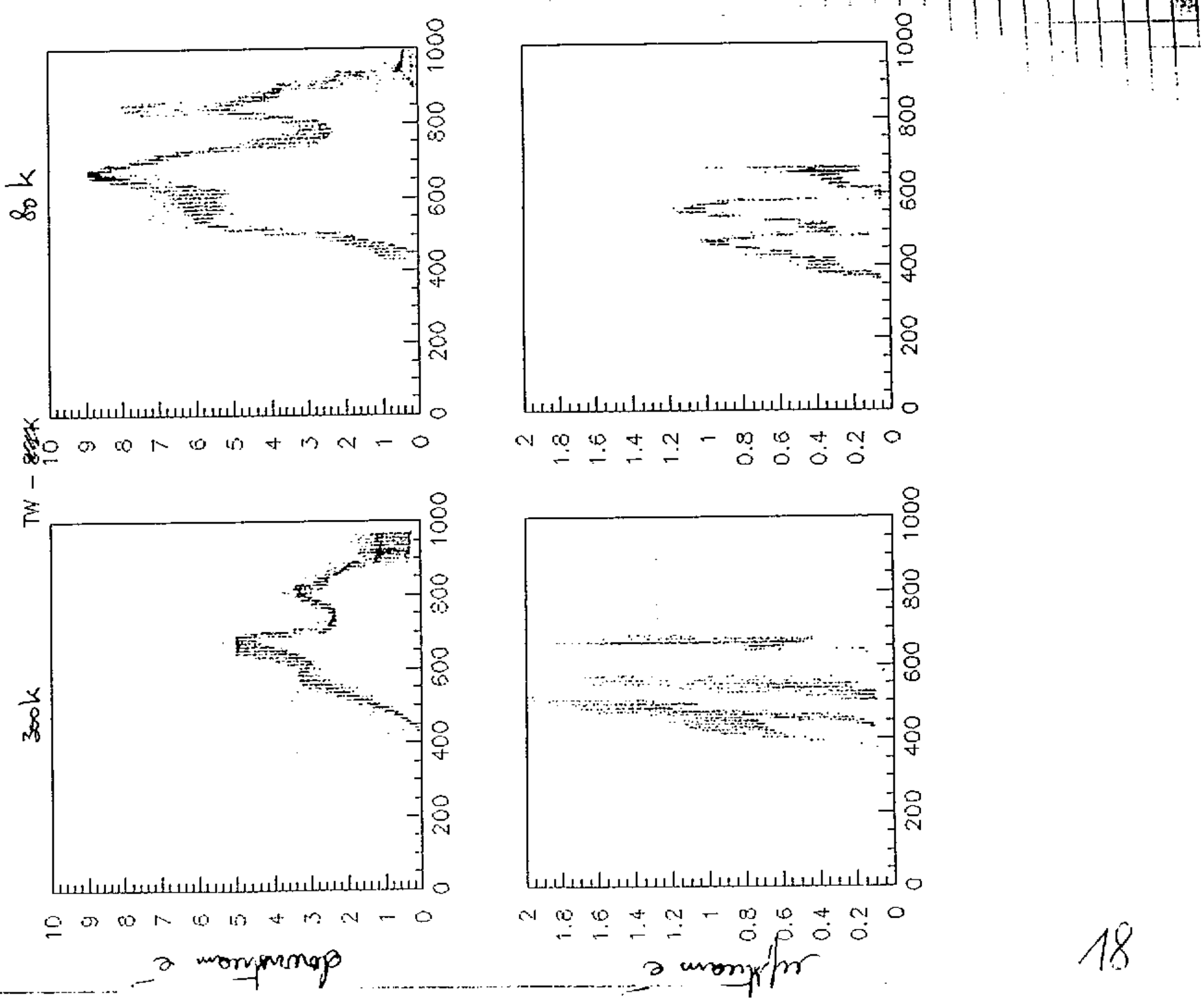

80 k
300k
TW - 80K
downstream e
upstream e

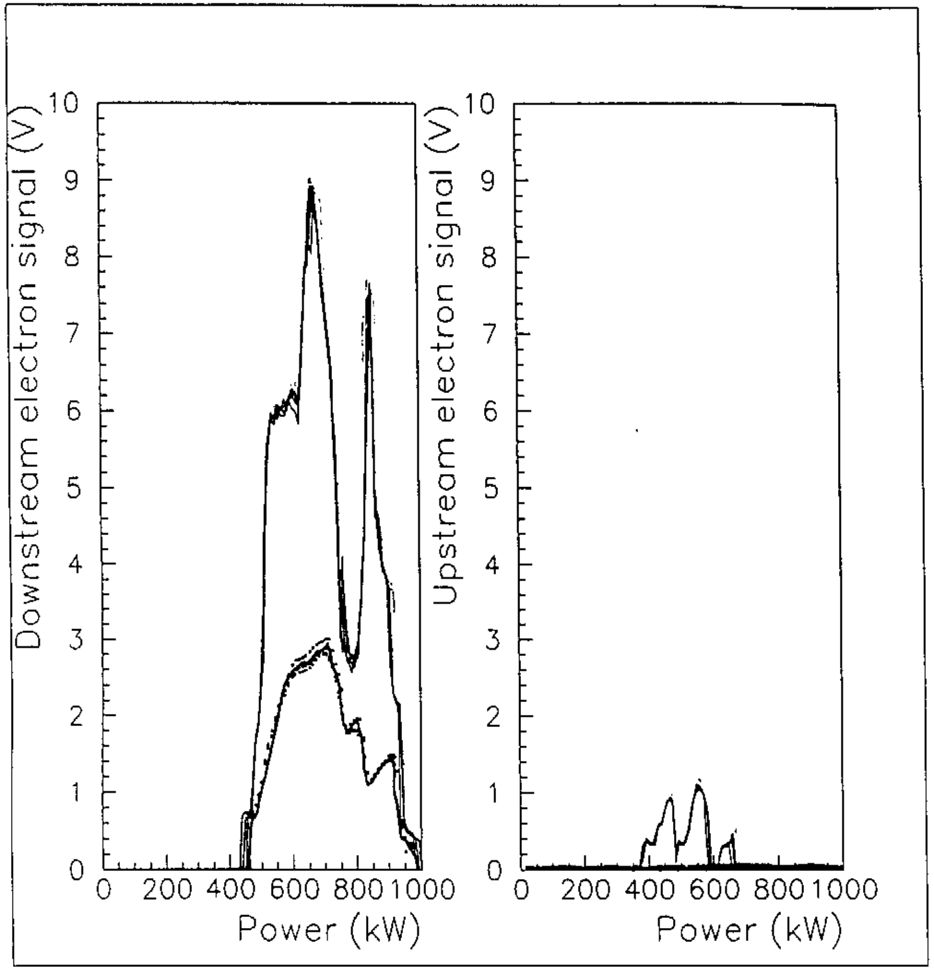

Figure 2: Multipactor as a function of power for TW operation, upstream and downstream sides: at some time (line) and 180,000 pulses later (dots).

DIELECTRIC LOSSES MEASUREMENTS

Temperature differences along copper braids give access to power flows.

Assuming negligible ohmic losses in ceramic, the losses in our system are the following:

- static losses: 7,58 W
- ohmic losses on inner conductor: 1.2 W (SW) @ 1MW
- dielectric losses in ceramic: 1.09 W (SW max)
  0,124 W (SW min) @ 1MW

From these measurements, we obtain:

$$\tan\delta = 5.8\ 10^{-4}$$

- for TESLA pulse @ 1MW, 1.3 ms, 10 Hz : 44 W
  @ 200 kW : 9 W.

19

Travelling wave window

Advantages	Drawbacks
•pure TW in ceramic •no direct view of cavity electrons •low field at brazing point •low dielectric loss •great flexibility in parameter choice •moderate cost •E field parallel to ceramic ➡ no multipactor	•large diameter •high field on noses •difficult to clean •narrow bandwidth

2 windows were fabricated by SICN and are ready to test

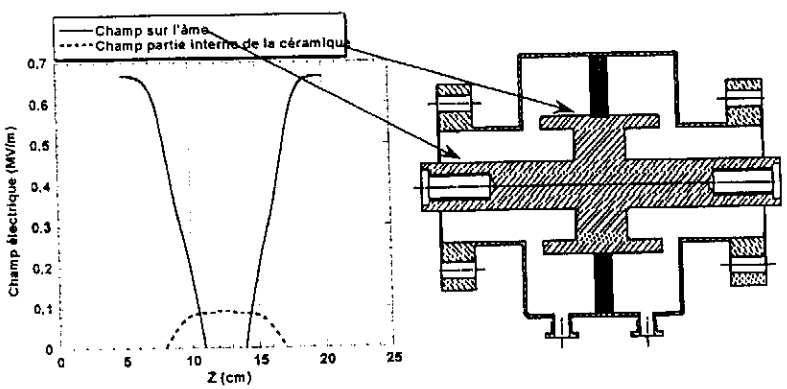

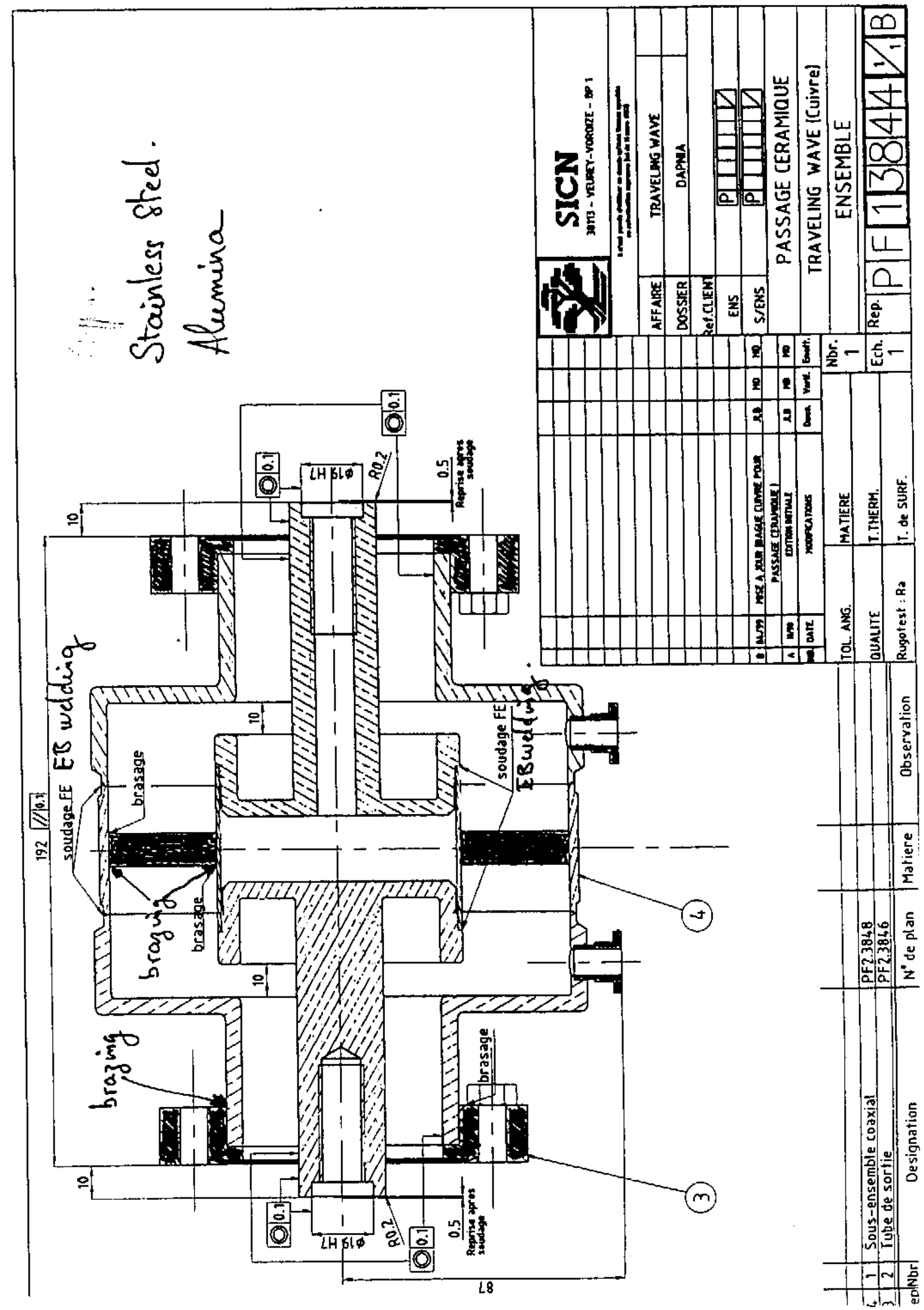

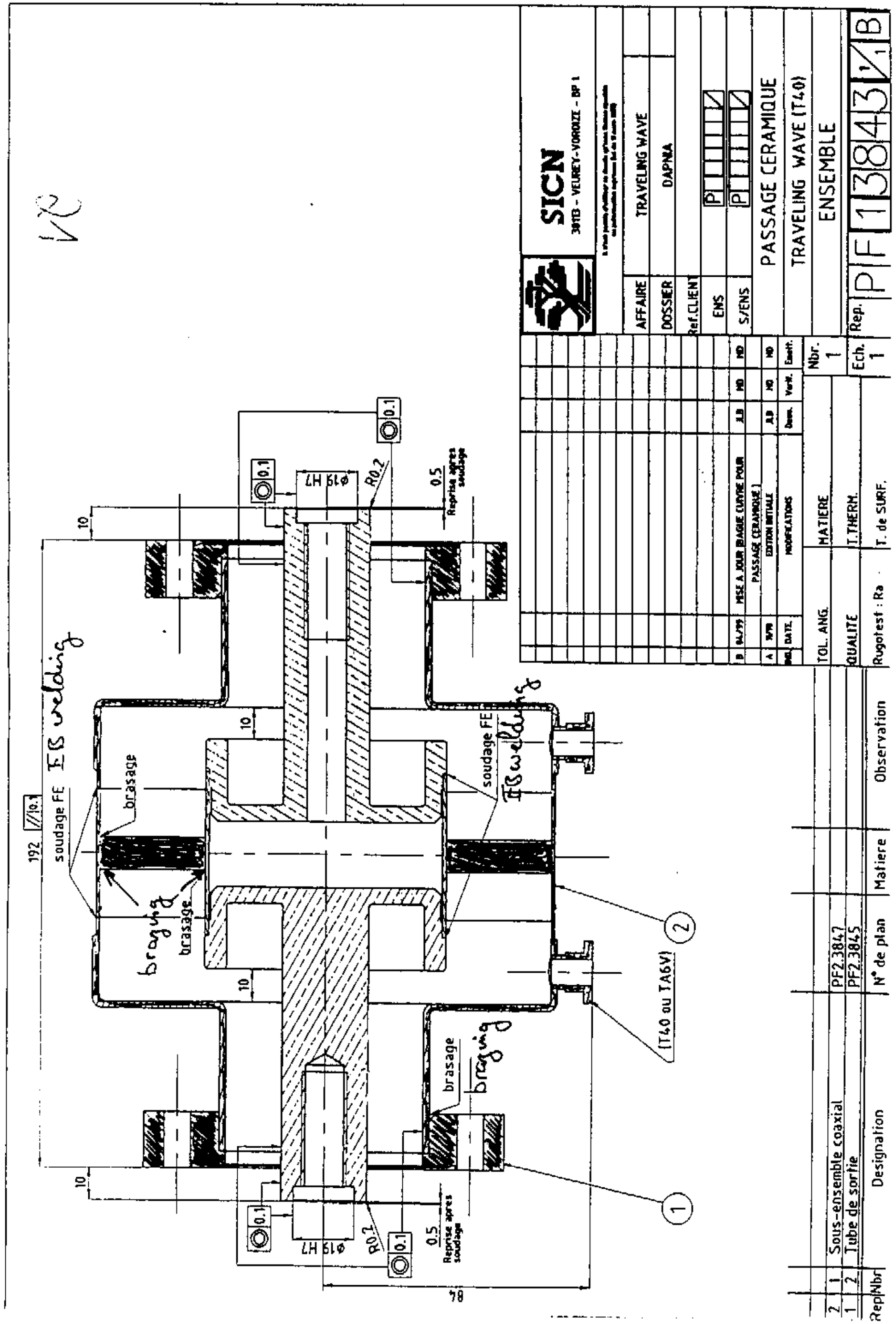

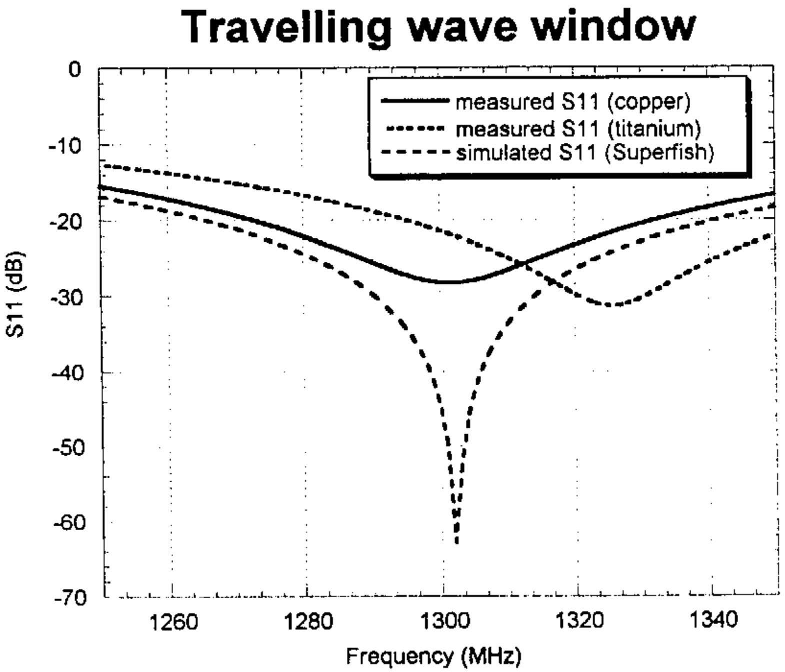

The titanium window is slightly off in frequency. There are some dimensions that were not respected that could explain this shift.

Ti Coating of Ceramics

B. Dwersteg, K. Kopalko, J. Lorkiewicz,
K. Twarowski,

+ MHF-SL Group electronic workshop
DESY

1. Problems with the DESY HIGH POWER WG WINDOW of the TTF Main COUPLER

- low power transmission,
- gas outbursts and vacuum breakdowns,
- light emission,
- electron emission - possibly resulting from multipacting effects originated on the ceramic surface.

22

FNAL TTF-Main-Coupler

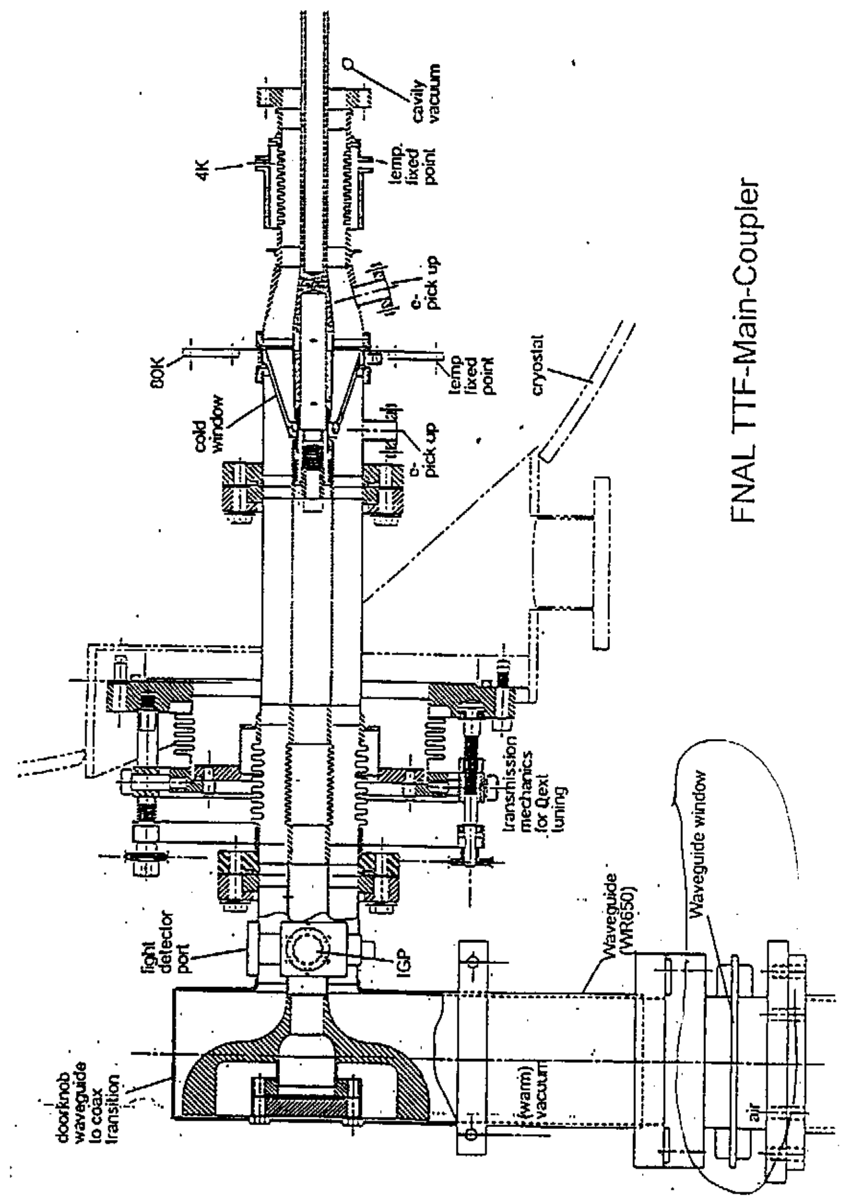

2. The choice of antimultipactor measures

- selection of TiN surface layer (low SEE, less processing time, good stability in RF fields),

- coating method and device,

  - sublimation of Ti from a heated filament (better suited in the case of limited access than sputtering methods), using a "point" Ti source,

    <u>advantages</u>: easy to manufacture in a v. short time, the shape and position of the wire depends weakly on thermal stresses,

    <u>drawbacks</u>: -the obtained layer is not homogeneous,
    -using of a thickness meter is not possible due to the lack of space,

- the on-line, continuous measurement of the layer resistance, preliminary Ti deposition tests,

- RF windows processing procedure, supplementary coating tests.

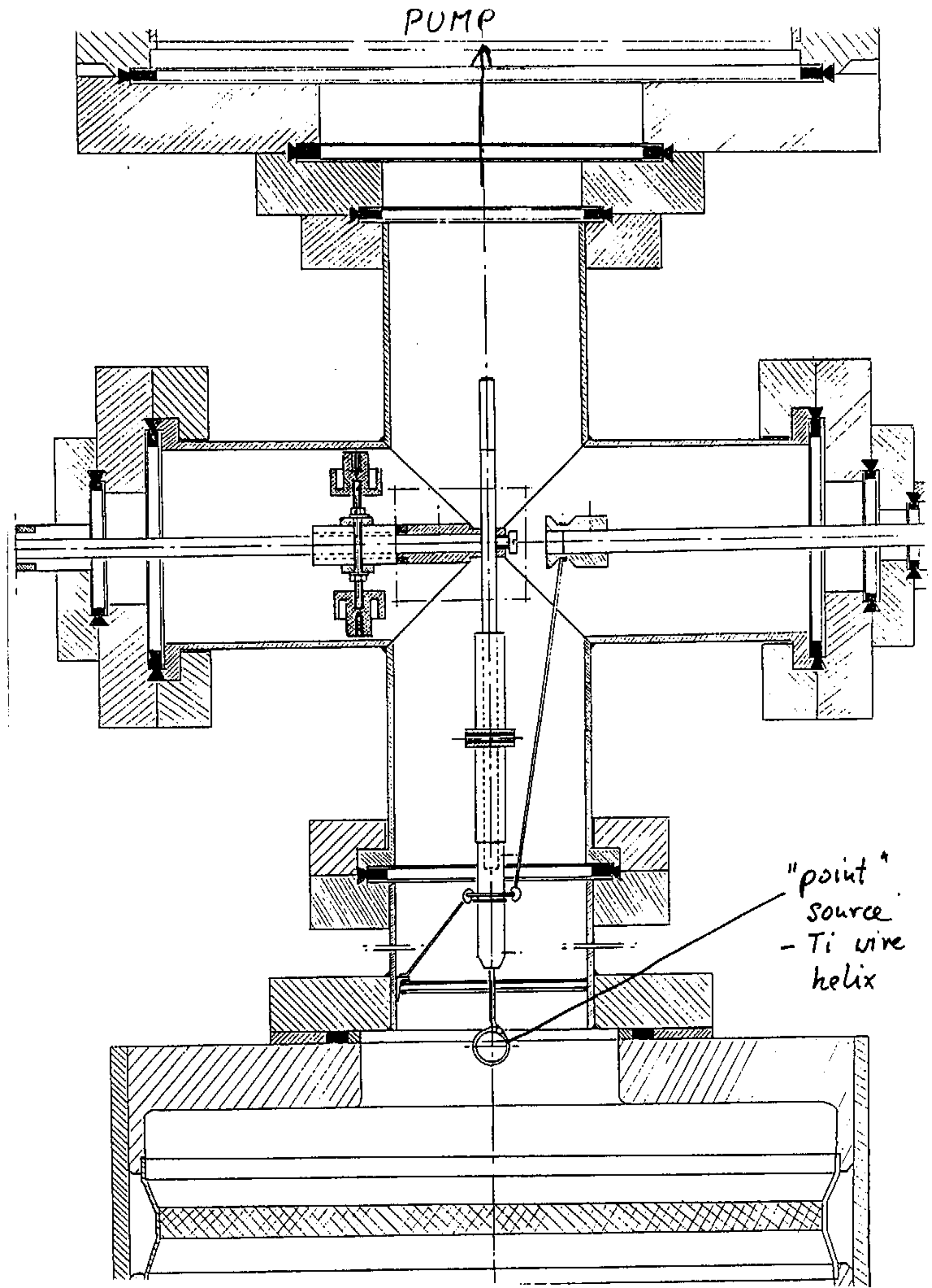

Ti layer resistance vs deposition time

average residual gas pressure = 10^{-7} mbar

Ti wire temperature = 1290 °C

sample 1

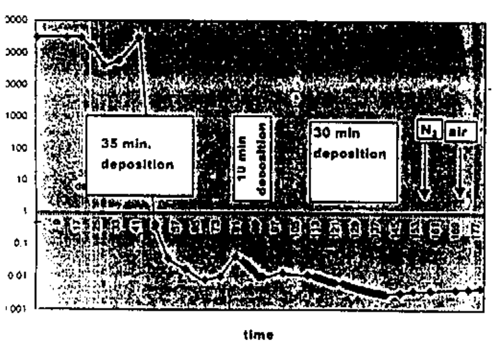

sample 2

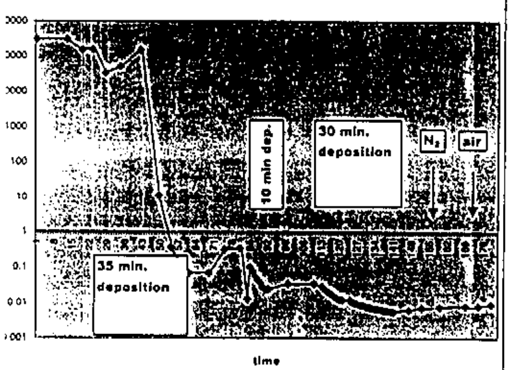

sample 3

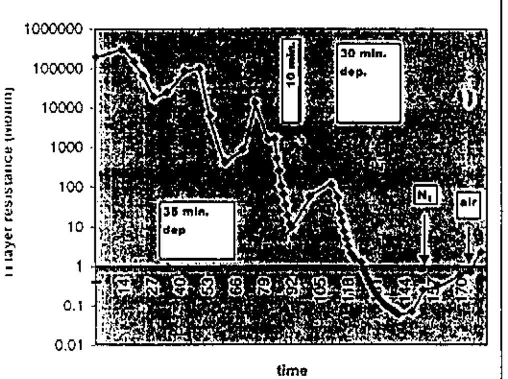

experimental setup

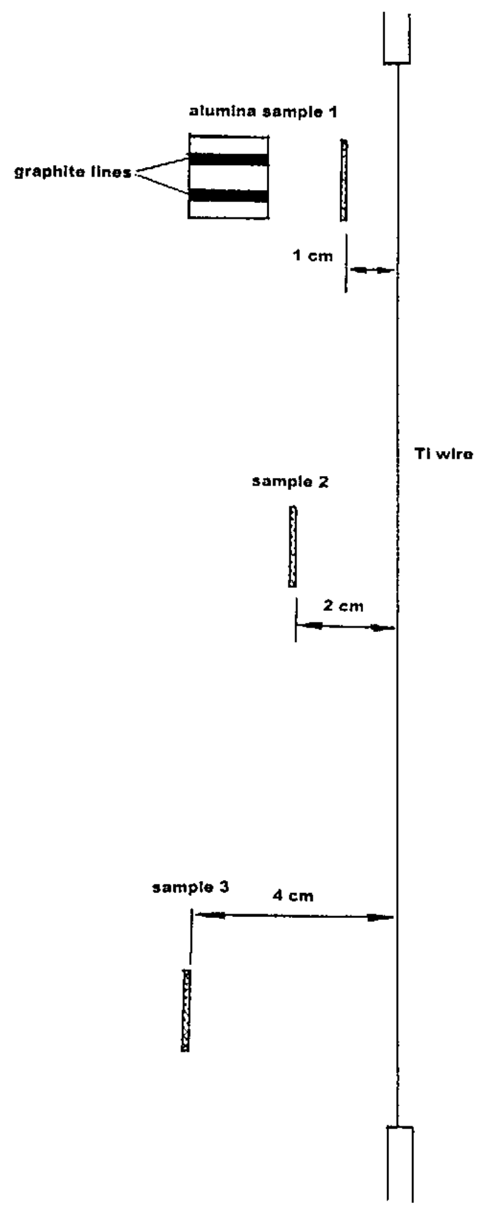

DESY
MHF-SL

Data of Ti coating of warm waveguide windows performed between 5 Feb and 1 March 1968

03.03.1999

Date of coating	Chamber pressure, atmosphere	Sublimation source	Exposition time	Heating current	The final resistance per sq. of the coated layer, at the end of the deposition	Colour of the layer
18-20.03.99	starting pressure:7E-8 after venting with NH_3:2E-4	point source, helix of 14.3 cm long Ti wire	36 min	12 amp	26 Mohm	slightly greyish with visible shadows
			3 h break, NH_3 pressure 10 mbar			
			20 min	12 amp	15 Mohm	
			21 h break, NH_3 pressure 10 mbar			
			7.5 min	12 amp	14 Mohm	
			2 h break, NH_3 pressure 10 mbar			
			10.5 min	12 amp	6 Mohm	
		total deposition time: 74 min				
22-24.03.99	starting pressure:7E-8 after venting with NH_3:2E-4	point source, helix of 14.3 cm long Ti wire	22 min	12 amp	15 Mohm	slightly yellowish colour of the window
			3 h break, NH_3 pressure 10 mbar			
			7 min	12 amp	14 Mohm	
			20 h break, NH_3 pressure 10 mbar			
			3.5 min	12 amp	19 Mohm	
			5 h break, NH_3 pressure 10 mbar			
			5 min	12 amp	12 Mohm	
			6.5 h break, NH_3 pressure 10 mbar			
			5 min	12 amp	12 Mohm	
			12 h break, NH_3 pressure 10 mbar			
			6 min	12 amp	17.5 Mohm	
			3.5h break, NH_3 pressure 10 mbar			
			10 min	12 amp	6 Mohm	
		total deposition time: 58.5 min				
25-26.03.99	starting pressure:7E-8 after venting with NH_3:2E-4	point source, helix of 14.3 cm long Ti wire	40min	12 amp	28 Mohm	
			4 h break, NH_3 pressure 10 mbar			
			7 min	12 amp	36 Mohm	
			5 h break, NH_3 pressure 10 mbar			
			6 min	12 amp	20 Mohm	
			14.5 h break, NH_3 pressure 10 mbar			
			4 min	12 amp	19 Mohm	
			4 h break, NH_3 pressure 10 mbar			
			10 min	12 amp	10.5 Mohm	
		total deposition time: 67 min				

Ammonia pressure:
2E-4 mbar
Average path length
≳ 10cm

RF window G15, Ti layer resistance vs time

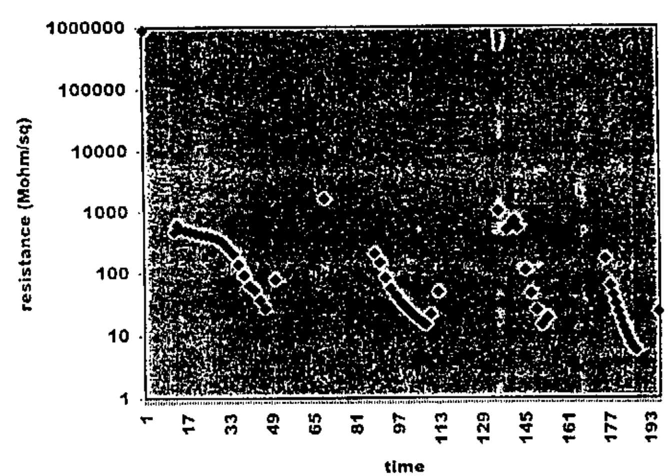

Coating score:

DESY WG windows:
12 pcs

Philips waveguide windows: 3 pcs

Coupler Workshop (DESY), April 26-27, 1999.

CONDITIONING EXPERIENCE

- Polarized transition (C. Travier)
- Experiment on coax (S. Ch...)

POLARIZED DOORKNOB TRANSITION

P. Lepercq (LAL Orsay)

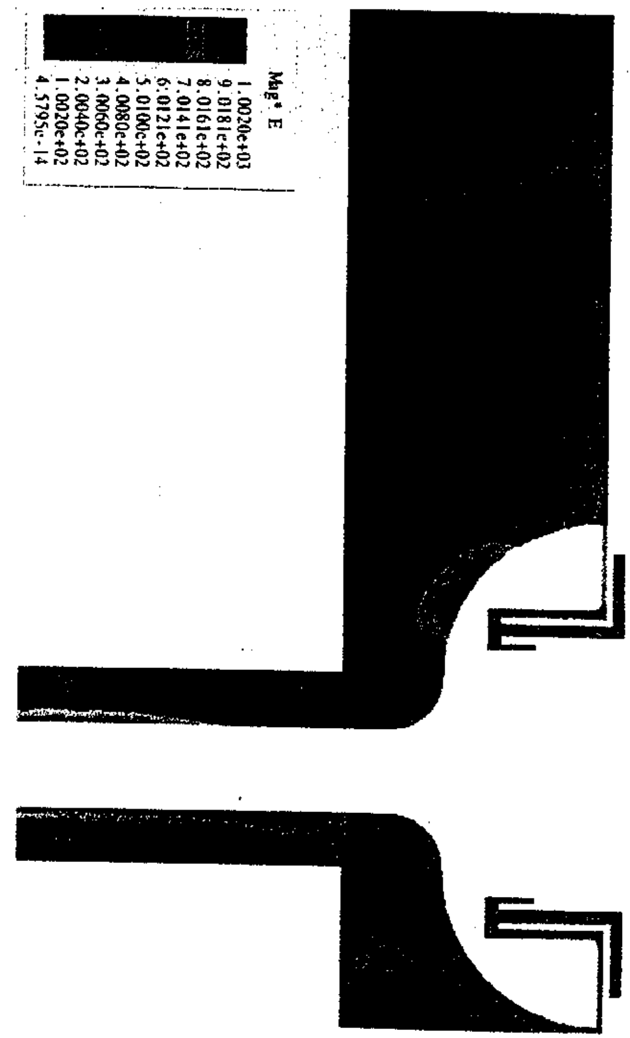

λ/2 WINDOW WITH POLARIZED TRANSITION

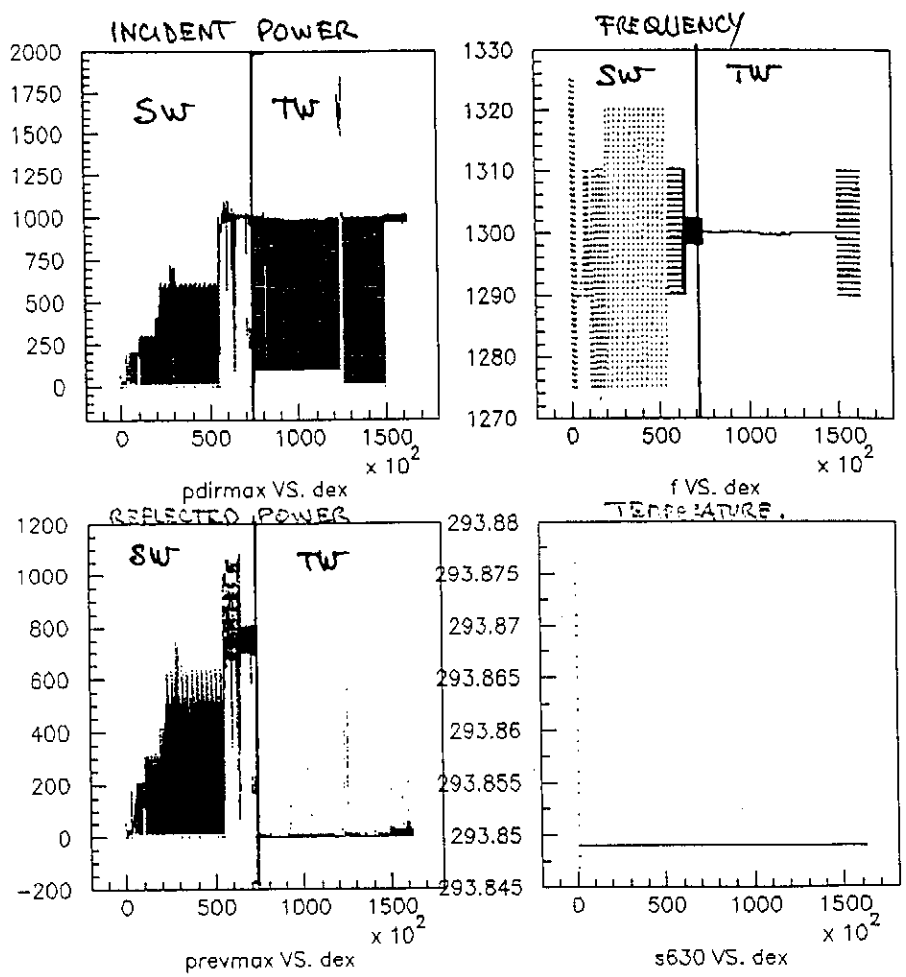

λ/2 window with polarized transition.

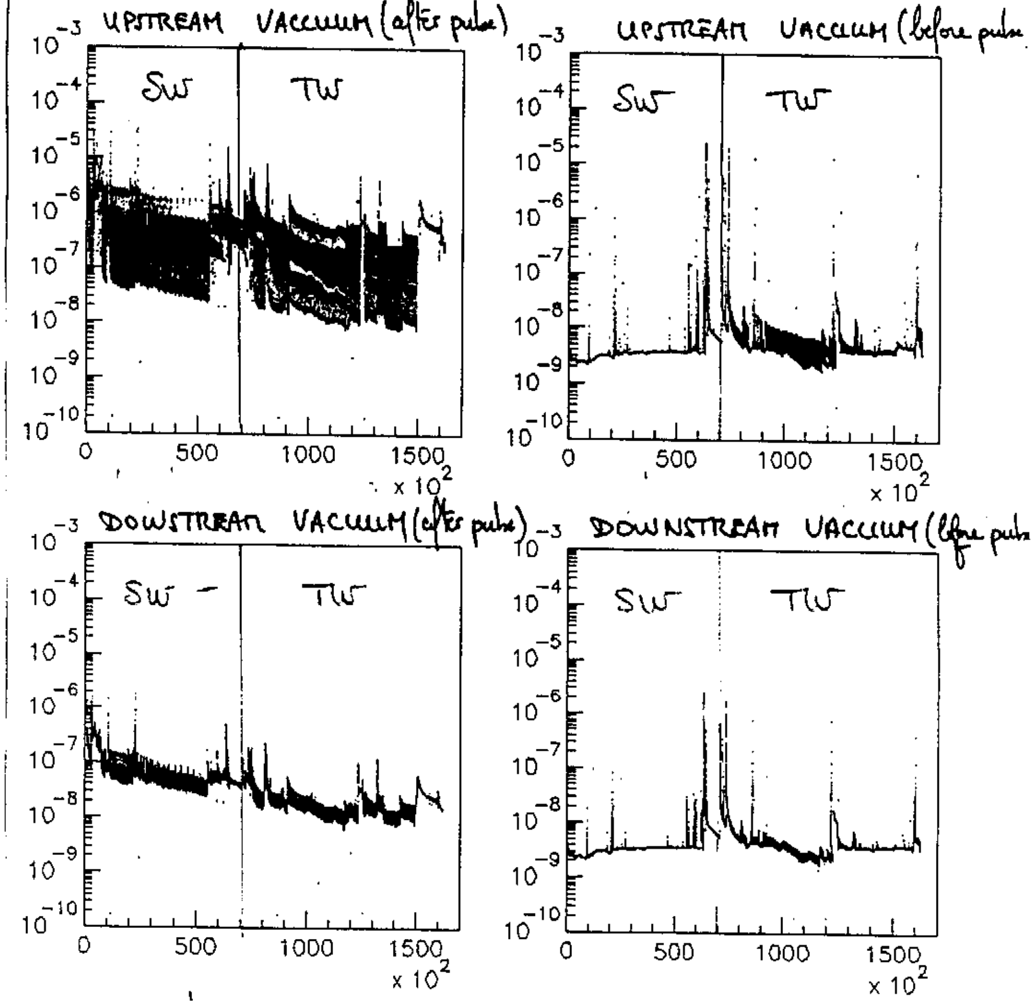

POLARIZED DOORKNOB TRANSITION

- Designed and built at LAL.
- tested in december 98 : 160,000 pulses.

2 problems :
- strong arcing in RF choke
- large RF leak through DC connector (> 1 kW)

However, one can still try to analyze the effect of polarisation on the downstream side of the window.

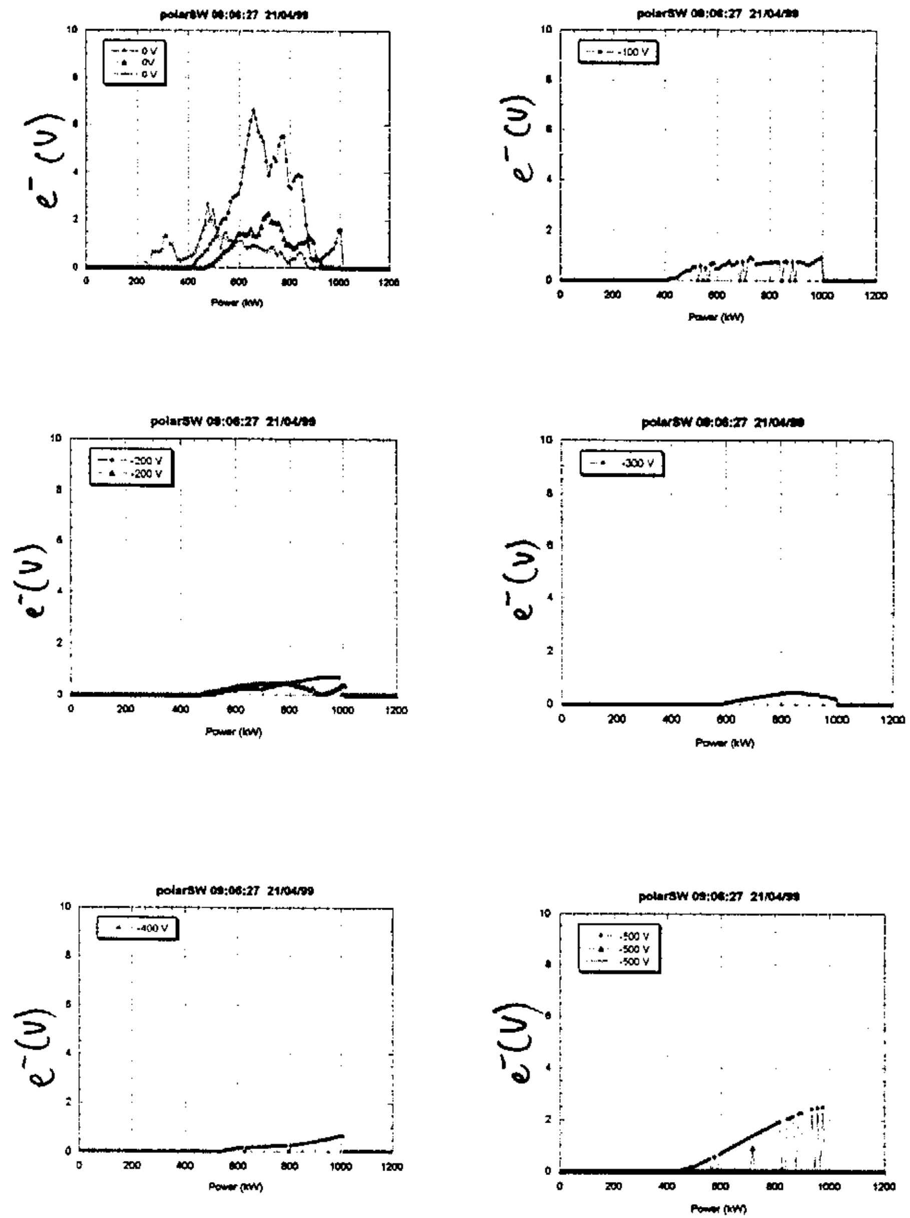

Standing wave.

28

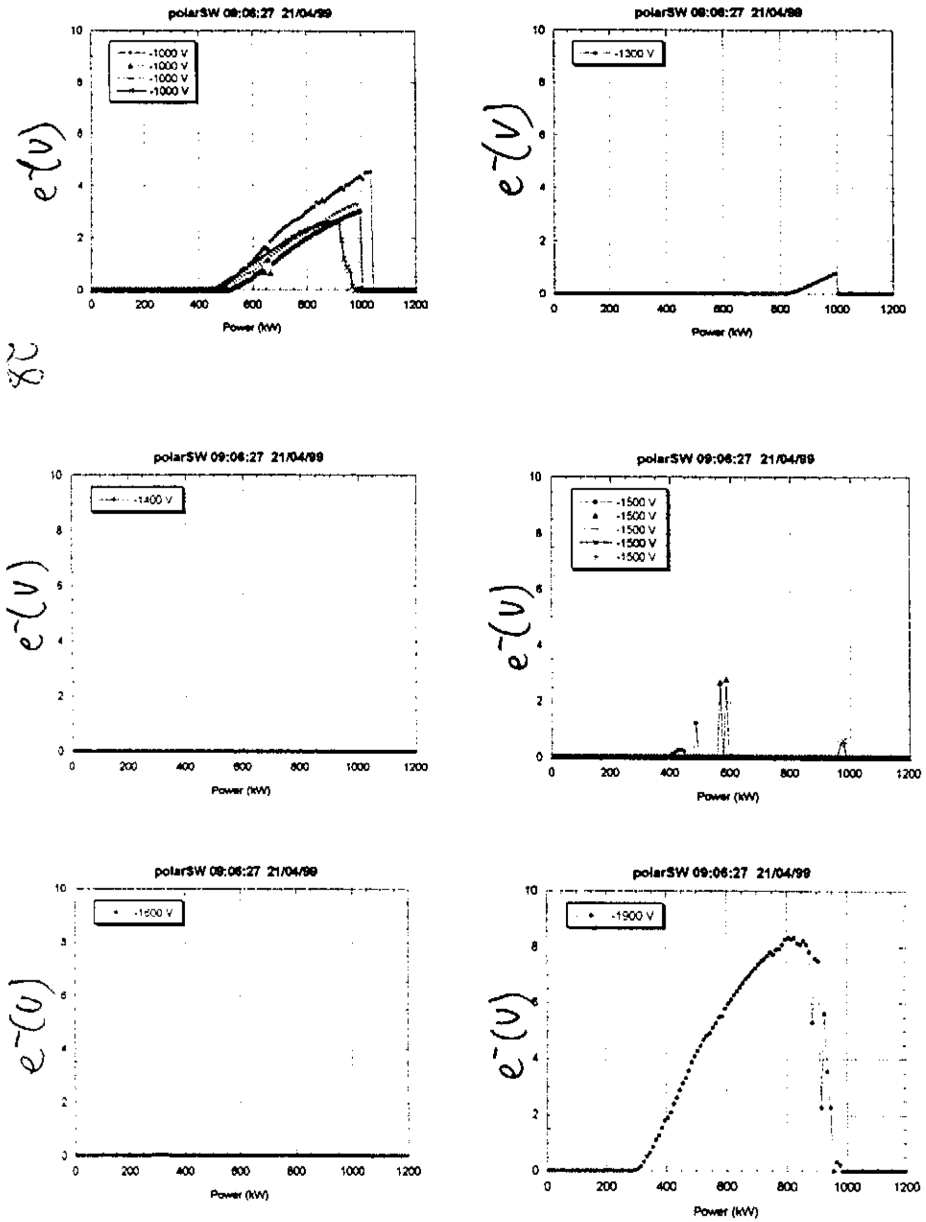

Standing wave

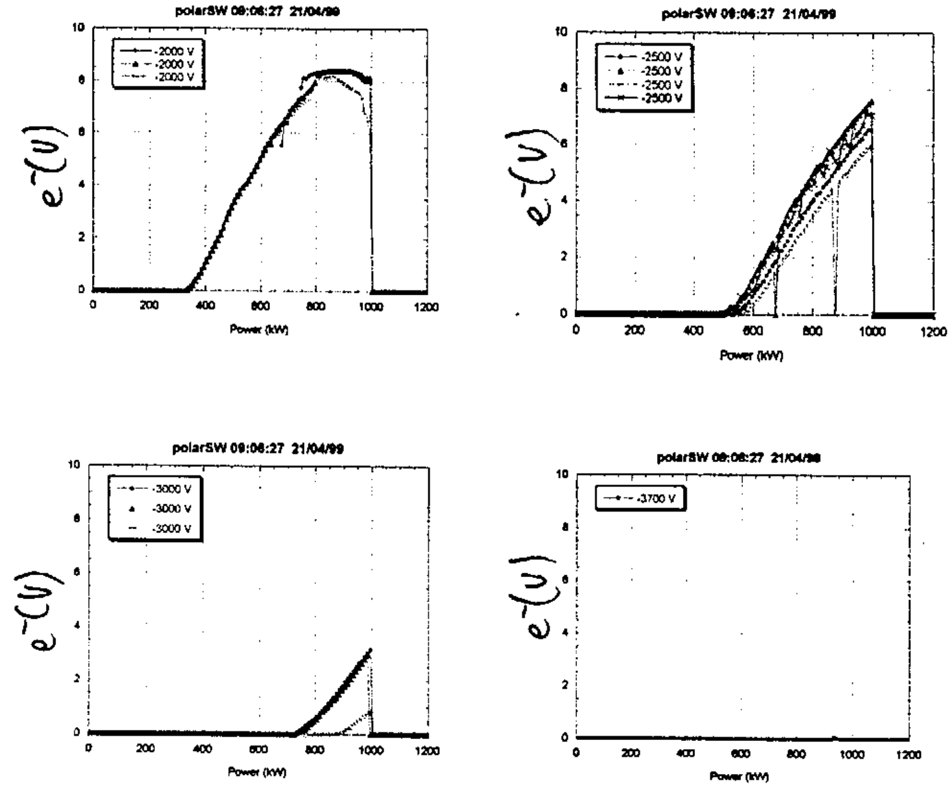

Standing wave

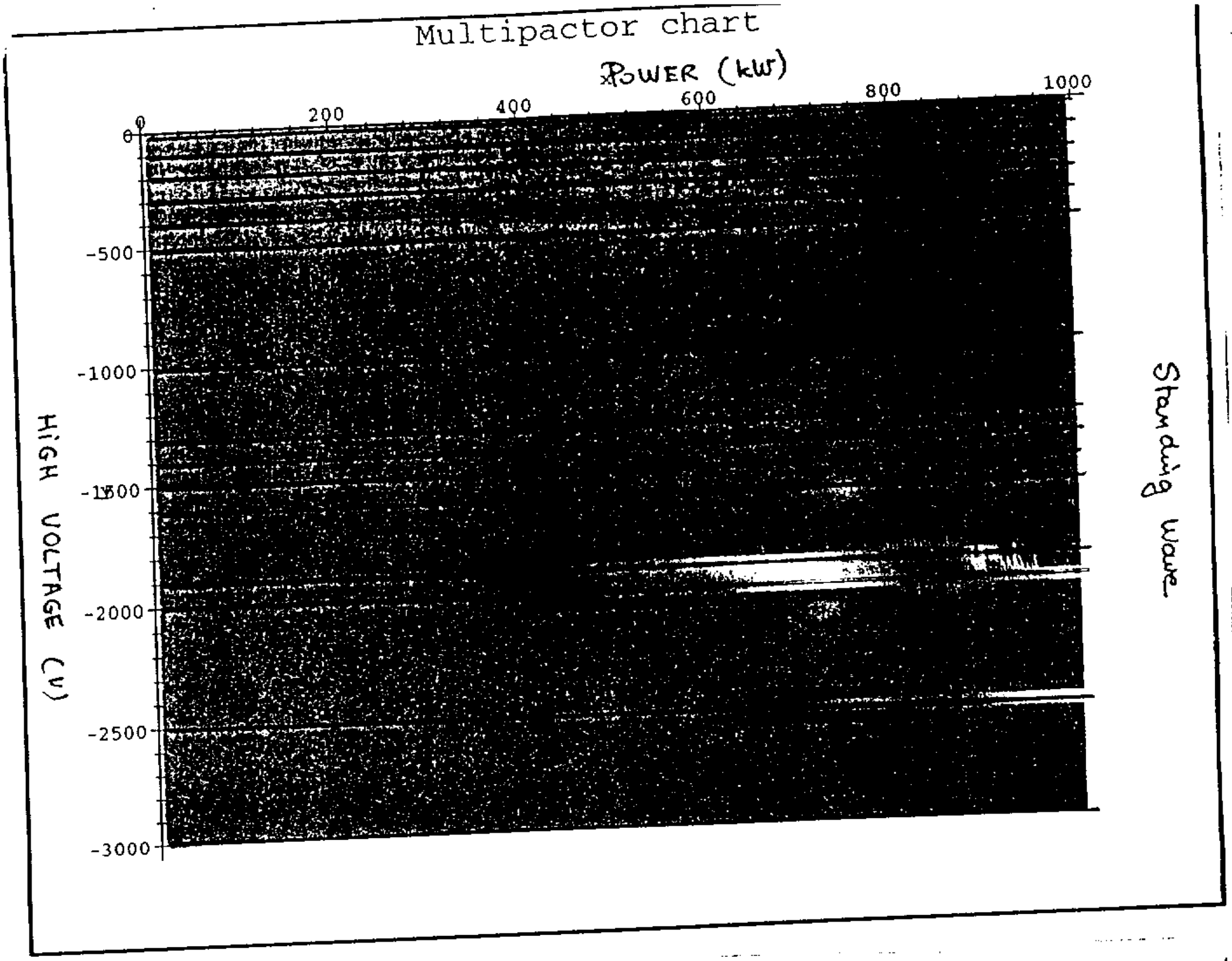
Multipactor chart
POWER (kW)
0
200
400
600
800
1000
0
-500
-1000
-1500
-2000
-2500
-3000
HIGH VOLTAGE (V)
Standing wave

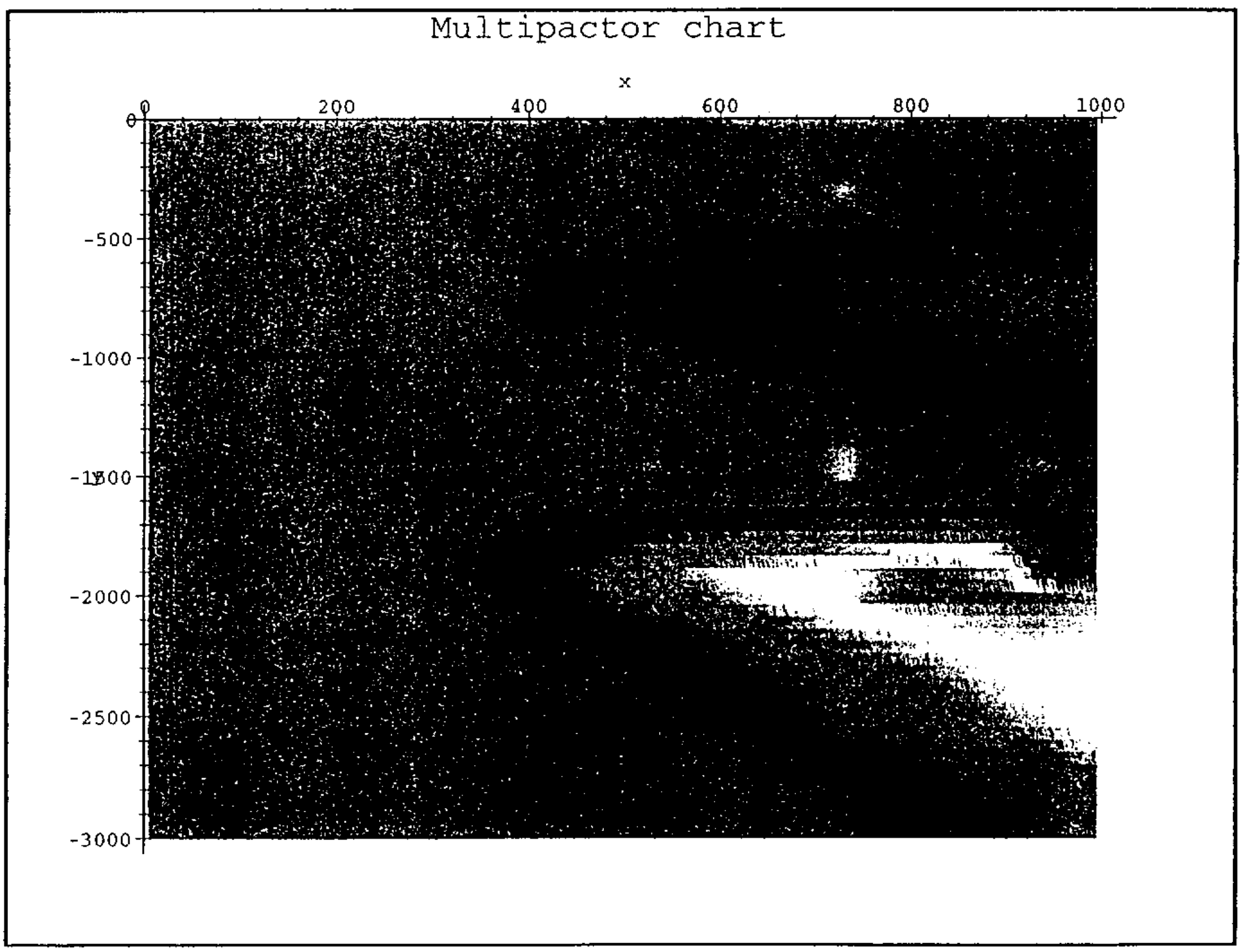
Multipactor chart
x
0
200
400
600
800
1000
0
-500
-1000
-1500
-2000
-2500
-3000

STANDING WAVE

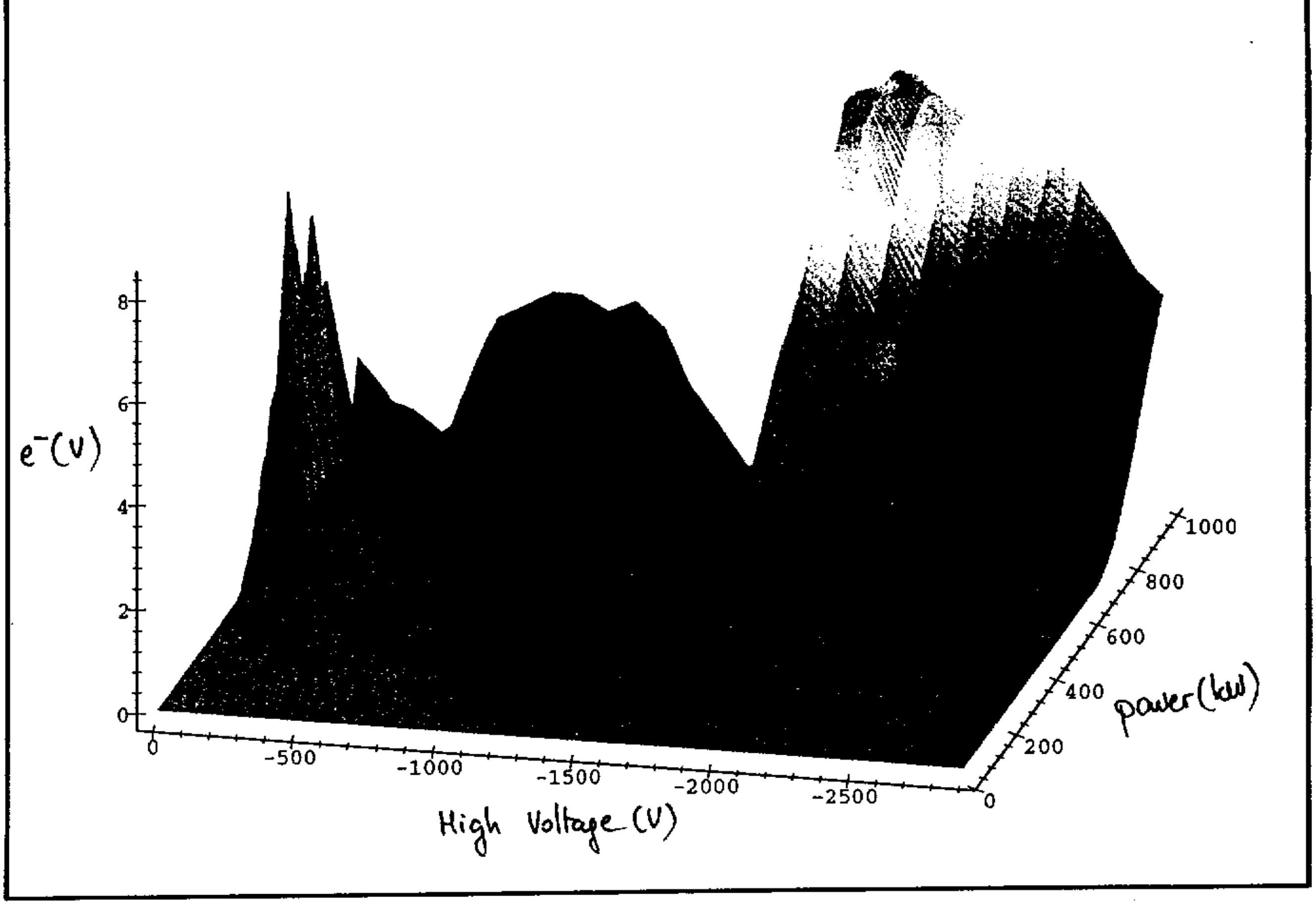

COMPARISON WITH CALCULATIONS.

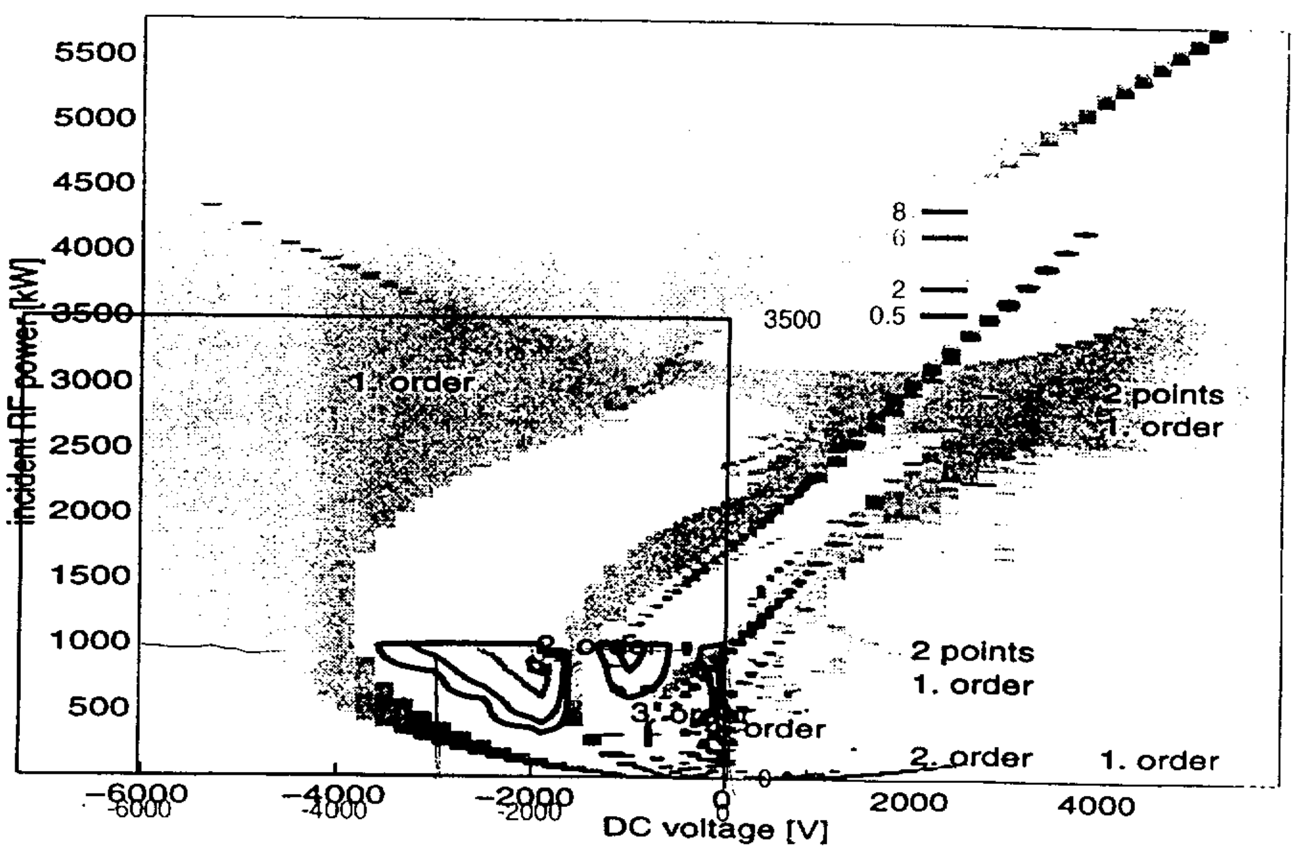

31

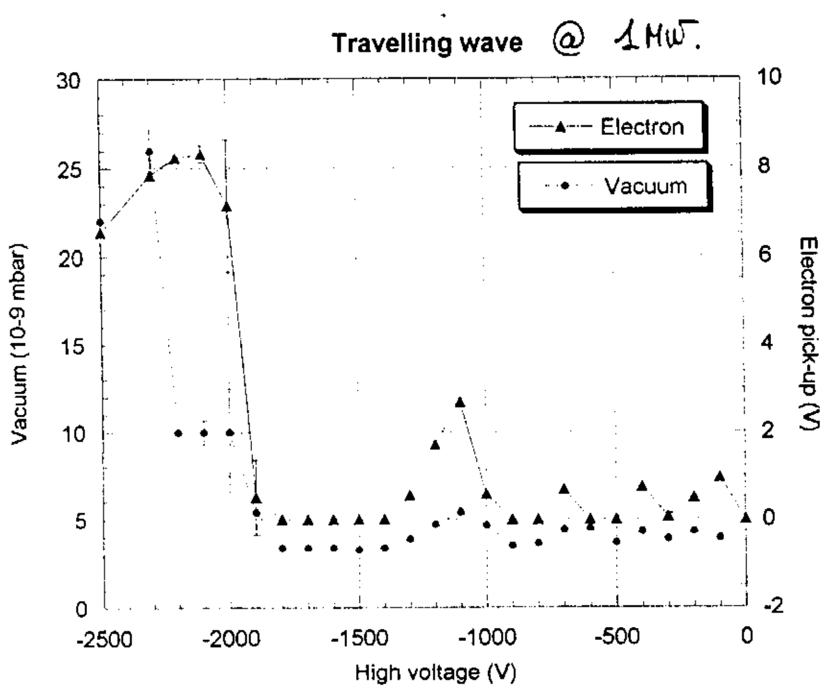
Travelling wave @ 1MW.
Electron
Vacuum
Vacuum (10-9 mbar)
Electron pick-up (V)
High voltage (V)
30
25
20
15
10
5
0
10
8
6
4
2
0
-2
-2500
-2000
-1500
-1000
-500
0

S. Chel

Processing of the Test Line #2

32

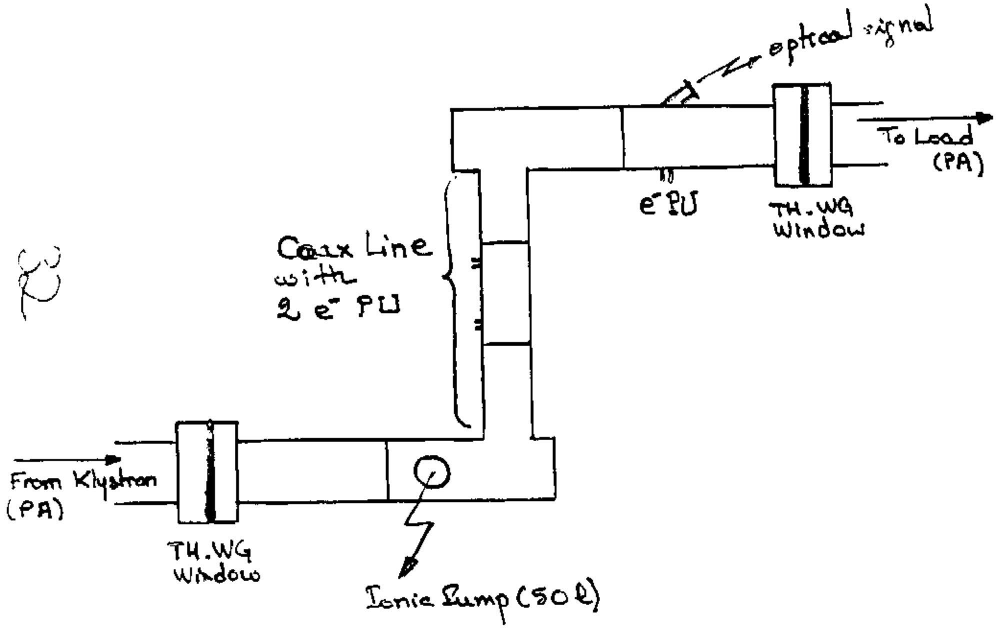

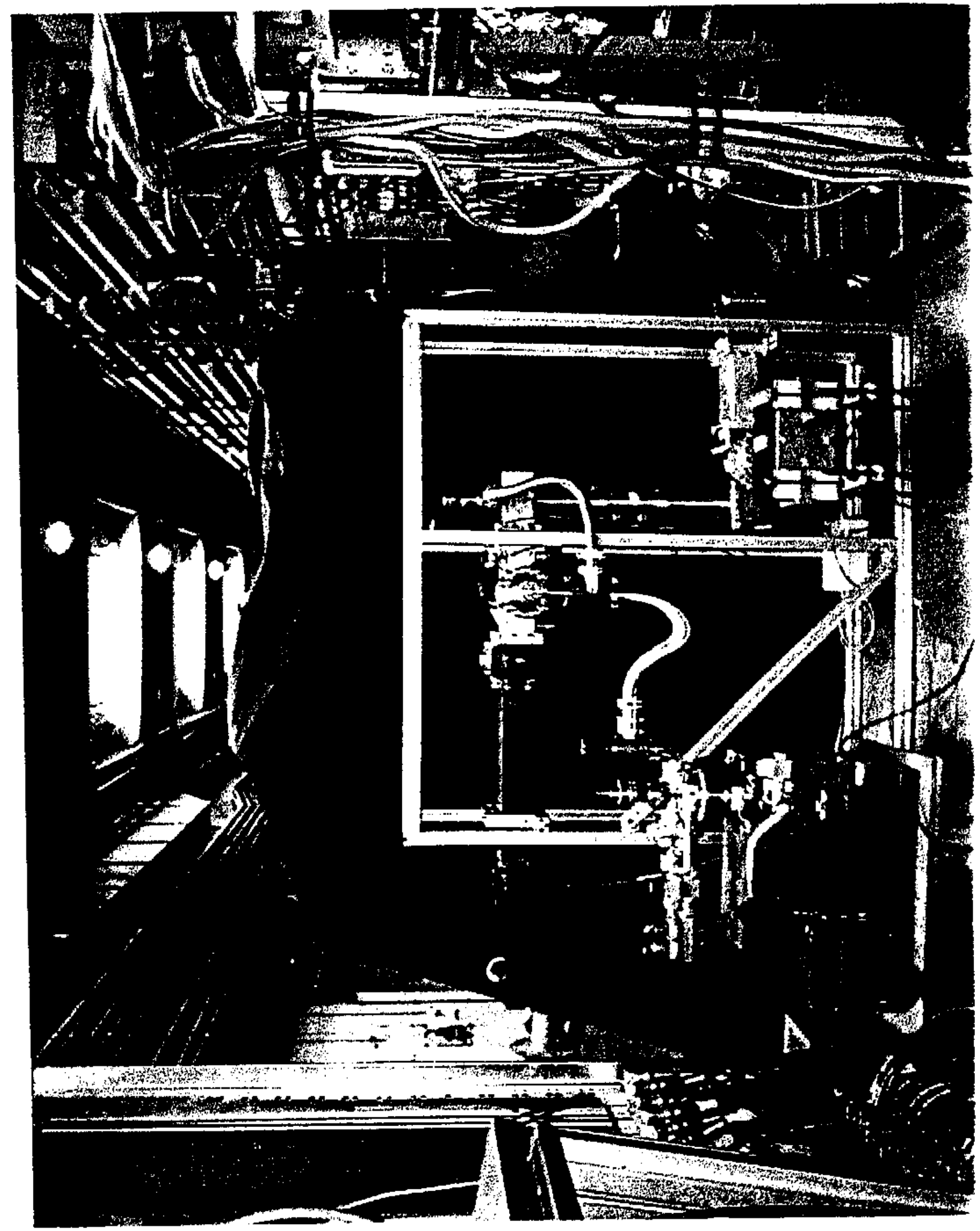

- All the pieces, except TH WG Windows, are in Stainless Steel (without Cu coating).
- Cleaning of the SS parts with alcohol.
- In gaskets for WG, CF for coax line.
- After assembly:
  - * Bake out of the coax line, the WG→coax transitions and some WG parts
    @ 320° C – 48 hrs
  - * Heating of WG Windows (main effect on the vacuum).
    @ 65° C – 48 hrs

(A) : RF power off during 5hrs.

but still pumping.

Vacuum very stable : 2-3 10^{-9}

With RF power, same behavior than after processing.

→ no deconditioning.

(B) : Calibrated leaks (ambiant air).

$P = 6.10^{-8}$, $P = 2.10^{-7}$ } $\Delta P_{th} = 10^{-8}$; $P = 1.10^{-6}$, $P = 3.10^{-6}$ } $\Delta P_{th} = 10^{-7}$

* the multipactor barriers (coax line) are larger
* Ve^- coax ≃ 99 V
* After less than 5 pulses / Power level : $\Delta P < 5 10^{-8}$ @ $P = 3 10^{-6}$ and Ve^- ↘

→ with 5 power rampings, the initial state is recovered, even with a pressure of $3 10^{-6}$ mbar

Test parameters :

- Room T°
- TW
- $f = 1300$ MHz
- $\tau_{RF} = 800\ \mu s$; $f_{rep} = 0{,}1$ Hz
- P_{RF} : Ramping from 100kW up to 1.2 MW
  → controled with vacuum ($\Delta P_{threshold} = 10^{-7}$ or 10^{-8})

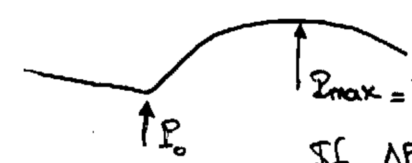

If $\Delta P > \Delta P_{th}$ → same RF power
If $\Delta P < \Delta P_{th}$ → RF power + 10kW

Initial RF processing :

* Initial Vacuum : 3.10^{-8} mbar
* Very strong vacuum bursts at the beginning : $\Delta P > 10^{-5}$ mbar → interlock
* After 180.000 pulses (~ 3weeks) : Vacuum = $2 10^{-9}$

- P_{RF} = 550 to 400 kW : - Ve^- in coax ~ 100mV
  - $\Delta P \leq 5 10^{-9}$ ($\Delta P_{th} = 10^{-8}$)
  - No light signals
  - No e^- detected close to the Window
- P_{RF} > 1.0 MW : - Some events detected probably localized near the window or transition
  - light signals ; no e^-
  - $\Delta P \leq 2\ 10^{-9}$
- All the other power levels are free of signals.

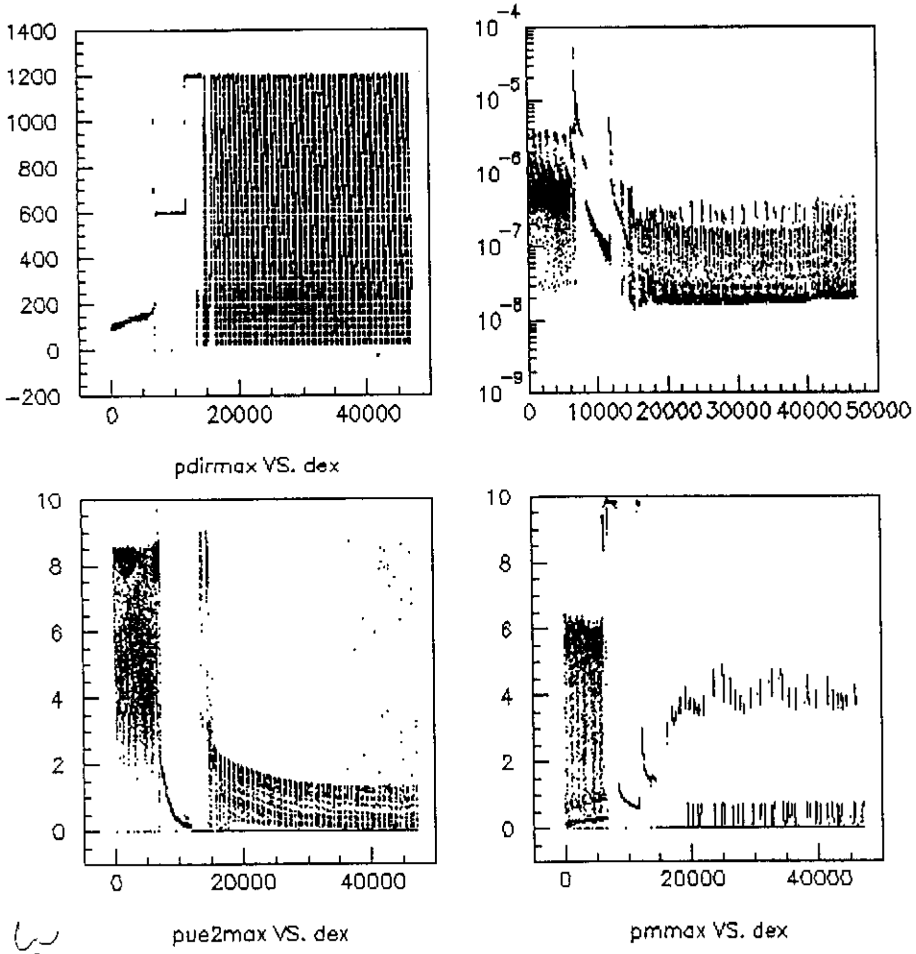

34

(C) 1 atm. during 2 hrs.

- Pumping down (1 night) : Vacuum = 10^{-6} mbar
- Very strong deconditioning :
  * same multipactor levels [200-400 kW] but very large
  * $V\bar{e}_{coax} \gtrsim 10V$ ⟹ interlock
  * $\Delta P_{max} \sim 3\ 10^{-6}$ mbar
- After 2.5 days of processing (~20 000 pulses) :
  * Vacuum = 10^{-7} mbar
  * Possible to make a complete ramping with $\Delta P_{th} = 10^{-7}$ mbar
- Last pulses observed :
  * $P = 10^{-7}$
  * $\Delta P \leq 5\ 10^{-8}$ in the range 360-410 kW
  * $V\bar{e}$ coax $\lesssim$ 200 mV
  * Rare pulses with light signals.

⟹ it is possible to recover an acceptable ~~the~~ behavior in some days with $\Delta P_{th} = 10^{-7}$.

But how long does it take to recover a full processed state with $\Delta P_{th} = 10^{-8}$?

Reports About Conditioning Experience With the Latest Module 3 Couplers

Input Coupler Workshop
DESY, 26. - 27. 04. 99

Wolf - Dietrich Möller,
DESY, Hamburg

1. Design of TTF DESY coupler 2 for module 3
2. Testresults
3. Some selected problems:
   - Kapton foil
   - WG windows
   - Qext tuning
4. Processing procedure
5. Vacuum behaviour

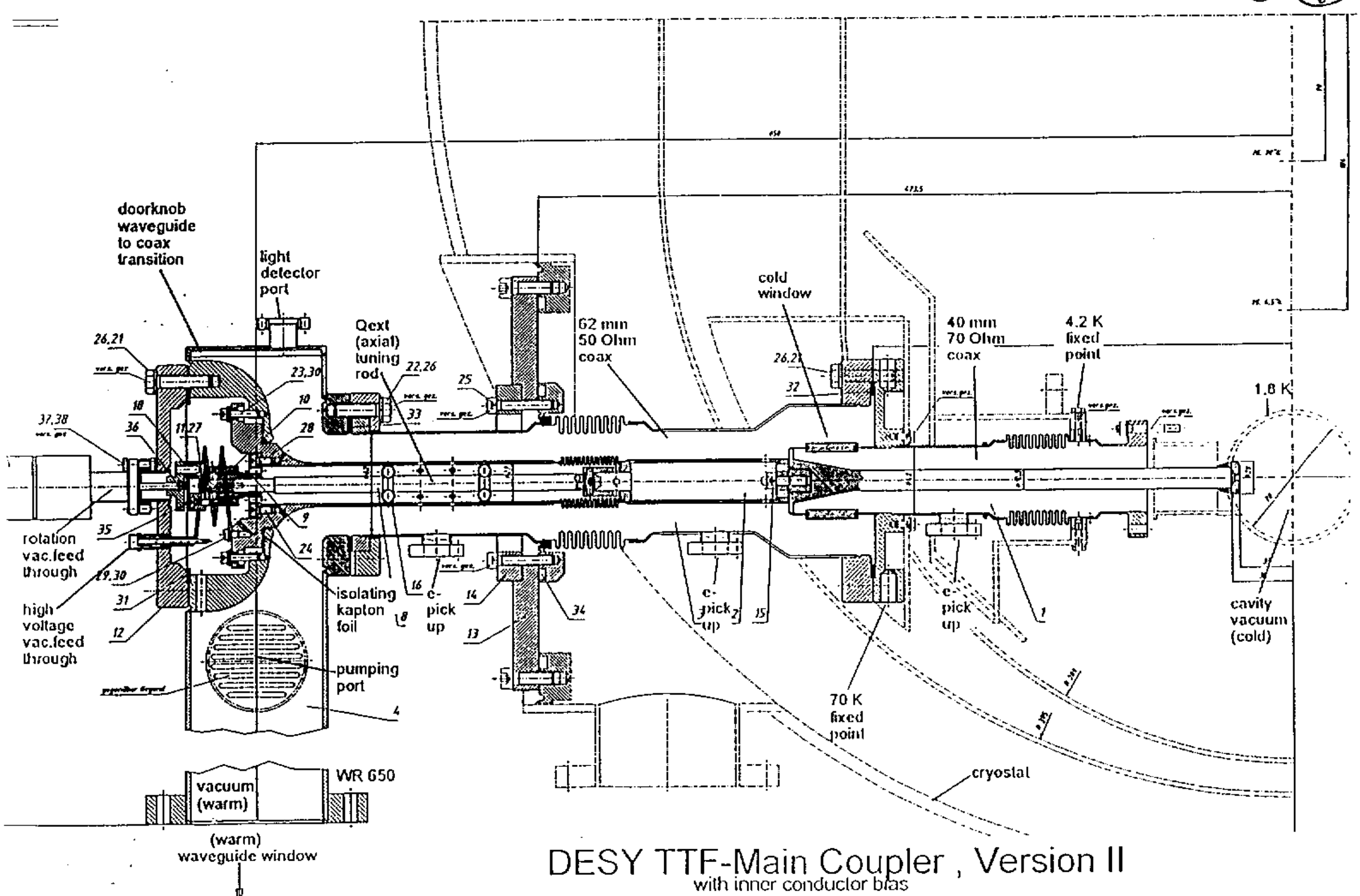

DESY TTF-Main Coupler , Version II
with inner conductor bias

35

Coupler Tests

coupler	*DE03 DE04*	*AC01 AC02*	*DE02 DE01*	*AC05 DE05*	*AC03 AC04*
WG window	Phillips	Desy	Desy	Desy	Desy
Ti	no	no	no	no	yes
window heating	no	no	300C	300C	300C
teststand heating	no	200C	200C	200C ← same warm parts	200C
500 μs	800 kW *	900 kW *	1MW	1MW	1MW
1.3 ms	250kW	250kW	250kW	250kW	250kW
processing time	23 d	16 d	5 d	2.5 d	3 d

* limited by e-, light and vacuum

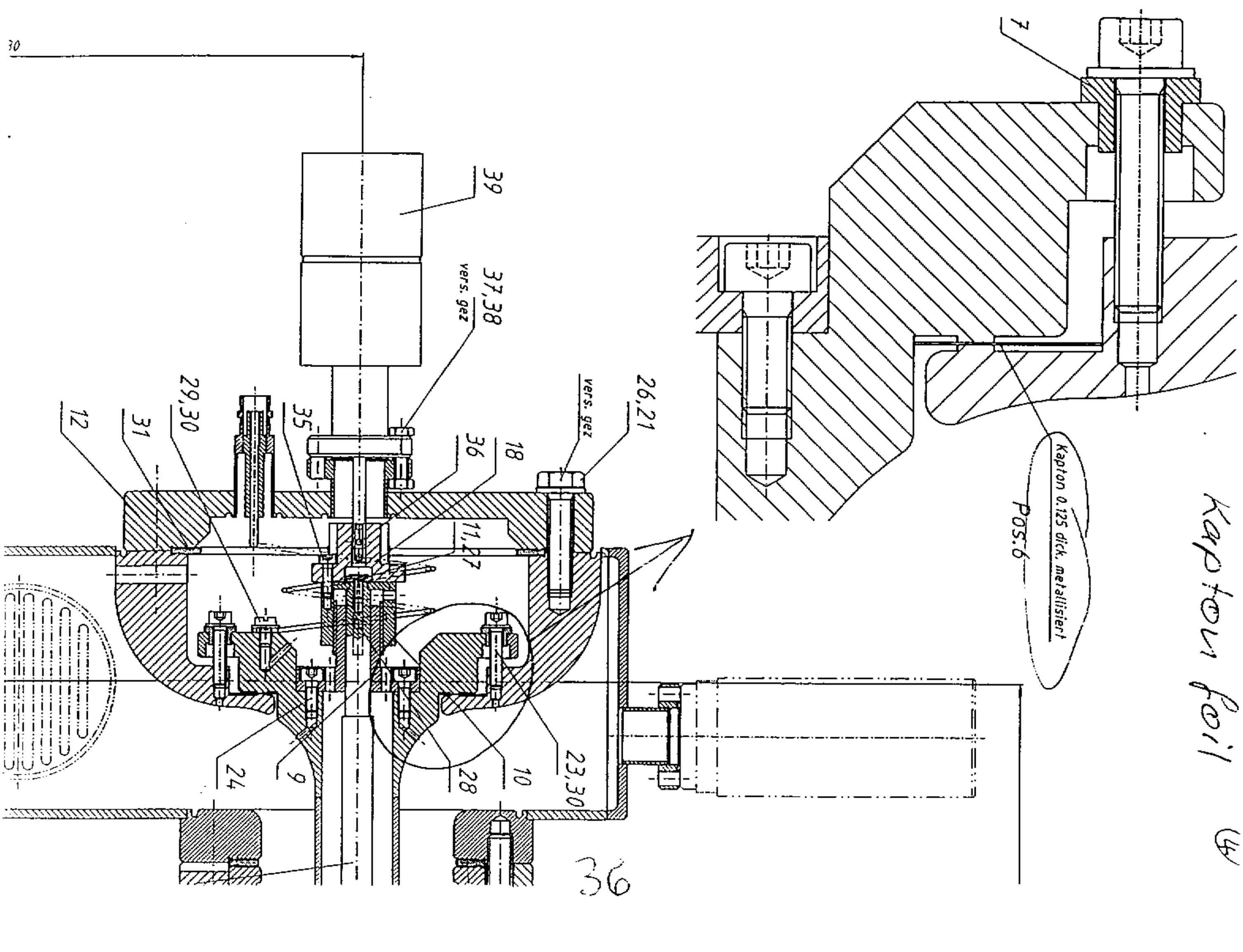

(5)

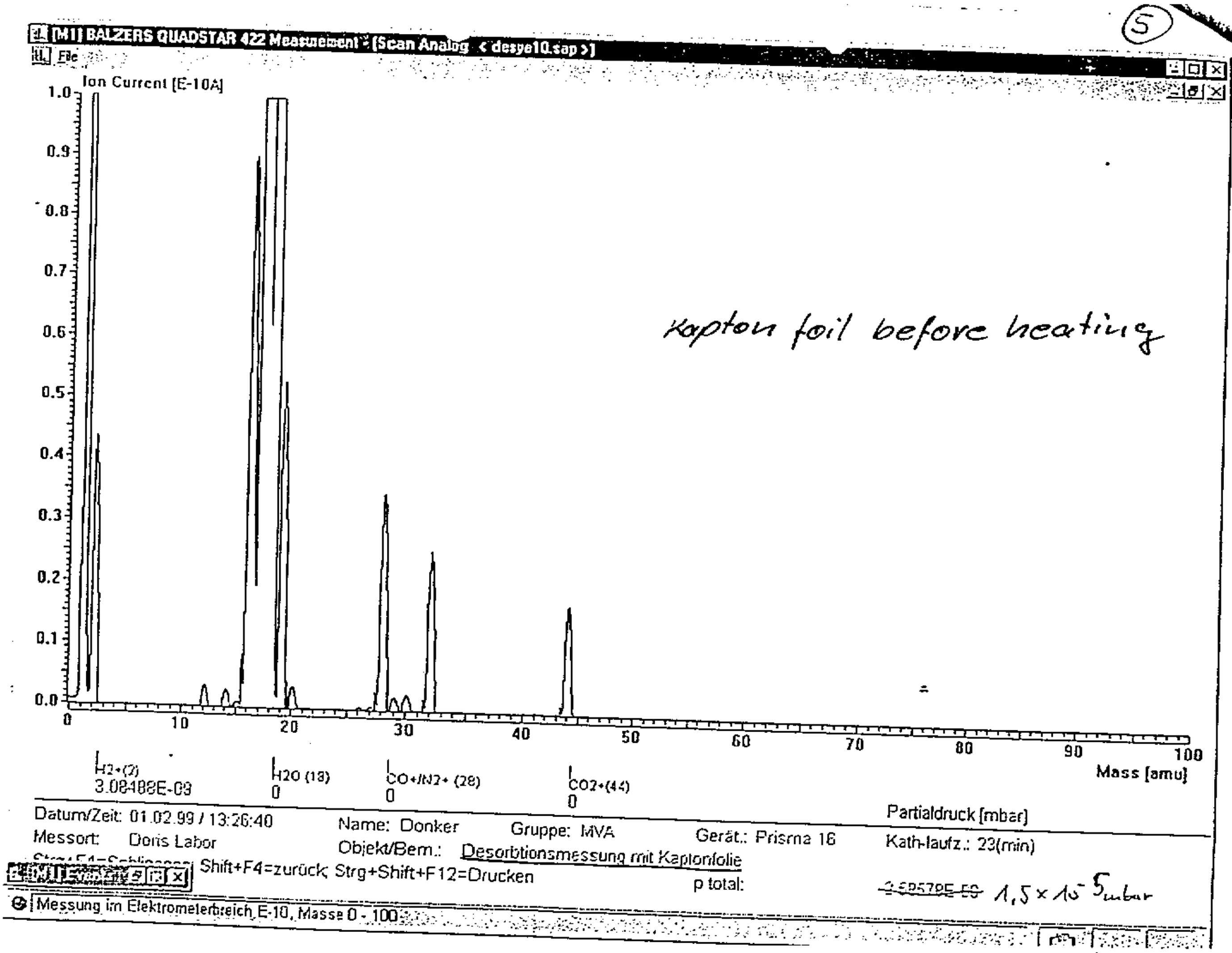
[M1] BALZERS QUADSTAR 422 Measurement - [Scan Analog < desye10.sap >]
File
Ion Current [E-10A]
Kapton foil before heating
Mass [amu]
H2+(2)
3.08488E-09
H2O (18)
0
CO+/N2+ (28)
0
CO2+(44)
0
Partialdruck [mbar]
Datum/Zeit: 01.02.99 / 13:26:40
Name: Donker
Gruppe: MVA
Gerät.: Prisma 16
Kath-laufz.: 23(min)
Messort: Doris Labor
Objekt/Bem.: Desorbtionsmessung mit Kaptonfolie
Shift+F4=zurück; Strg+Shift+F12=Drucken
p total:
~~3.58579E-09~~ 1,5 × 10⁻⁵ mbar
Messung im Elektrometerbreich E-10, Masse 0 - 100

(6)

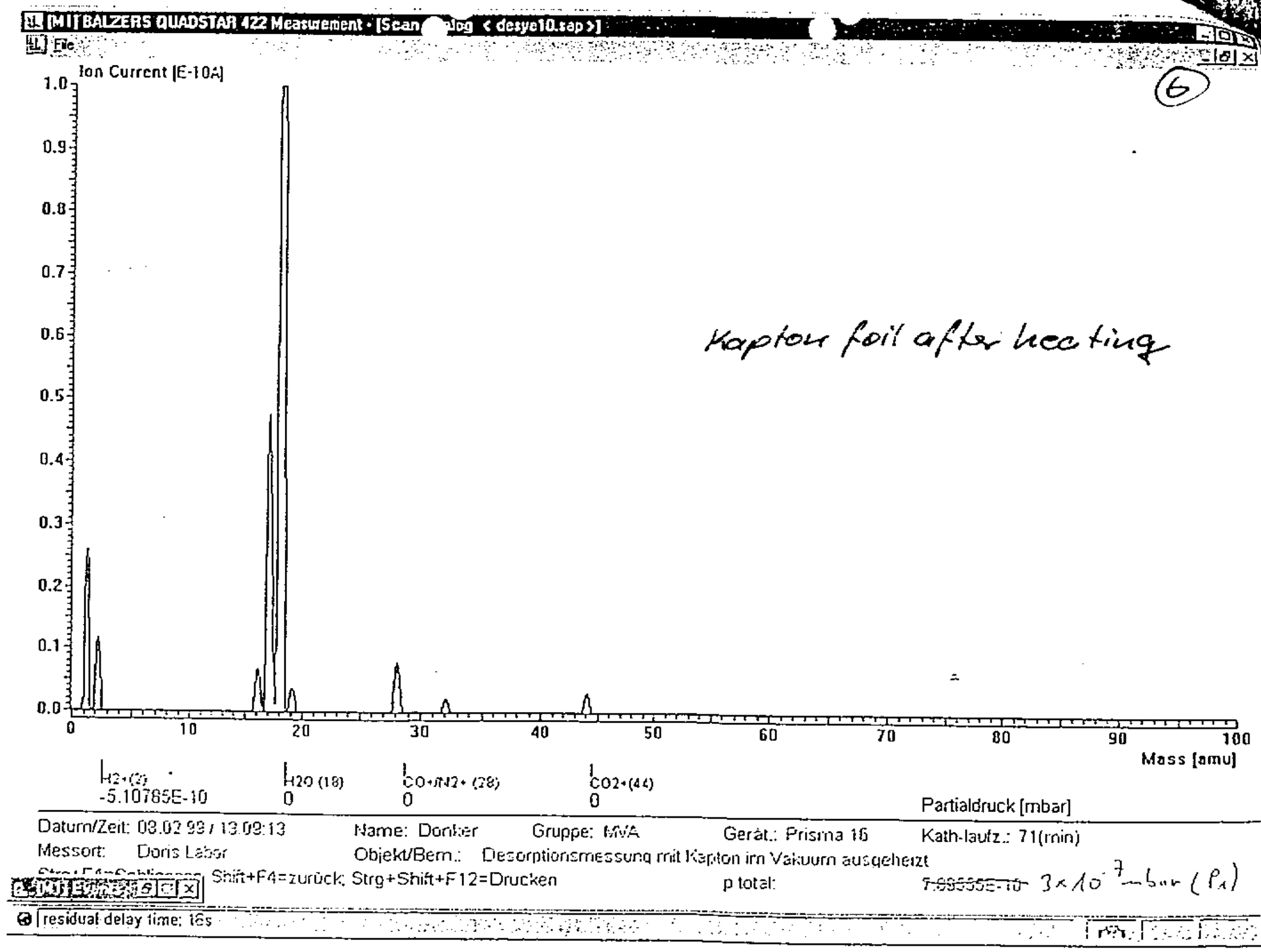
[M1] BALZERS QUADSTAR 422 Measurement - [Scan Analog < desye10.sap >]
File
Ion Current [E-10A]
Kapton foil after heating
Mass [amu]
H2+(2)
-5.10785E-10
H2O (18)
0
CO+/N2+ (28)
0
CO2+(44)
0
Partialdruck [mbar]
Datum/Zeit: 08.02.99 / 13:09:13
Name: Donker
Gruppe: MVA
Gerät.: Prisma 16
Kath-laufz.: 71(min)
Messort: Doris Labor
Objekt/Bem.: Desorptionsmessung mit Kapton im Vakuum ausgeheizt
Shift+F4=zurück; Strg+Shift+F12=Drucken
p total:
~~7.99555E-10~~ 3 × 10⁻⁷ mbar (P₁)
residual delay time: 18s

(7)

7. Fazit der Desorptionsmessung

Zeit (h)	Desorptionsrate des Rezipienten EDELSTAHL SS (mbar*l/cm²*s)	Desorptionsrate der Probe KAPTON (mbar*l/cm²*s)	Desorptionsrate der Probe nach Stickstoffausheizung after heating with N_2 (mbar*l/cm²*s)	Desorptionsrate der Probe nach Vakuumausheizung after heating in vacuum (mbar*l/cm²*s)	Desorptionsrate der Probe nach Vakuum-Ausgeheizung u. 10-Tägiger Lagerung im Exicator (mbar*l/cm²*s)
2	1,4 E-09	1,8 E-06	1,0 E-07	**1,8 E-08**	2,0 E-07
20	1,6 E-10	5,2 E-08	2,0 E-09	**5,5 E-11**	5,0 E-09
100	5,7 E-11	2,0 E-08	1,0 E-10	**5,2 E-11**	1,6 E-10

after 10d in an exicator

38

Die Desorptionsmessung der „Kapton-Folie" zeigt, das die besten Werte durch die vorherige Ausheizung unter Vakuum erreicht werden.

Da Kapton die Neigung zur Wasserbindung hat, ist es besser, die „Kapton-Folie" gleich nach der Vakuumausheizung in das UHV-System einzubauen, und nicht erst im Exicator zwischenzulagern.

Ist es dennoch erforderlich „Kapton - Folien" über einen längeren Zeitraum zu lagern, so ist empfehlenswert die Kaptondichtungen in eine metallbedampfte Folie, unter Vakuum, einzuschweißen.
Eine metallbedampfte Folie ist weitgehend wasserundurchlässig, spült man vor dem Vakuumeinschweißen der Kaptondichtungen die Folie mit Stickstoff N_2, so verbleibt im Restgas so gut wie kein Wasser H_2O, das sich in die Kaptondichtungen einlagern könnte.

- main outgassing is water
- best is to assemble direct after vacuum heating
- 2nd best: store after heating in metal foil
- 3rd best: store after heating in exicator

(8)

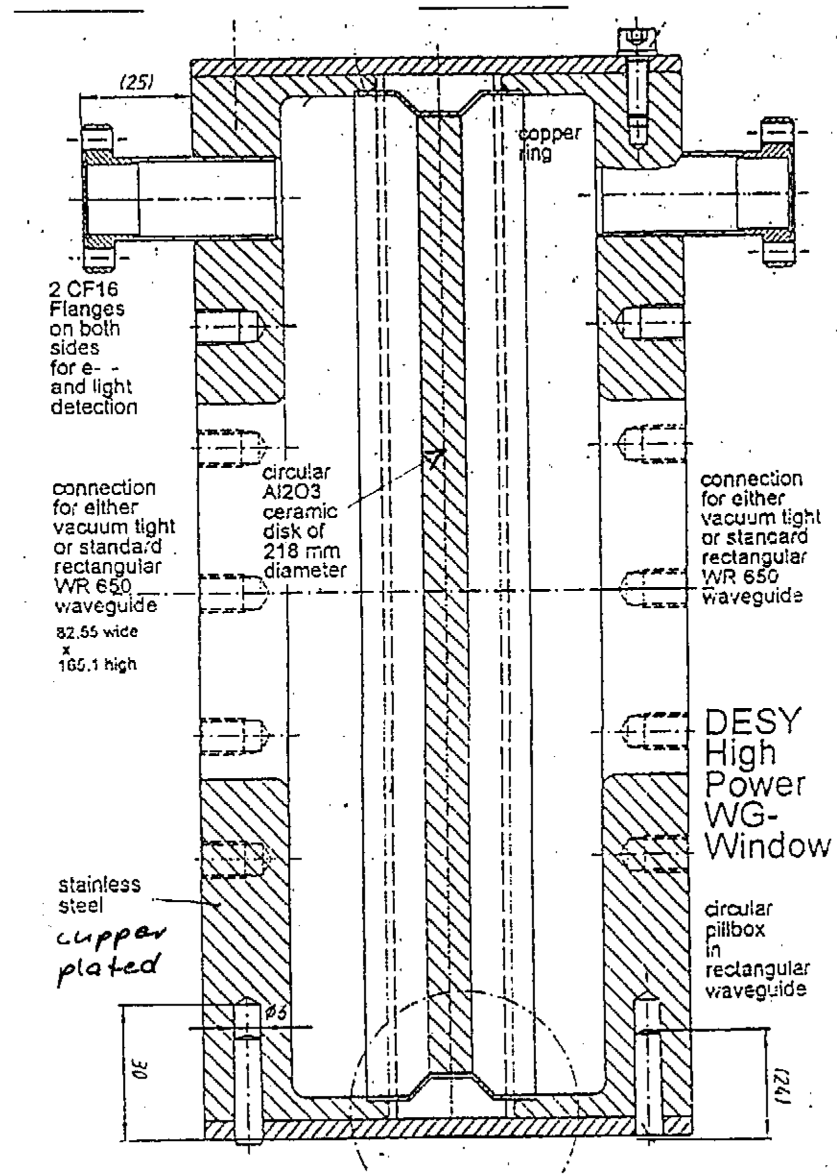

Desy wave guide window

Desy wave guide windows

20 windows were brazed / 15 windows are leaktight:
-dark ceramic discolouration
-blisters in copper plating

14 windows:-sandblasted
-sealing surface polished
-washed & us cleaned

3 tests on teststand & on cavity (horizontal cryostat)
-strong light
-in one case bad vacuum even after heating at 200C (10e-7 mbar)
-ceramic showed some discolouration after test, no temperature increase

12 windows heated in vacuum furnace (showed strong outgassing)
on all 12 windows the ceramic was then Ti coated (evaporation)

tests with Ti:-two windows connected with a straight wave guide
-we could not reach the 1 MW at 20μs pulses, vacuum is the limitation
-visual inspection: no hint
-next 2 windows tested on coupler teststand showed much better vacuum behaviour but still strong light & e-

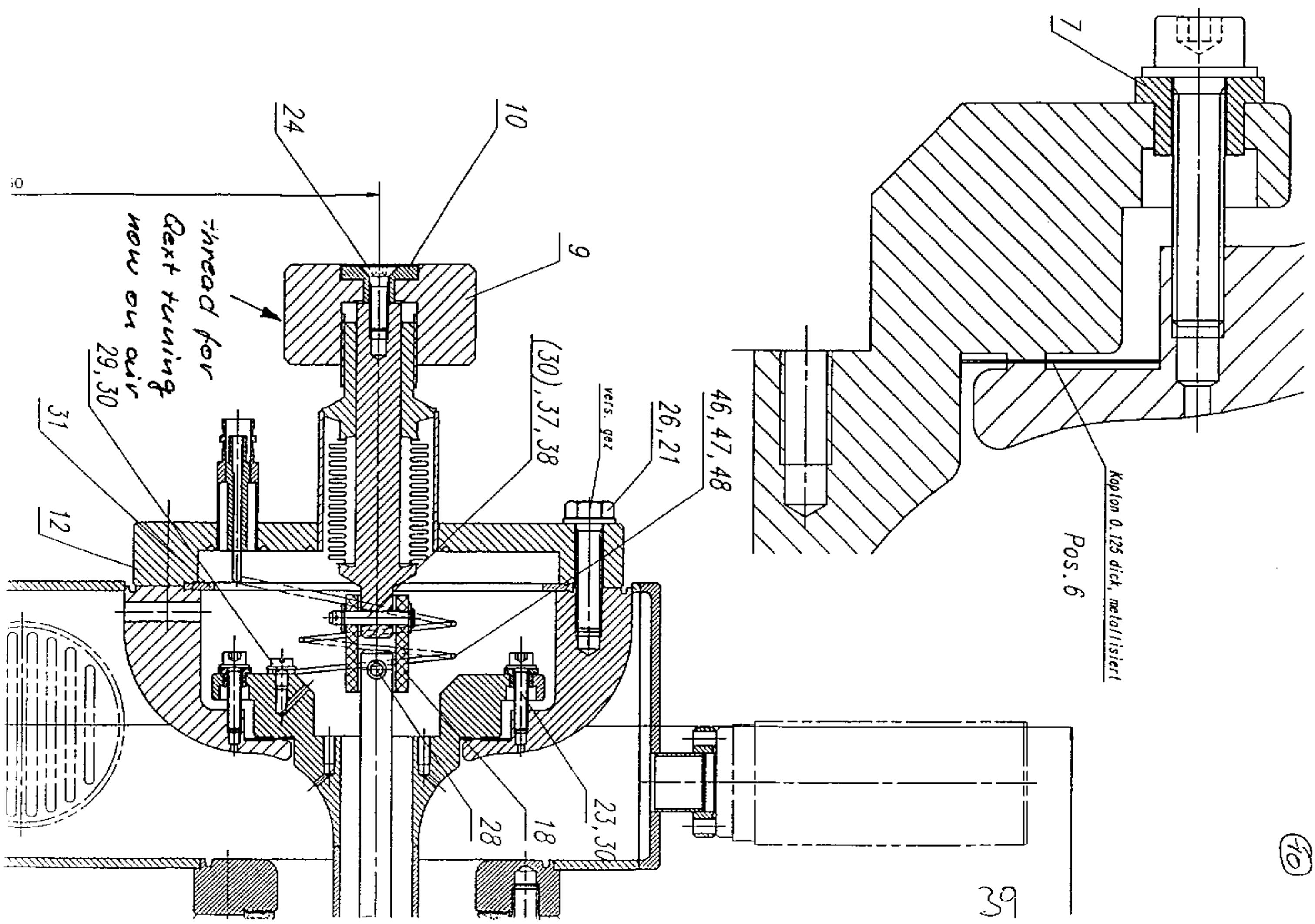

N2 heating

goal and idea:

Heating of the coupler in situ on the test stand under a Nitrogen atmosphere.
Reduce the adsorbed gases on the surface and replace them with Nitrogen.
Nitrogen is easer to desorb ⇒ faster RF processing.

Test:

The teststand was heated at a temperature of 200C.
3 times pumped and purged with N2 at that temperature.
Cooled down under vacuum to RT.

Results:

No significant changes in the RF behaviour.
The Cu surfaces were discolourated after the test.

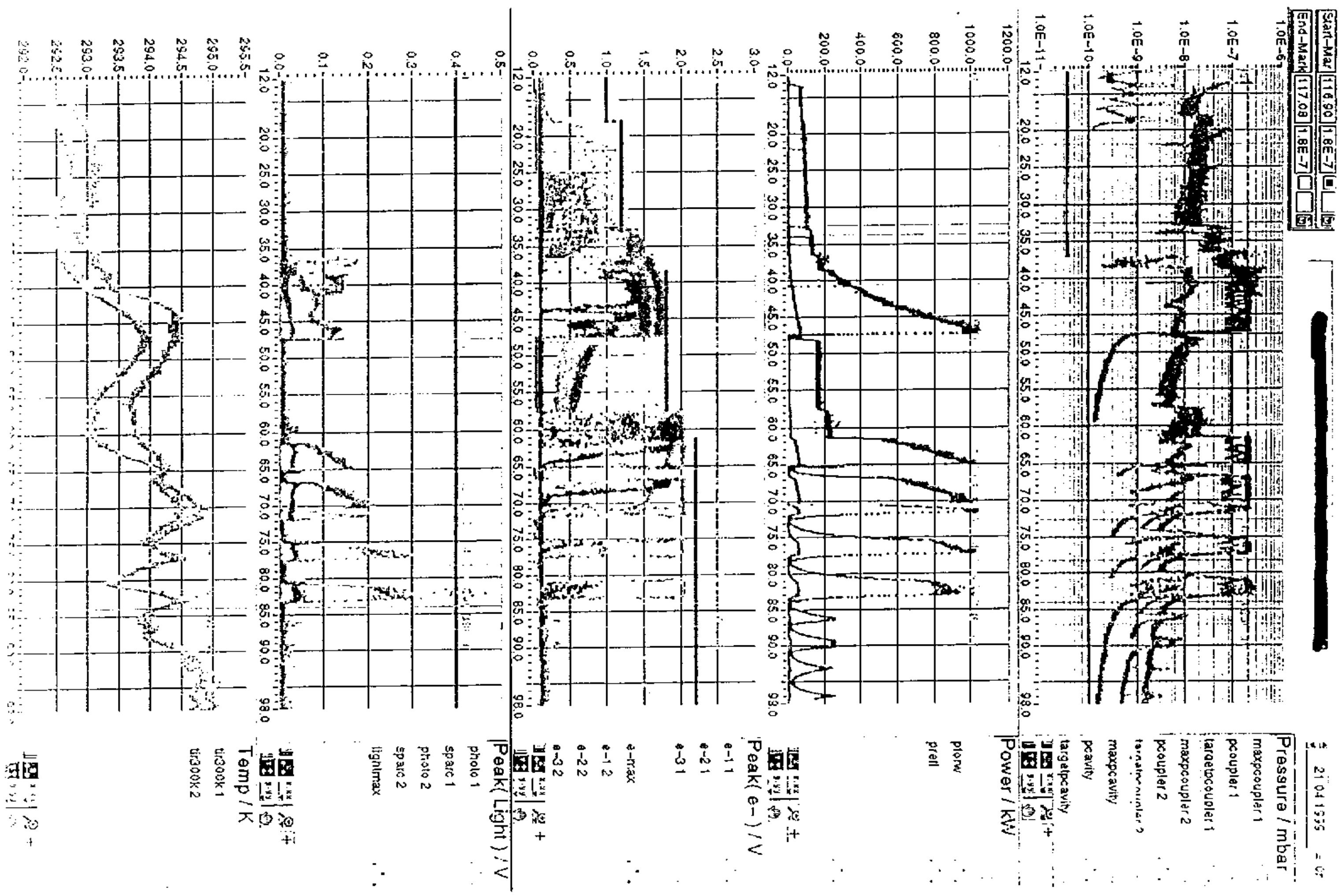

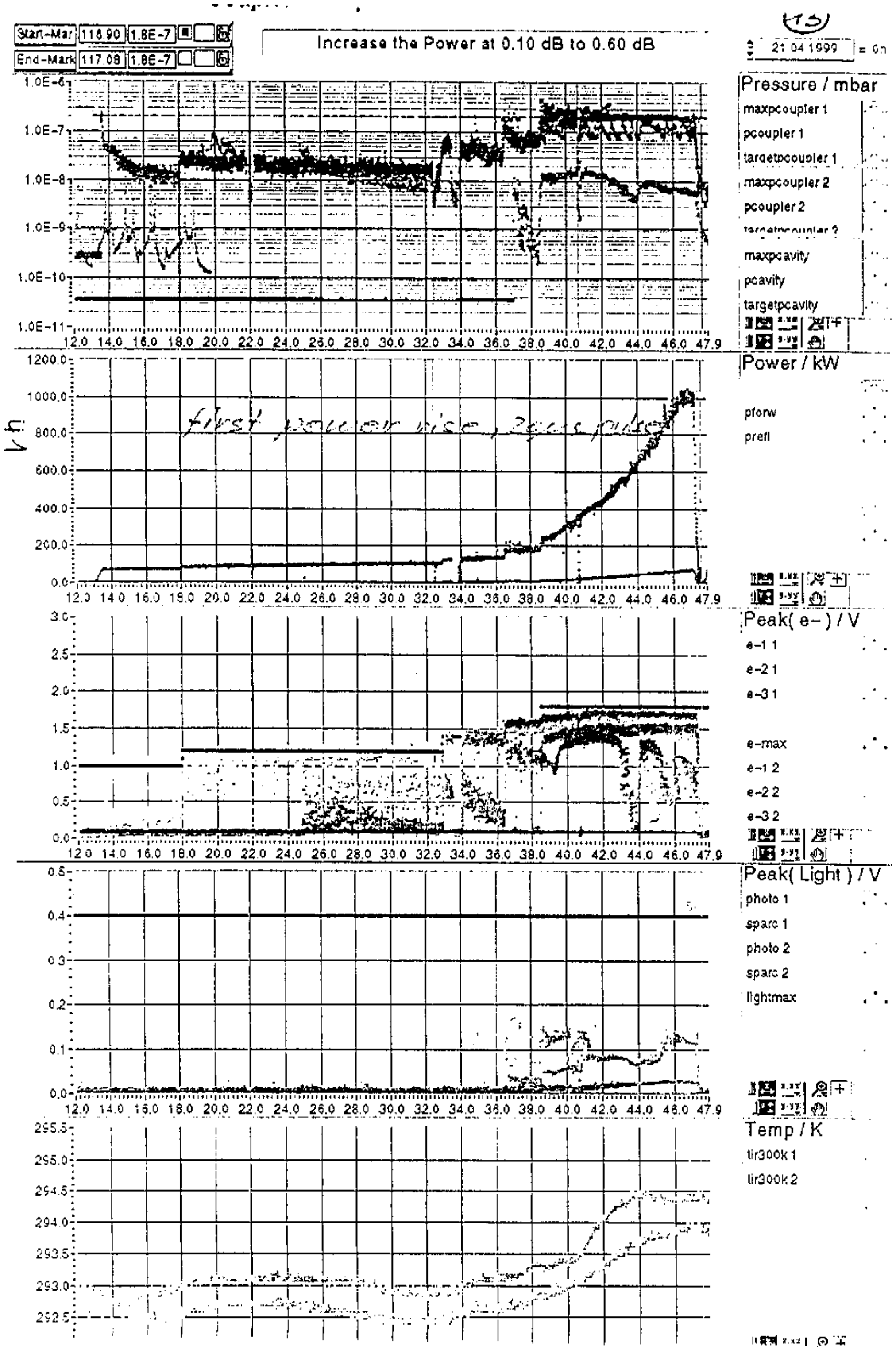

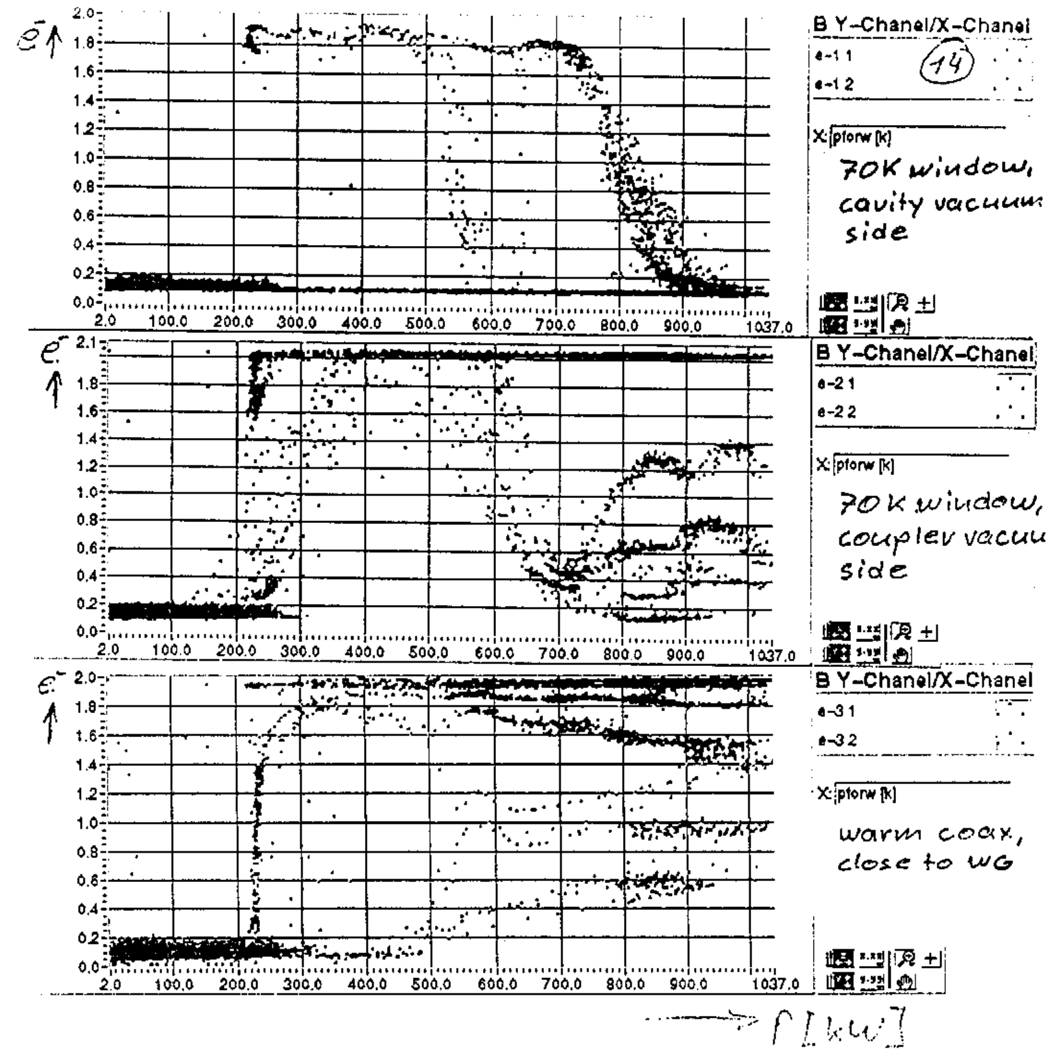

e⁻ signals vs power for the whole test

- several power sweeps with different pulslength

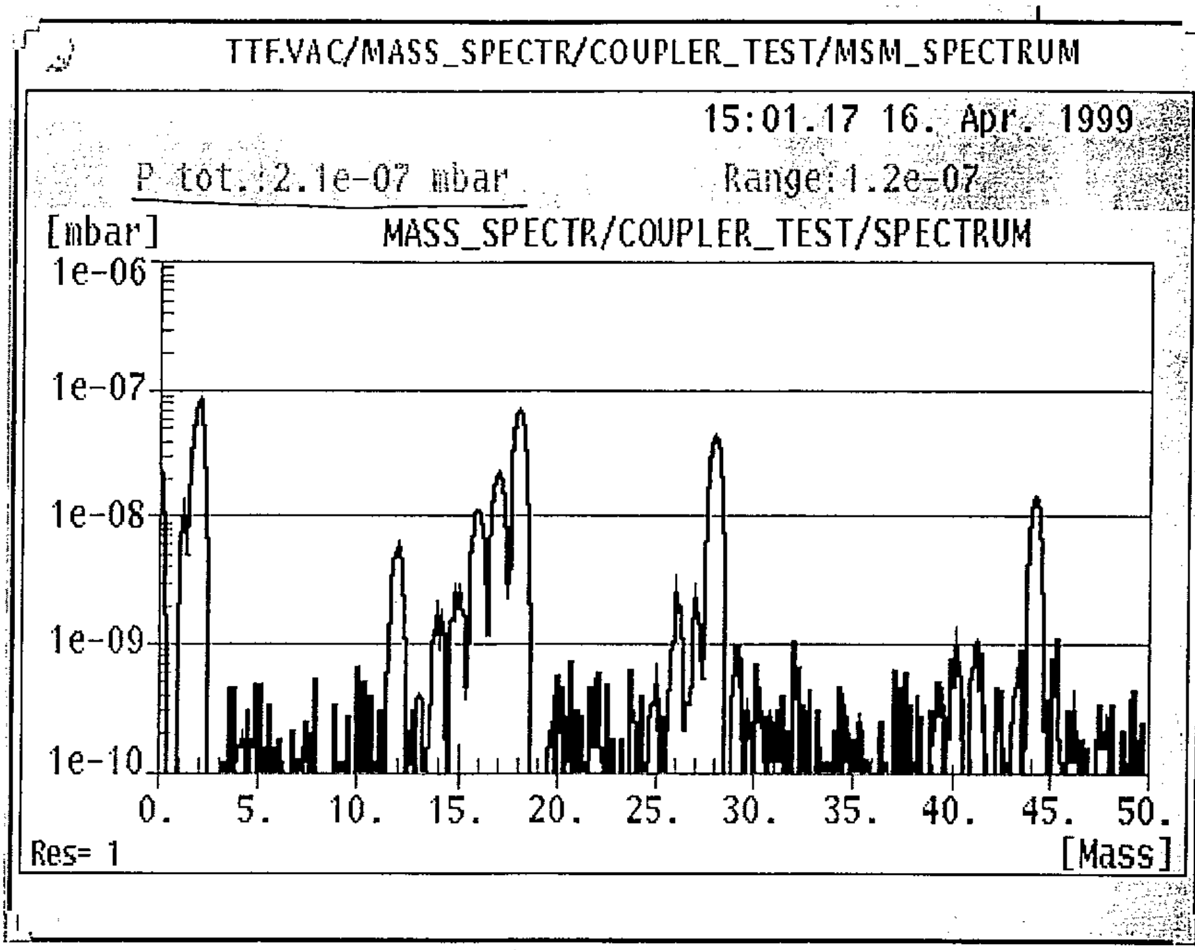

AC03/AC04 before heating

(16)

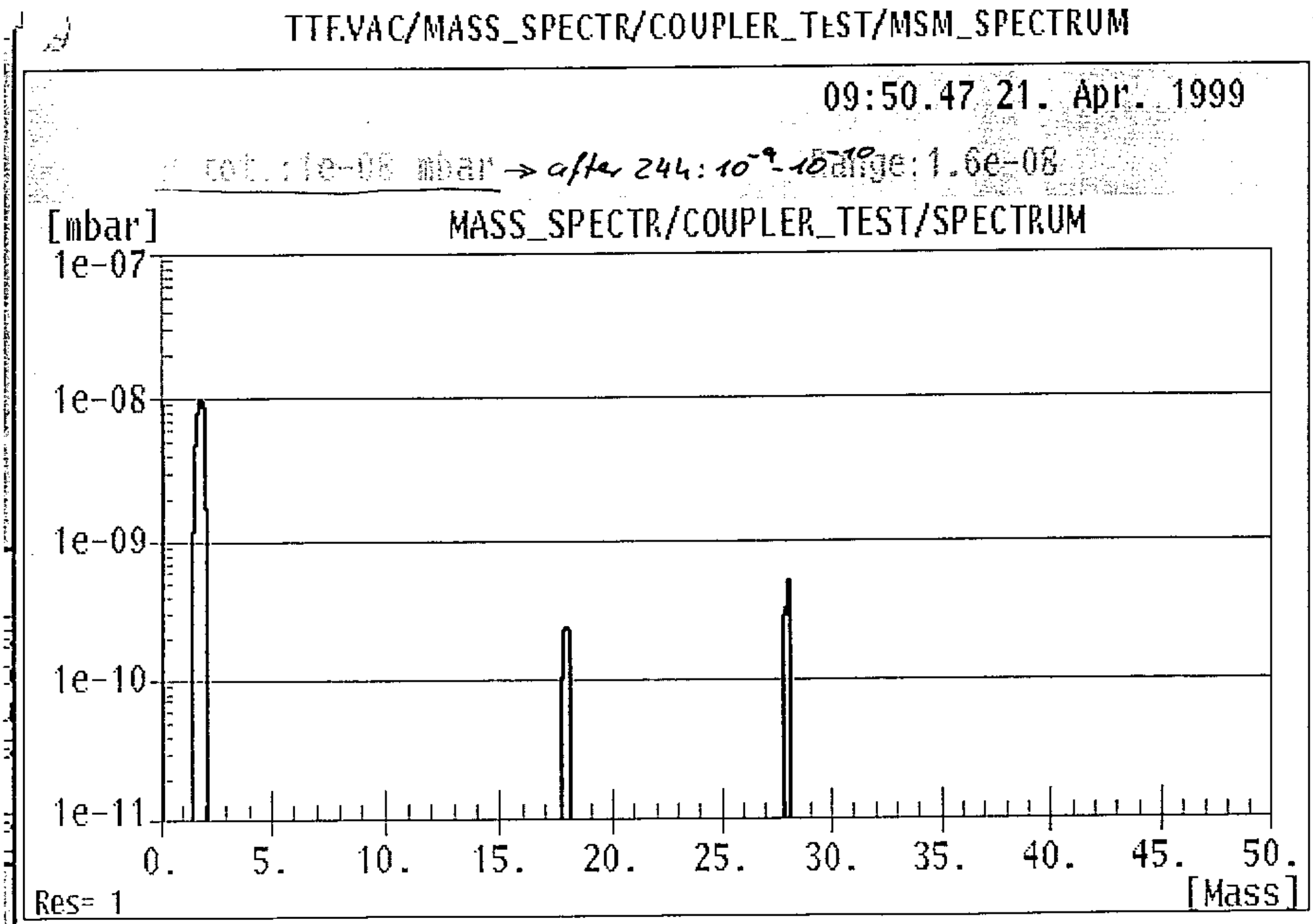

AC03/AC04 after heating

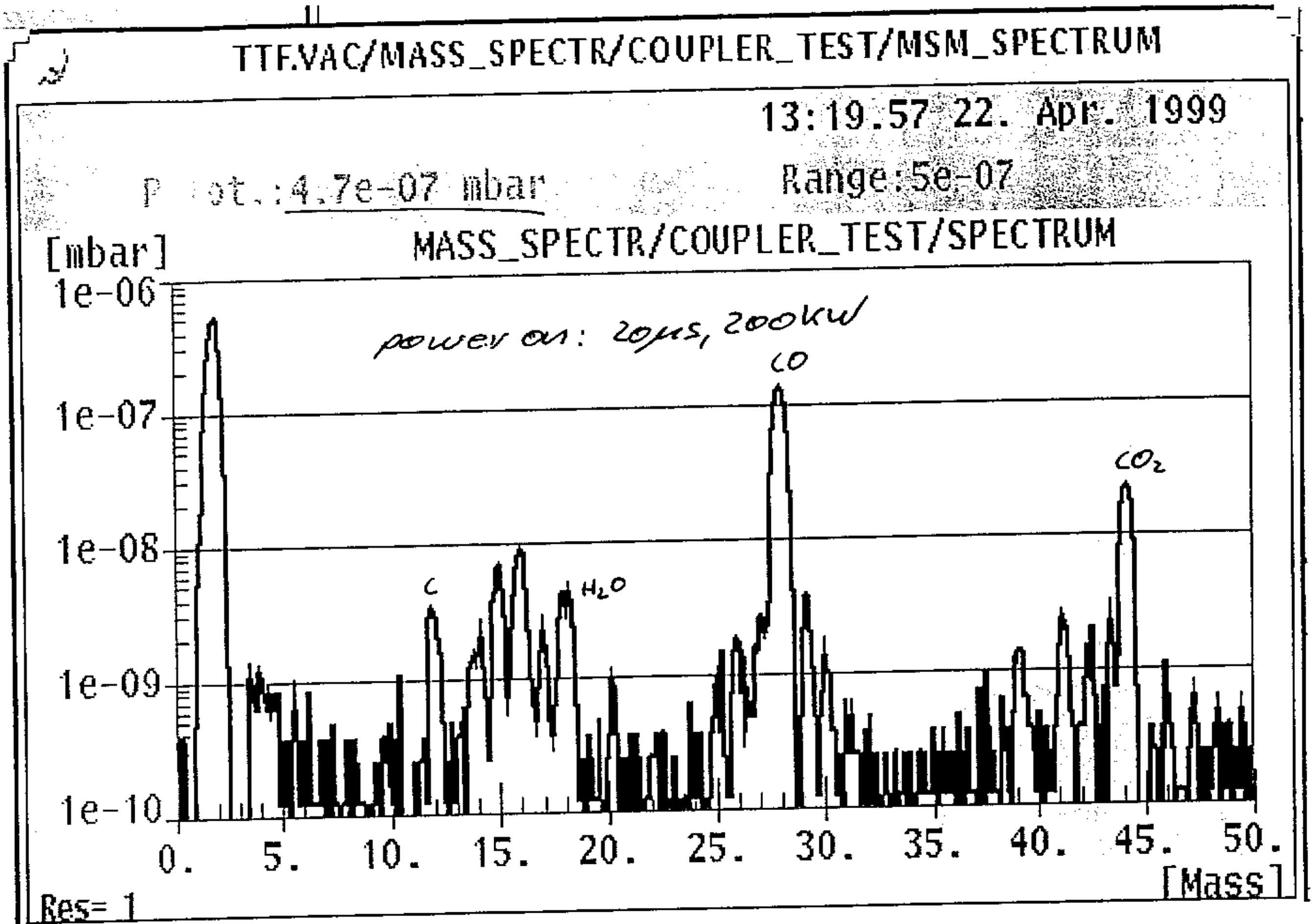

AC03, AC04 20µs, 200kW

FM coupler for the proposed 4x7-cell superstructure: RF requirements

R. Brinkmann, J. Sekutowicz, S. Simrock

44

Normal operation at 21.7 MV/m and I_{beam} = 11.3 mA

$V = 21.7\ \mathrm{MV/m} \cdot 4 \cdot 0.807\ \mathrm{m} = \mathbf{70.1\ MV}$

$Z = 70.1\ \mathrm{MV} / 11.3\ \mathrm{mA} = \mathbf{6.2\ G\Omega}$

$Q_{ext} = 6.2\ \mathrm{G\Omega} / 2930\ \Omega = \mathbf{2.12 \cdot 10^6}$

$\Delta f_{3dB} = 1300\ \mathrm{MHz} / 2.12 \cdot 10^6 = \mathbf{614\ Hz}$

$P_{beam} = 11.3\ \mathrm{mA} \cdot 70.1\ \mathrm{MV} = \mathbf{792\ kW}$

Additional power needed to compensate for the Lorentz force detuning is about 7% and for the phase and amplitude stabilization almost 20 % (S. Simrock). The total input power is :

Pin = 792 *1.27 = 1006 kW

For the energy upgrade the voltage and the current will be almost proportional increased by 40% . This will required **to double Pin** but Qext will stay **unchanged**.

HPP processing

By proper tuning of 7-cell structures half of the input power P_{in} will be transferred to the processed structure.

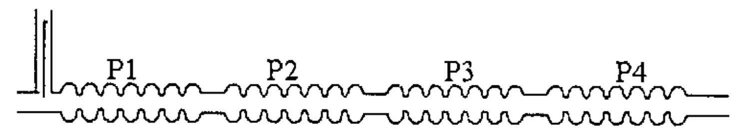

Processed structure	Structure # 1 Δf [kHz]	Structure # 2 Δf [kHz]	Structure # 3 Δf [kHz]	Structure # 4 Δf [kHz]
Structure # 1	-100	0	0	+100
Structure # 2	0	-200	0	0
Structure # 3	0	0	-200	0
Structure # 4	100	0	0	-100

Example:

When Pin = 800 kW almost 400 kW goes into 7cell structure.

45

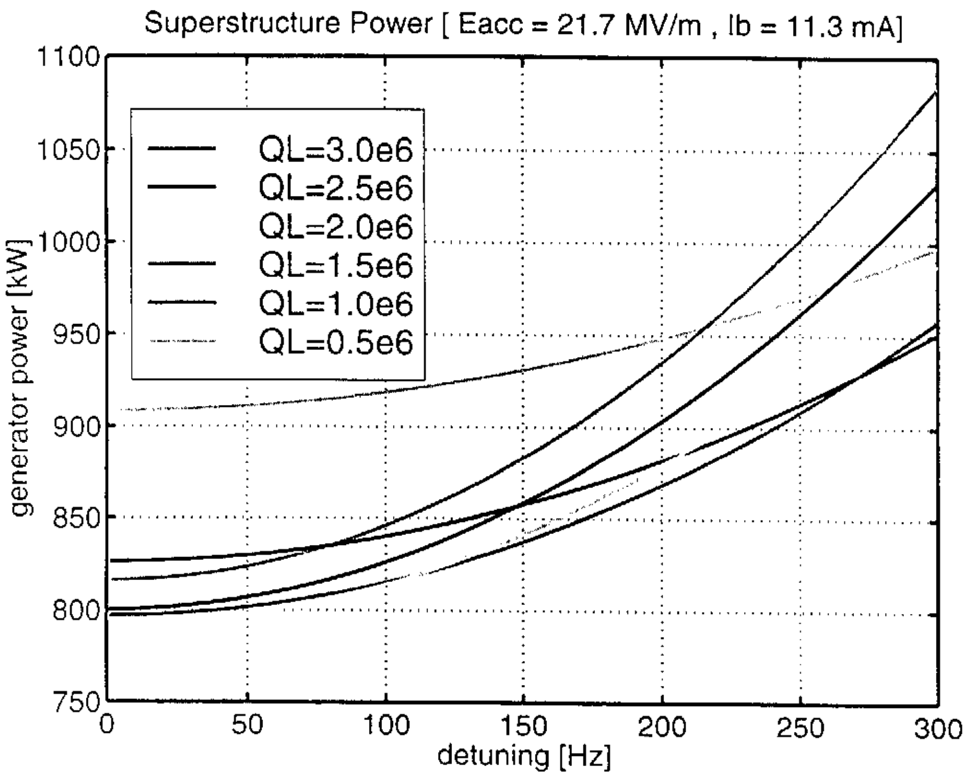
Superstructure Power [Eacc = 21.7 MV/m , Ib = 11.3 mA]
generator power [kW]
detuning [Hz]
QL=3.0e6
QL=2.5e6
QL=2.0e6
QL=1.5e6
QL=1.0e6
QL=0.5e6
1100
1050
1000
950
900
850
800
750
0
50
100
150
200
250
300

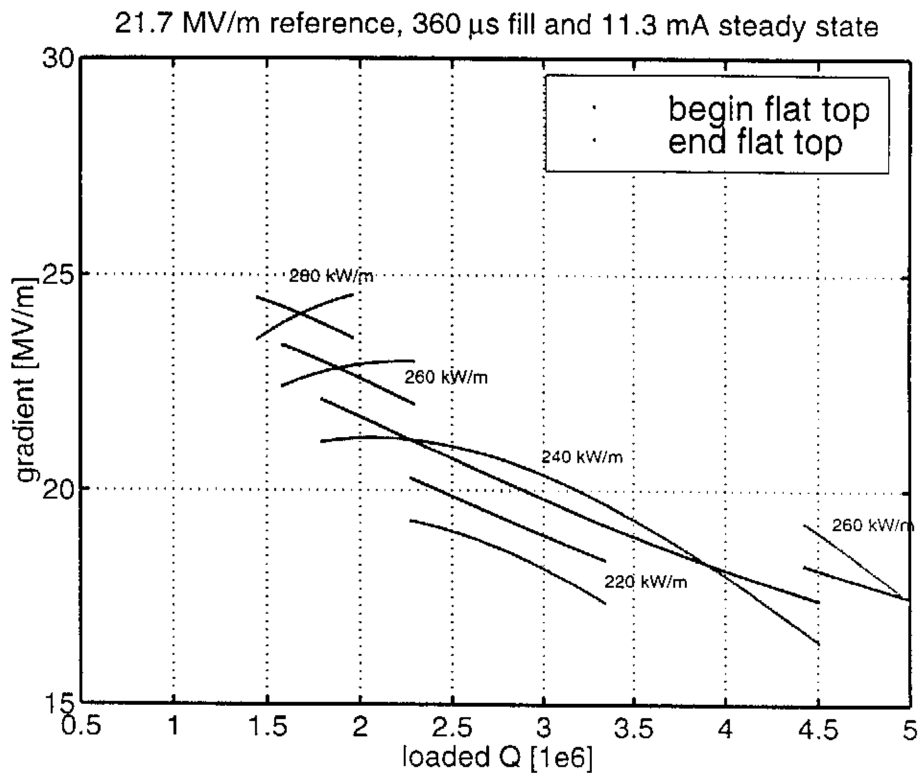
21.7 MV/m reference, 360 µs fill and 11.3 mA steady state
gradient [MV/m]
loaded Q [1e6]
begin flat top
end flat top
280 kW/m
260 kW/m
240 kW/m
220 kW/m
260 kW/m
30
25
20
15
0.5
1
1.5
2
2.5
3
3.5
4
4.5
5

TESLA Waveguide Coupler

J.Boster, J.Dicke, M.Dohlus, A.Gamp, H. Hartwig, K.Jin, A.Jöstingmeier,
C.Martens, V.Kaljuzhny, S.Yarigin, A.Zavadsev

1. Versions
2. Waveguides
3. Windows
4. Integrated Waveguide-Coupler / Window
5. Tuning

1. Versions

1.1 Rectangular waveguide: at coupler 165mm x 30mm

a) coupler for 2*28 cells: 2L solution; Report: TESLA 99-01

problem with space !

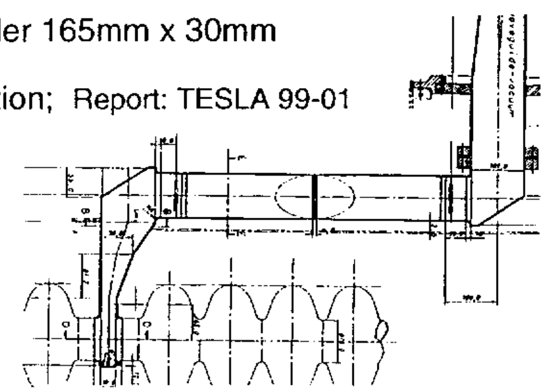

b) coupler for 2*28 cells: Zavadtsev's straight solution

problem with space !
→ 2L solution

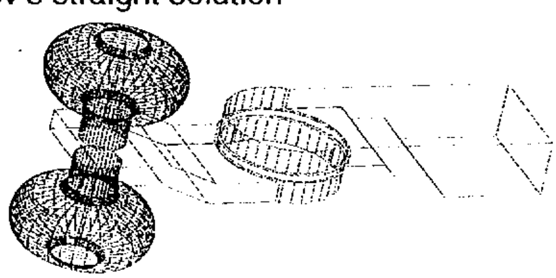

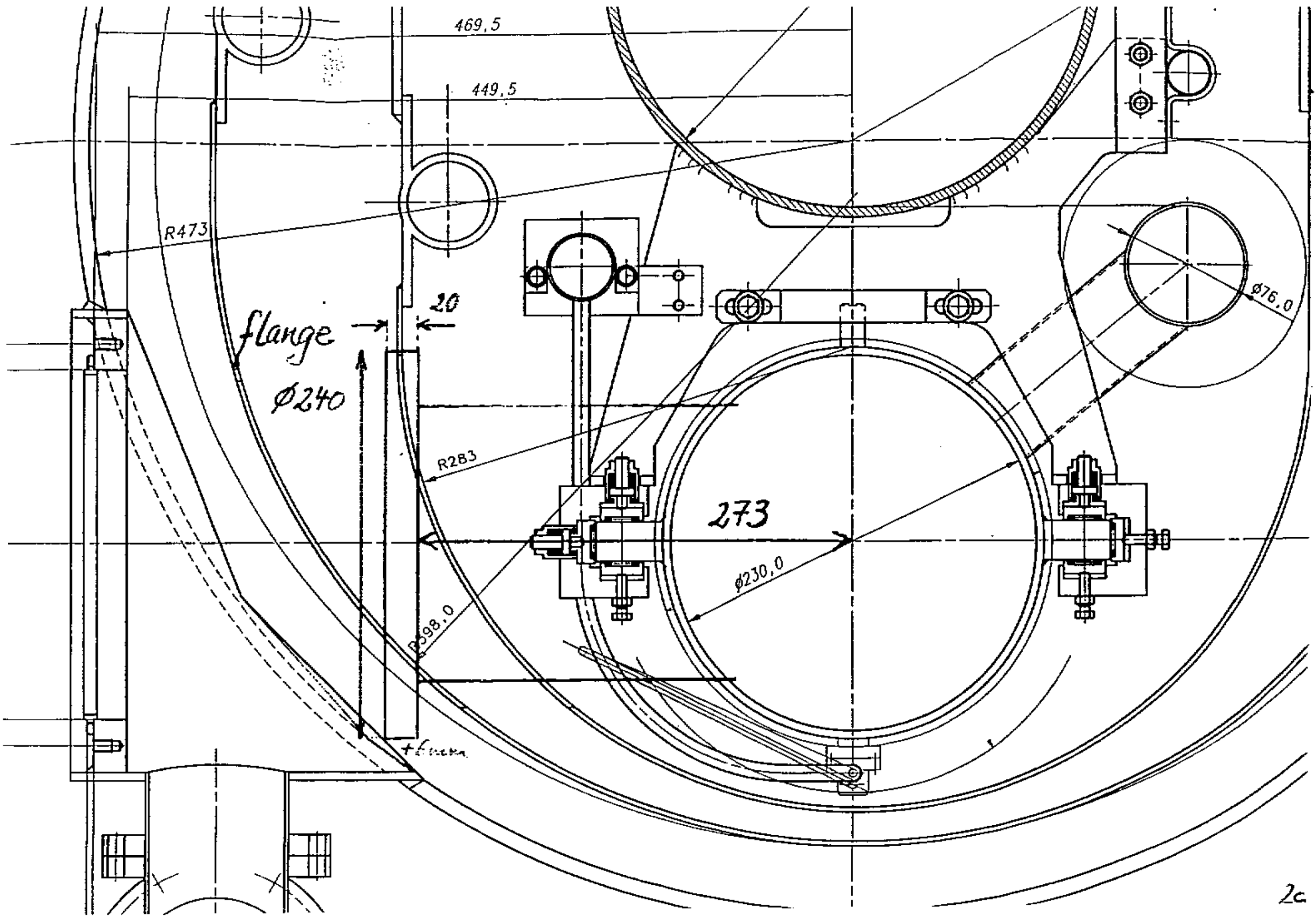

1.2 Beam pipe hidden by wall

a) asymmetric solution

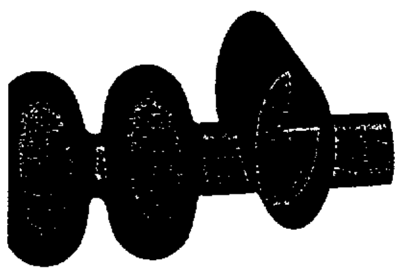

9 cell version investigated
elliptical waveguide 170mm x 85 mm
r_{pipe}=39mm

problems: additional resonator; field asymmetry

b) symmetric solution

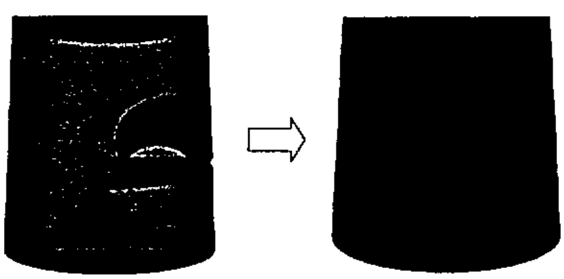

elliptical waveguide 170mm x 85 mm
r_{pipe}=39mm

problem: weak coupling → high Q of additional resonator
→ high losses or SC

c) symmetric solution with rectangular waveguide (165mm x 30mm), big pipe (r_{pipe}=57mm), small wall

A. Zavadtsev

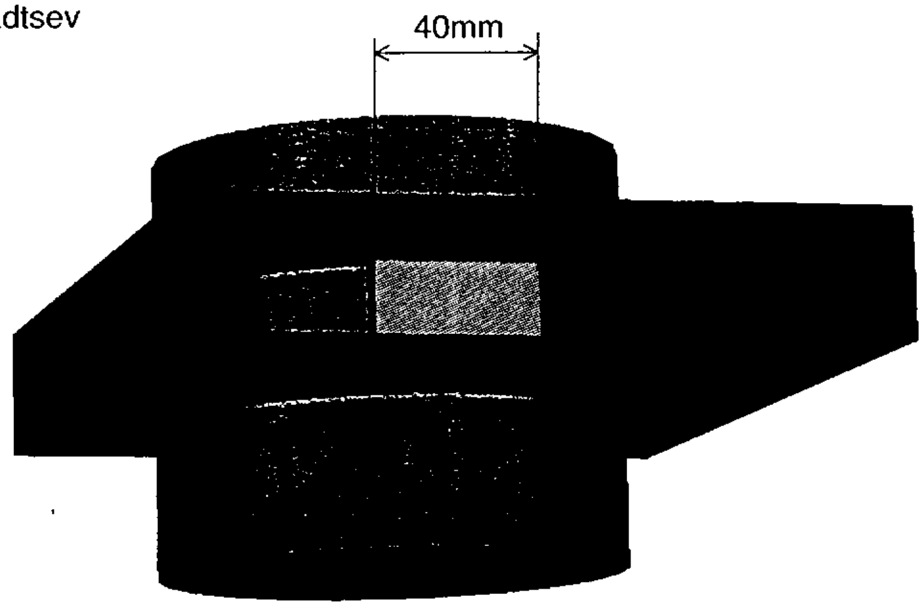

4

1.3 Beam pipe hidden by chicane

a) symmetric chicane

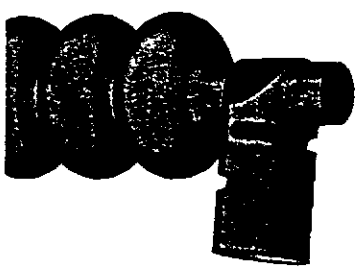

9 cell version investigated
elliptical waveguide 170mm x 85 mm
r_{pipe}=39mm

problem: space

b) asymmetric chicane

problem: E_{max}

1.4 Circular Waveguide

a) "organ pipe"

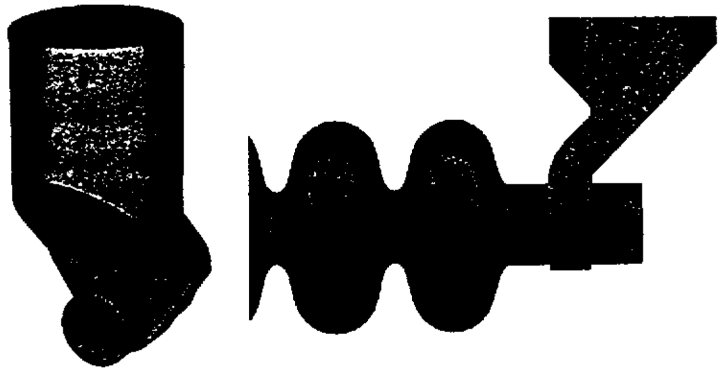

problems: space (z,x),
thermal flow,
waveguide modes

b) "elephant" 

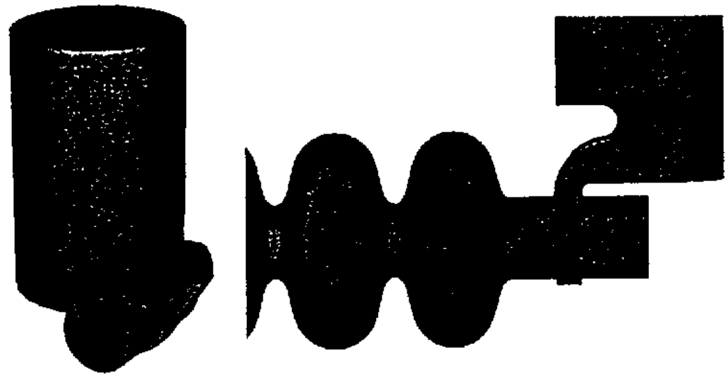

problems: space (z),
thermal flow,
waveguide modes

6

c) modification : reduce wg. size (f_c = const.)
increase f_c of higher modes

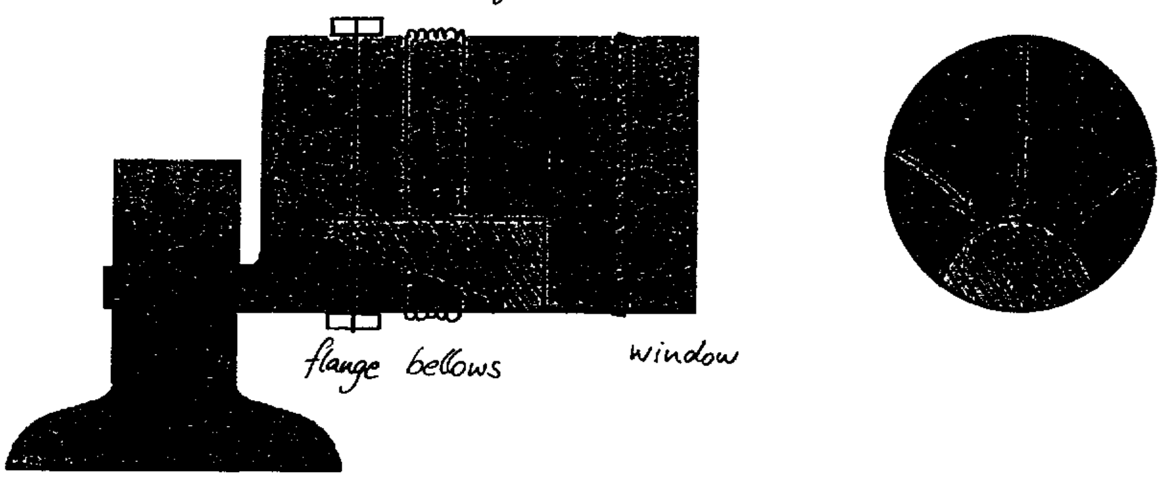

to be investigated !

2. Waveguides

2.1 Coax Transmission Line (70 Ω):

	total	outer conductor	inner conductor
radius		20 mm	6.22 mm
α	$5.4\cdot10^{-4}$ N/m	23.7 %	76.2 %
losses, κ=10^9 S/m, P=1MW	1090 W/m	258 W/m	830 W/m
losses 1.4ms, 5Hz	7.63 W/m	1.81 W/m	5.81 W/m
E-field		0.507 MV/m	1.628 MV/m
B-field		$1.690\cdot10^{-3}$ T	$5.43\cdot10^{-3}$ T

f_c(TE) = 3.7 GHz

	total	outer conductor	inner conductor
radius		30 mm	9.34 mm
α	$3.6\cdot10^{-4}$ N/m	23.7 %	76.2 %
losses, κ=10^9 S/m, P=1 MW	723 W/m	172 W/m	552 W/m
losses 1.4ms, 5Hz	5.06 W/m	1.20 W/m	3.86 W/m
E-field		0.338 MV/m	1.086 MV/m
B-field		$1.127\cdot10^{-3}$ T	$3.622\cdot10^{-3}$ T

f_c(TE) = 2.5 GHz

copper
≈ 47K

2.2 Rectangular Waveguide:

geometry	165mm × 82.5mm
f_c(H10)	909 MHz
α (κ=10^9 S/m)	$1.5\cdot10^{-4}$ N/m
losses, κ=10^9 S/m, P=1MW	302 W/m
losses 1.4ms, 5Hz	2.1 W/m
max E-field	0.393 MV/m
f_c(H20) = f_c(H01)	1.82 GHz

geometry	165mm × 30mm
f_c(H10)	909 MHz
α (κ=10^9 S/m)	$3.3\cdot10^{-4}$ N/m
losses, κ=10^9 S/m, P=1MW	660 W/m
losses 1.4ms, 5Hz	4.6 W/m
max E-field	0.652 MV/m
f_c(H20)	1.82 GHz

2.4 Elliptical Waveguide:

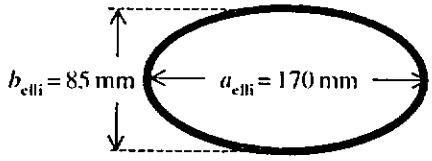

mode 1 type=TE ↓ f_c = 1.051 GHz
mode 2 type=TE ↓↑ f_c = 1.918 GHz
mode 3 type=TE → f_c = 1.983 GHz
mode 4 type=TM f_c = 2.119 GHz

$$f_0 = 1.3\text{GHz}$$

$$\max\{\vec{E}\}_{P=1\text{MW}} = \underline{449\,\text{kV/m}}$$

$$\alpha = 2.10 \cdot 10^{-4}\ \text{N/m} \quad \text{for } \underline{\kappa = 10^9\ 1/(\Omega\text{m})}$$ copper ≈ 47k

$$P = 1\ \text{MW}\ (\kappa = 10^9\ \text{S/m}) \Rightarrow 420\ \text{W/m}$$

$$t = 1.4\ \text{ms},\ f_{rep} = 5\ \text{Hz} \Rightarrow 2.94\ \text{W/m}$$

2.3 Circular Waveguide:

2·radius	150 mm	165 mm	200 mm
f_c(H11) c+s	1.171 GHz	1.065 GHz	0.879 GHz
α (κ=10^9 S/m)	$2.27 \cdot 10^{-4}$ N/m	$1.38 \cdot 10^{-4}$ N/m	$0.71 \cdot 10^{-4}$ N/m
losses, κ=10^9 S/m, P=1MW	454 W	276 W	142 W
losses 1.4ms, 5Hz	3.18 W	1.93 W	0.99 W
max E-field	0.454 MV/m	0.359 MV/m	0.261 MV/m
f_c(E01)	1.53GHz	1.39 GHz	1.15 GHz
f_c(H21)	1.94 GHz	1.77 GHz	1.46 GHz

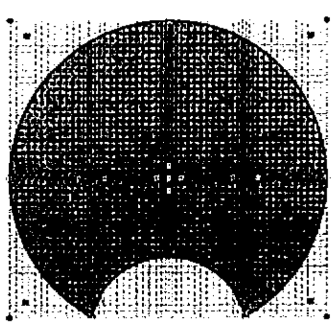

2 · r = 150 mm

mode 1 type=TE↓ f_c = 1.052 GHz
mode 2 type=TE→ f_c = 1.321 GHz
mode 3 type=TM f_c = 1.718 GHz
mode 4 type=TE f_c = 1.842 GHz

3. Windows

3.1 Window with Shifted Waveguides

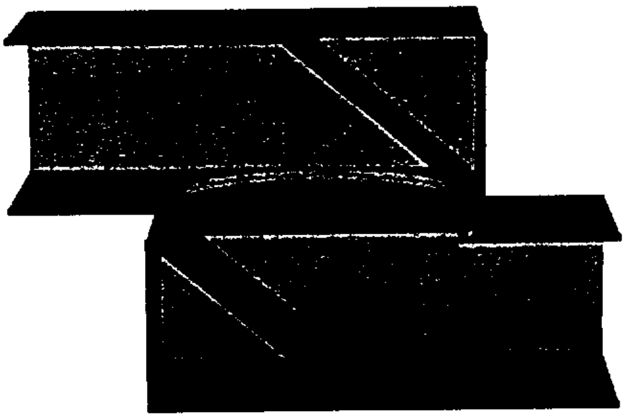

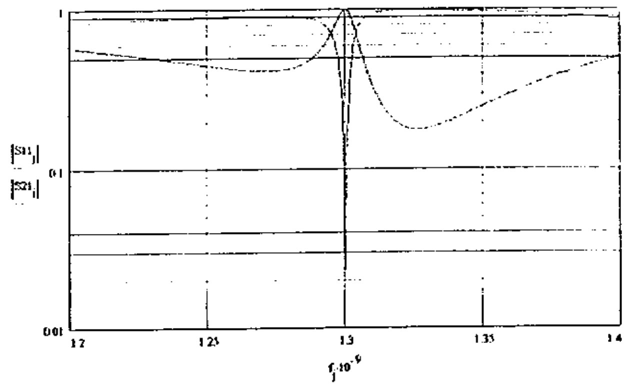

very narrow,
high E-peak (especially on ceramic)

3.2 Window for 165mm x 30mm Waveguide (A.Zavadtsev)

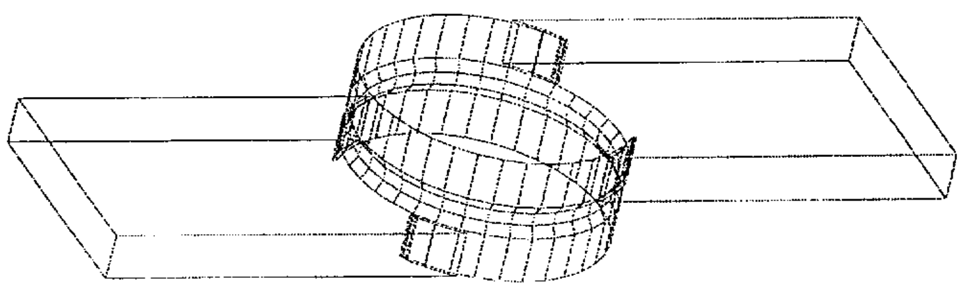

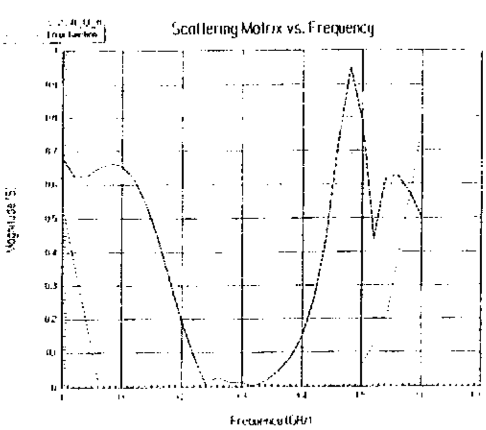

Table 2: Parameters of the window variants in the frequency range 1.0-1.6 GHz. $P = 1.3$MW

Variant	Mode	f_0, MHz	Δf, MHz ($S_{11}=0.1$)	E_{cer} kV/cm
One-mode variant with h=90 mm.	TM_{010}	1155	10	12.3
	TE_{111}	1225	<10	11.0
	TE_{211}	1400	10	11.0
Tree-modes variant with h=114 mm.	TM_{010} $+TE_{111}$ $+TE_{211}$	1300	170	5.0

0.44 MV/m @ 1MW

3.3 Symmetric Window with Posts

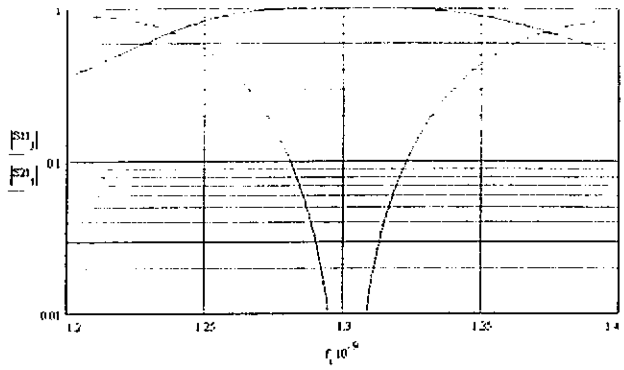

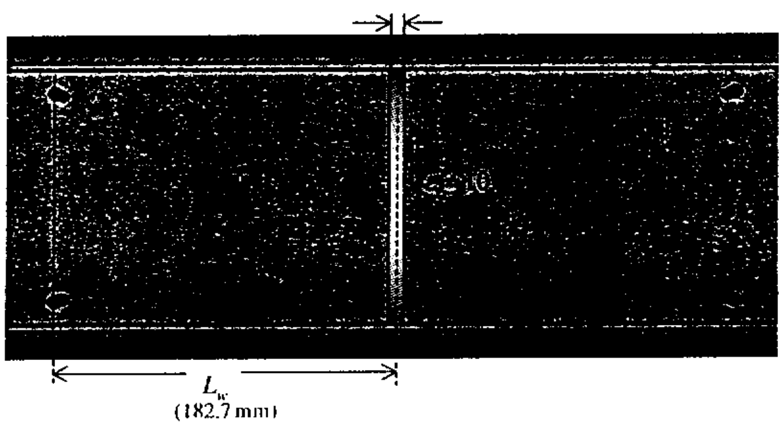

/3

a) Fields

Normalized Transverse E-Field in Waveguide ($r = -1 .. 0$)

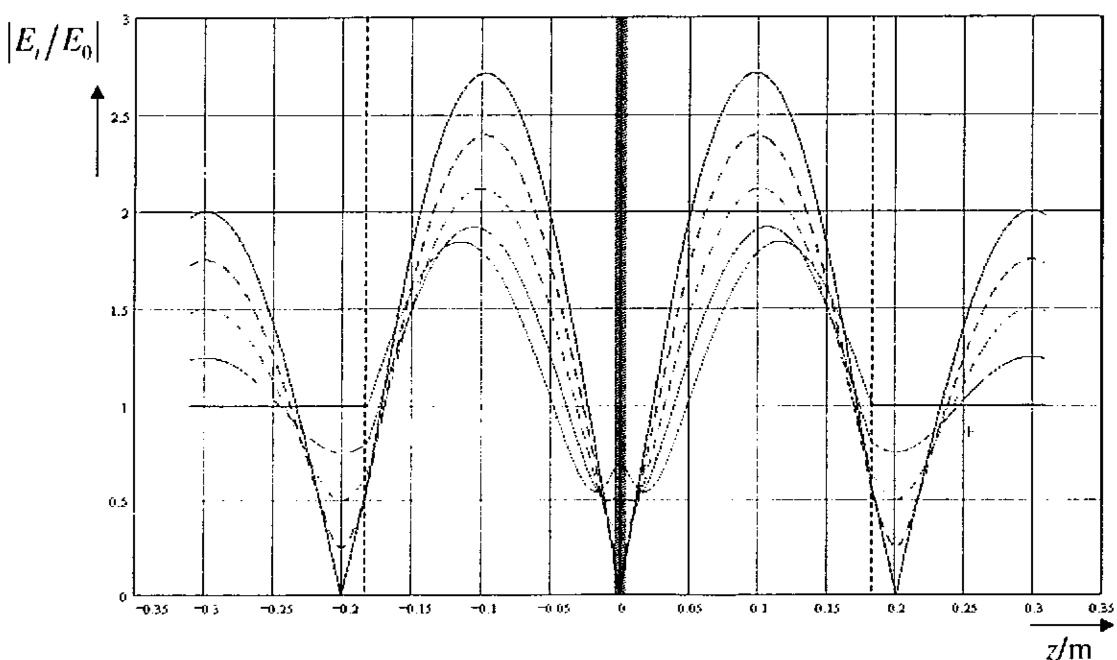

$E_0(P = 1\,\mathrm{MW}) = 0.449\,\mathrm{MV/m}$

b) Losses

Losses in Ceramic:

1996 International Accelerator School in Japan

DEVELOPMENT OF A HIGH POWER RF-WINDOW AT S-BAND

H. Matsumoto
KEK, High Energy Accelerator Research Organization
1-1 Oho, Tsukuba, Ibaraki 305, Japan

Table 3 Physical properties of high-purity alumina ceramic.

	99.5%	99.9%	99.9% (no MgO)
Thermal conductivity: cal/cm·h·°C	0.060	0.070	0.075
$\tan\delta$ ($\times 10^{-4}$): (at 2853 MHz)	13.0	3.0	0.27 (at 10 GHz)

C. Travier
$\tan\delta \approx 5.8\cdot 10^{-4}$
1MW, 1.4ms 10Hz!
$\Rightarrow$ 14.3 W

$$a_{\text{ceramic}}(\tan\delta = 0.27\cdot 10^{-4}) = \frac{1}{2}\cdot\frac{47.7\,\text{W}}{1\text{MW}} = 2.38\cdot 10^{-5}\,\text{N}$$

$$\overline{P}_c(P = 1\text{MW}) = 2a_{ceramic}\cdot P\cdot 1.4\,\text{ms}\cdot 5\,\text{Hz} = 333\,\text{mW}$$

Losses in Metal (κ=const):

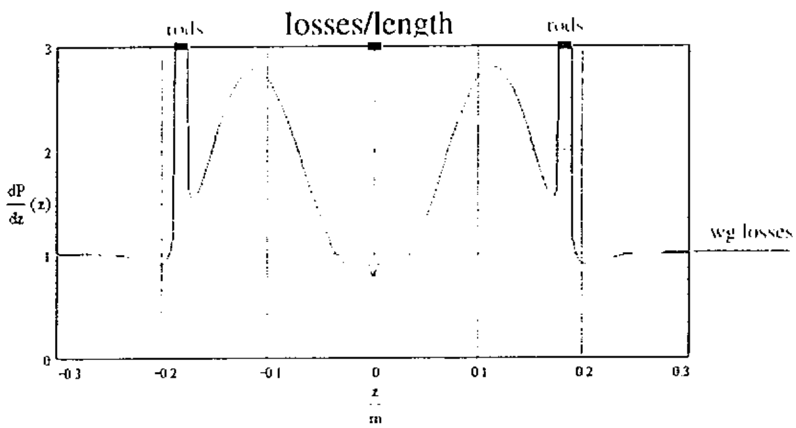

$$a_{\text{metall}} = \alpha_{WG}\cdot(\text{length} + 425\,\text{mm}) \qquad (\text{length} = 365.4\ \text{mm})$$

losses of one rod ≈ losses of 4cm waveguide
(not optimized)

$$\overline{P}_M(P = 1\text{MW}, \text{copper}(40\,\text{K})) = 1.98\,\text{W}$$

3.5 Window with Posts and Chicane (sym. operation)

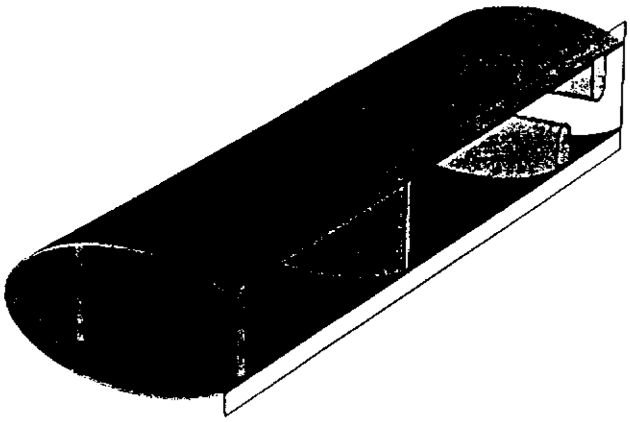

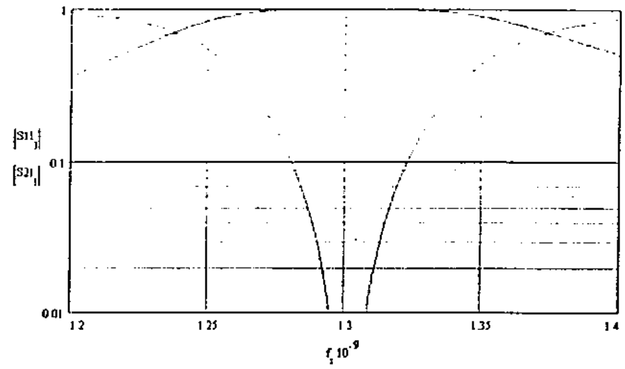

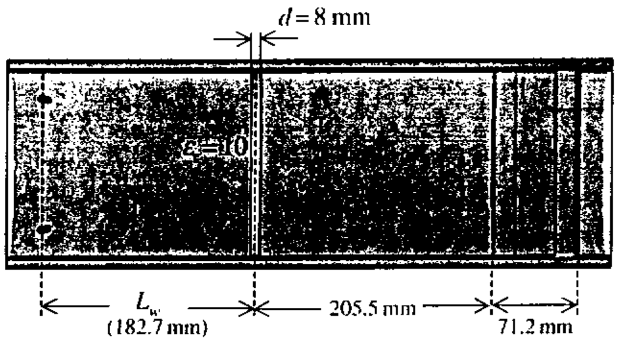

a) Fields $E_0(P = 1\,\text{MW}) = 0.449\,\text{MV/m}$

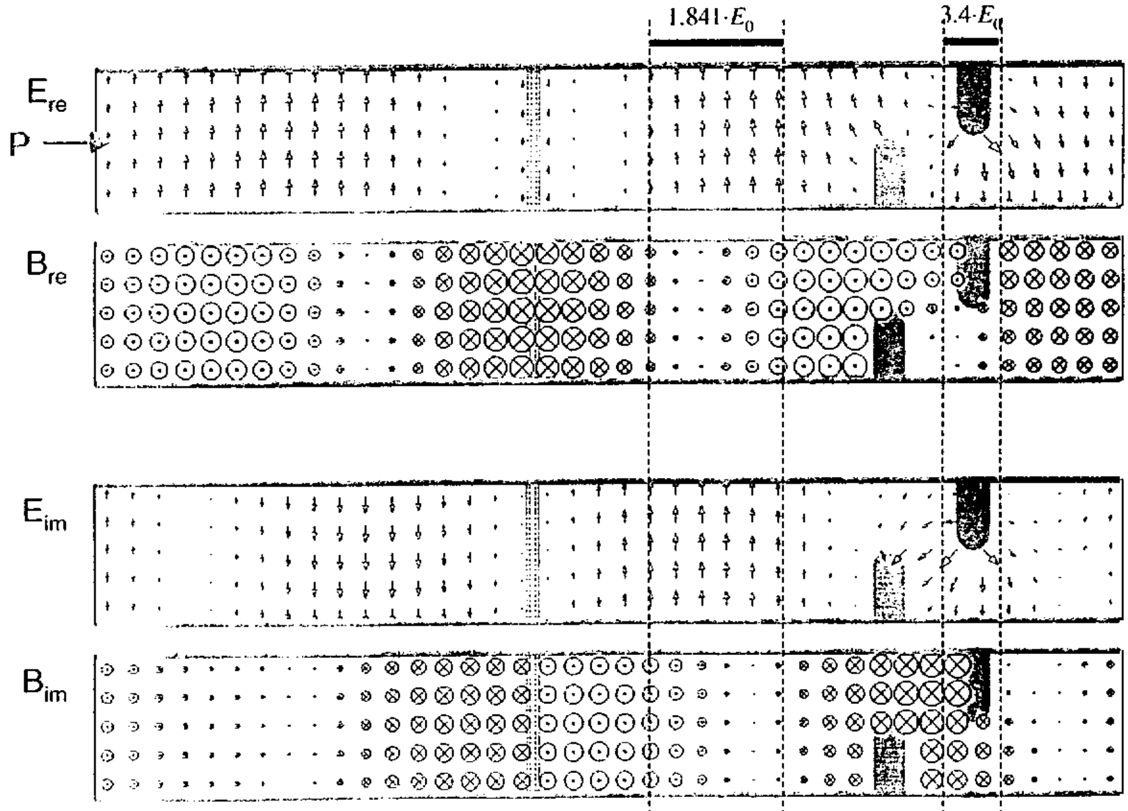

b) Losses

Losses in Ceramic: see 3.3 sym. window

e.g. $\overline{P}_c(P = 1\,\mathrm{MW}) = 2a_{ceramic} \cdot P \cdot 1.4\,\mathrm{ms} \cdot 5\,\mathrm{Hz} = 333\,\mathrm{mW}$

Losses in Metal (κ=const):

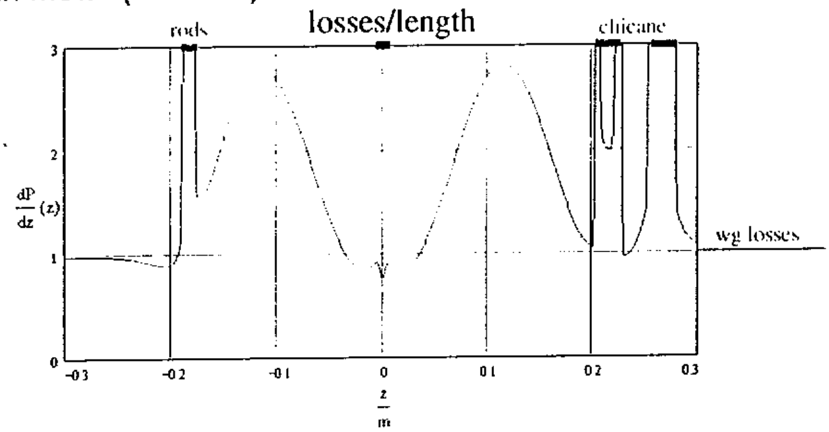

$$a_{metall} = \alpha_{WG} \cdot (\mathrm{length} + 508\,\mathrm{mm}) \qquad (\mathrm{length} = 459.325\,\mathrm{mm})$$

losses of one rod ≈ losses of 4 cm waveguide (not optimized)
losses in chicane ≈ losses of 20 cm waveguide

$$\overline{P}_M(P = 1\,\mathrm{MW}, \mathrm{copper}(40\mathrm{K})) = 2.41\,\mathrm{W}$$

3.6 Window with Posts and asym. Chicane

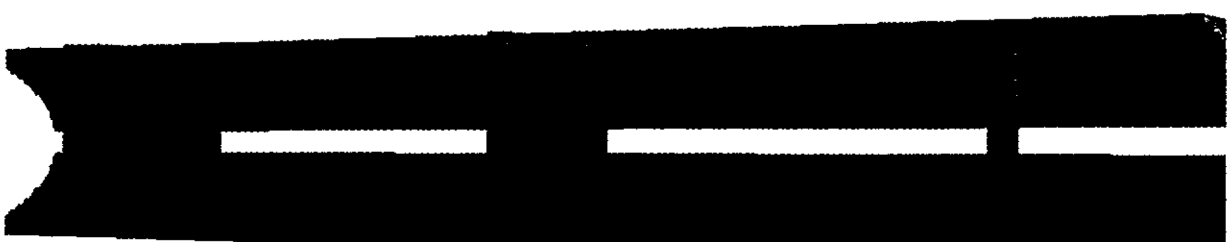

energy density of E-field

P ⇒

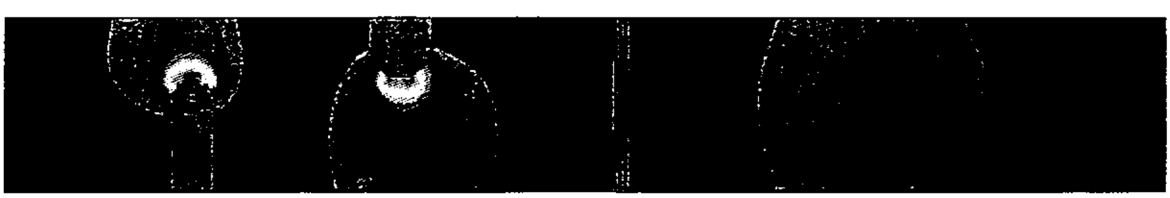

≈ $5 \cdot E_0$ ≈ $4.4\,E_0$ ≈ $1.84\,E_0$

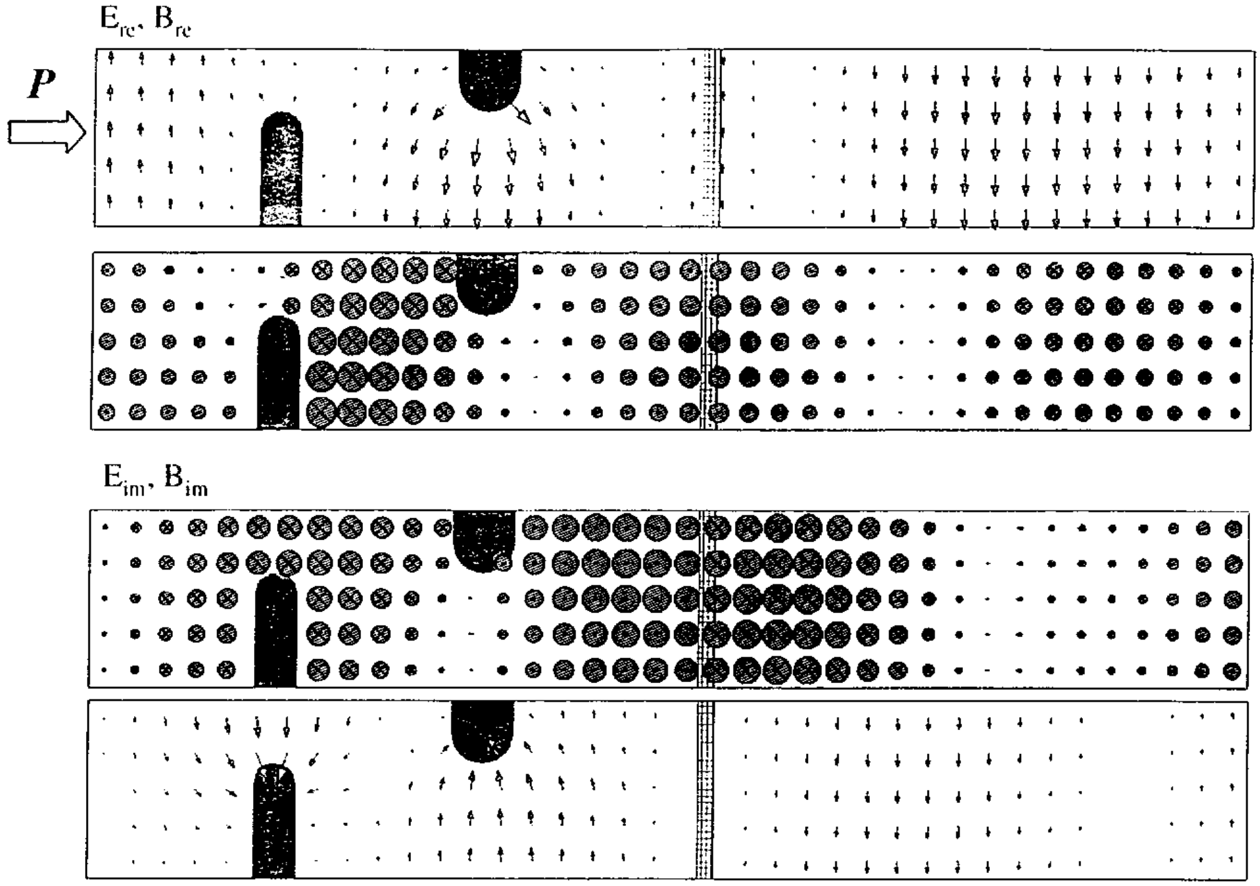

4. Integrated Waveguide-Coupler / Window

4.1 Version 1: coupler with wall and straight waveguide + integrated window

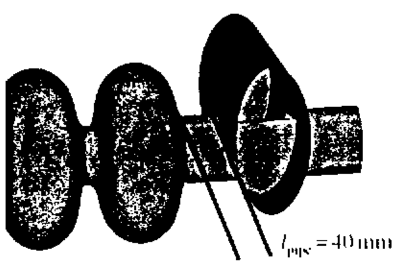

$Q_{ext} = 3.1 \cdot 10^6$
ceramic in SW minimum
for $t << t_{fill}$

Problems:
"resonator" losses
kick: $\vec{K} = 16.0\,\text{kV}\,\vec{e}_x + 11\,\text{kV}\,\vec{e}_y$

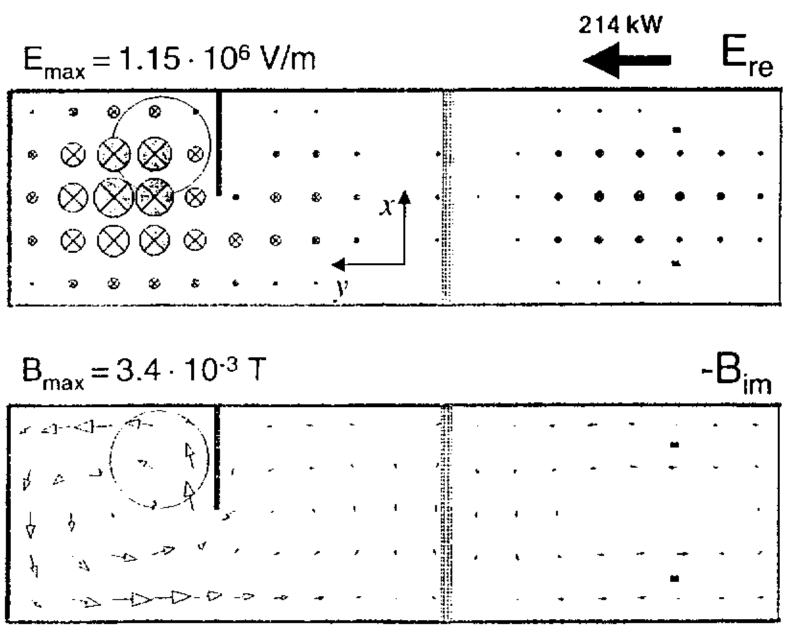

4.2 Version 2: coupler with "chicane" and straight waveguide + integrated window

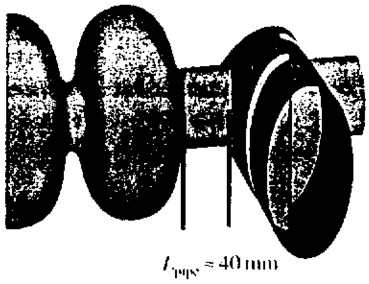

$Q_{ext} \approx 3.1 \cdot 10^6$
ceramic in SW minimum
for $t << t_{fill}$

a) Fields

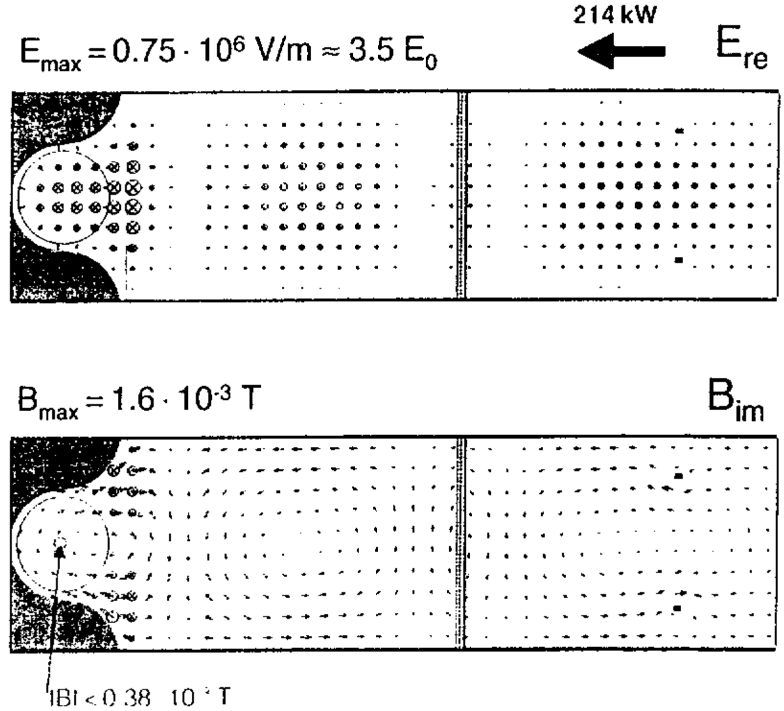

b) Kick

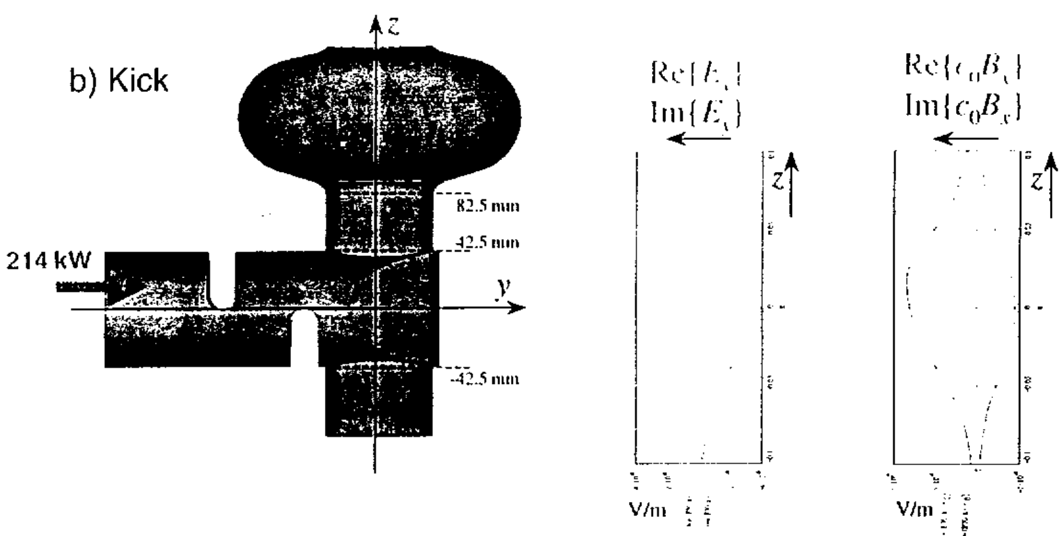

$$F_y = (E_y + c_0 B_x)\exp(j\beta[z - z_{offset}])$$

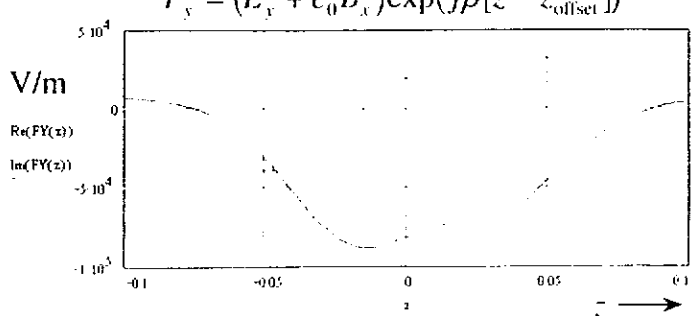

kick

$$\int F_y dz = (0.7 - j\,7.7)\,\mathrm{kV}$$

c) Losses

setup 1:

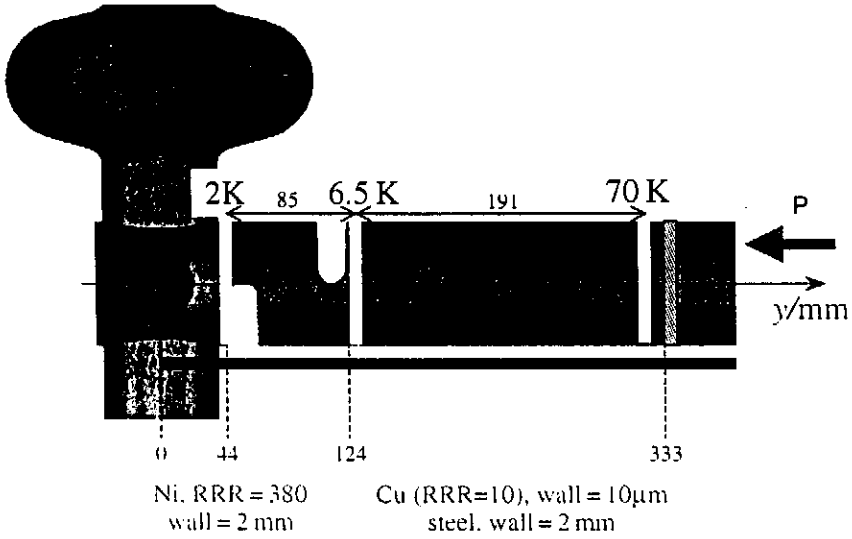

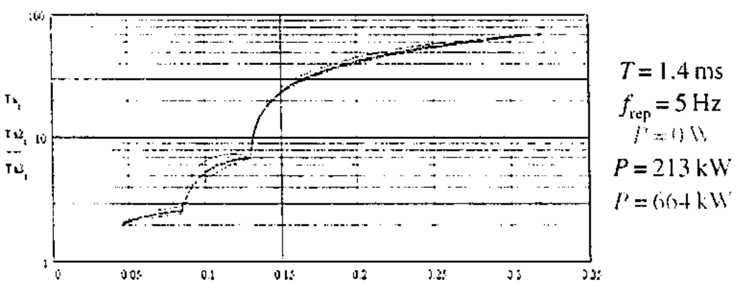

2 K losses: 0.061 W, 0.093 W, 0.162 W

4 K losses (6.5 K): 1.74 W, 1.96 W, 2.43 W

setup 2:

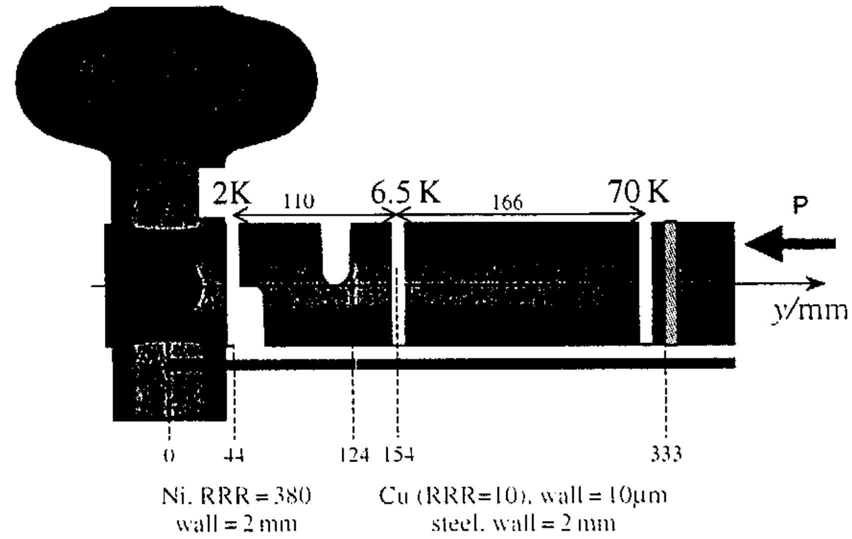

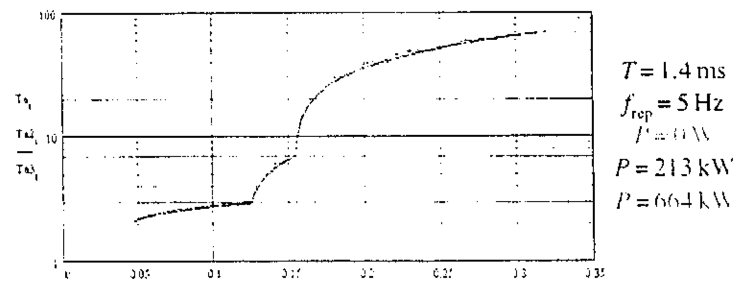

2 K losses: [illegible] W, 0.101 W, 0.124 W

4 K losses (6.5 K): [illegible], 2.16 W, 2.54 W

setup 3:

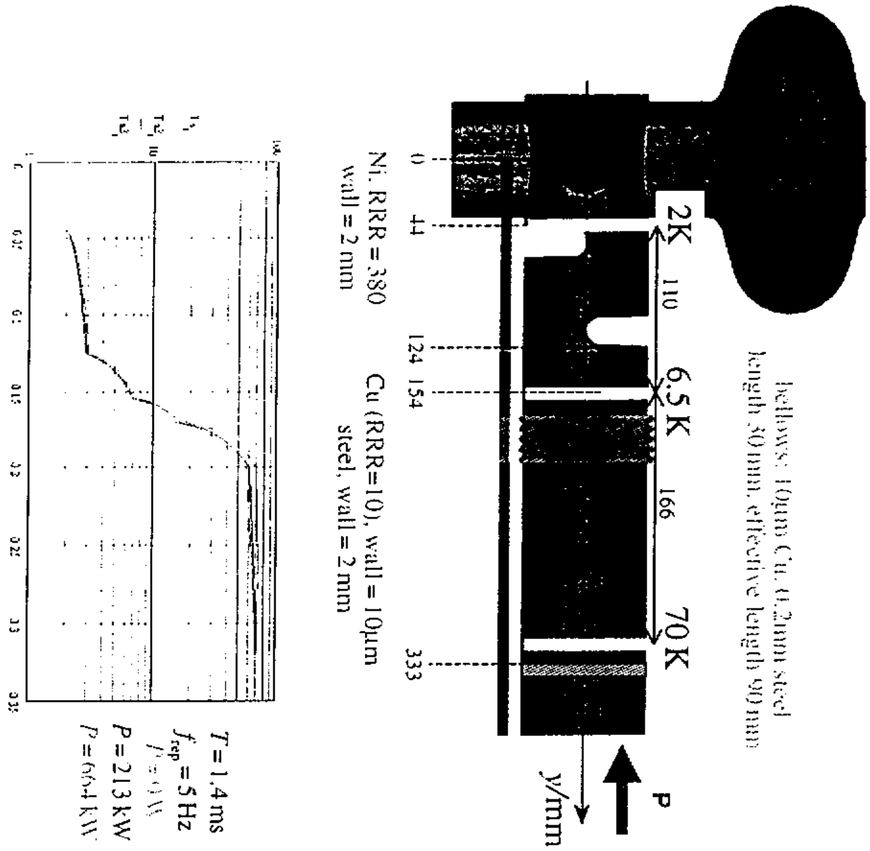

2 K losses: [illegible] W, 0.101 W, 0.124 W

4 K losses (6.5 K): [illegible] W, 0.99 W, 1.46 W

31

5. Tuning

5.1 Coupler with adjustable coupling: ???

5.2 External Tuning

design: $Q_{ext} = 3.10 \cdot 10^6$

e.g. wrong coupling: beam pipe 5 mm too long $\rightarrow Q_{ext} = 5.44 \cdot 10^6$

beam pipe 5 mm too short $\rightarrow Q_{ext} = 1.80 \cdot 10^6$

reflection by external tuner: $|r| = \left| \frac{Q_{ext}^{design} - Q_{ext}}{Q_{ext}^{design} + Q_{ext}} \right|$ example $|r| = 0.27$

field distribution in window $r = -0.27, 0, +0.27 \quad P_{\text{forward}}=\text{const}$

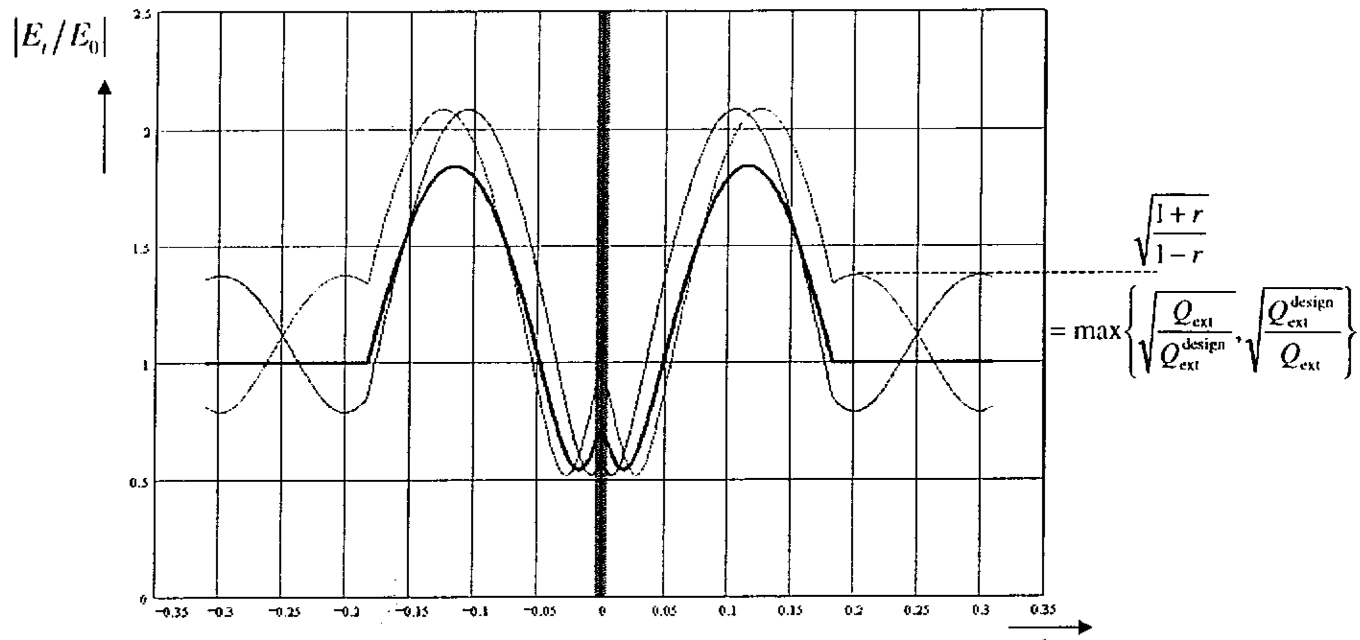

$E_0(P = 1\,\text{MW}) = 0.449\,\text{MV/m}$

Martin Dohlus Deutsches Elektronen Synchrotron Apr.99

Proposal 3.99

TW Test Setup

1. Prinzip

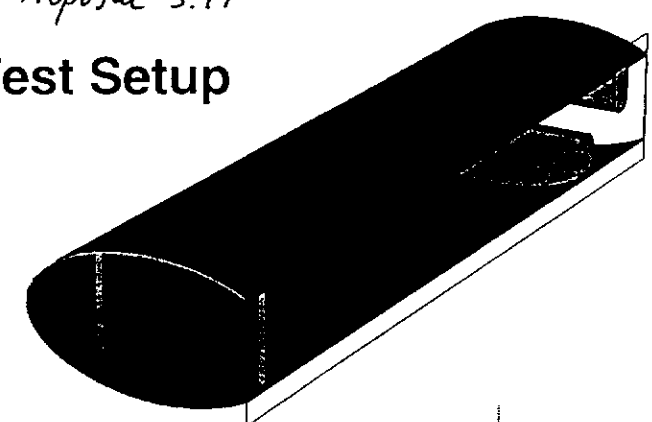

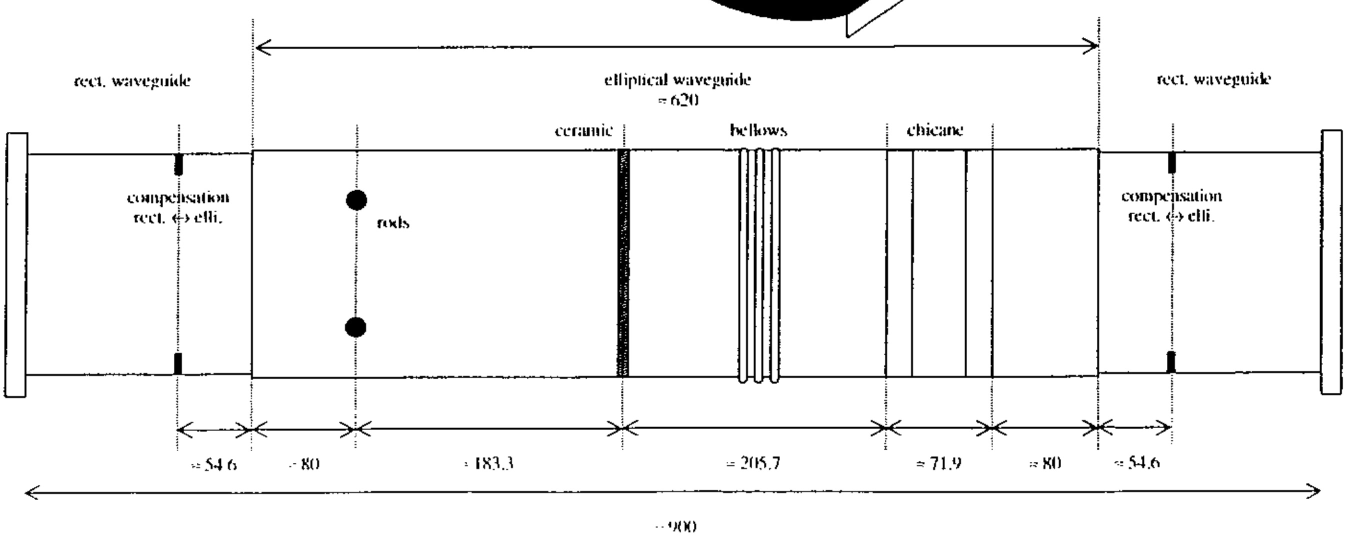

Martin Dohlus Deutsches Elektronen Synchrotron Mar.99

Coupler Meeting April 26 .. 27 , 1999

Status of Coaxial Coupler Development

For Superstructure

B. Dwersteg , DESY
A.Zavadsev, Chen HuaiBi

62

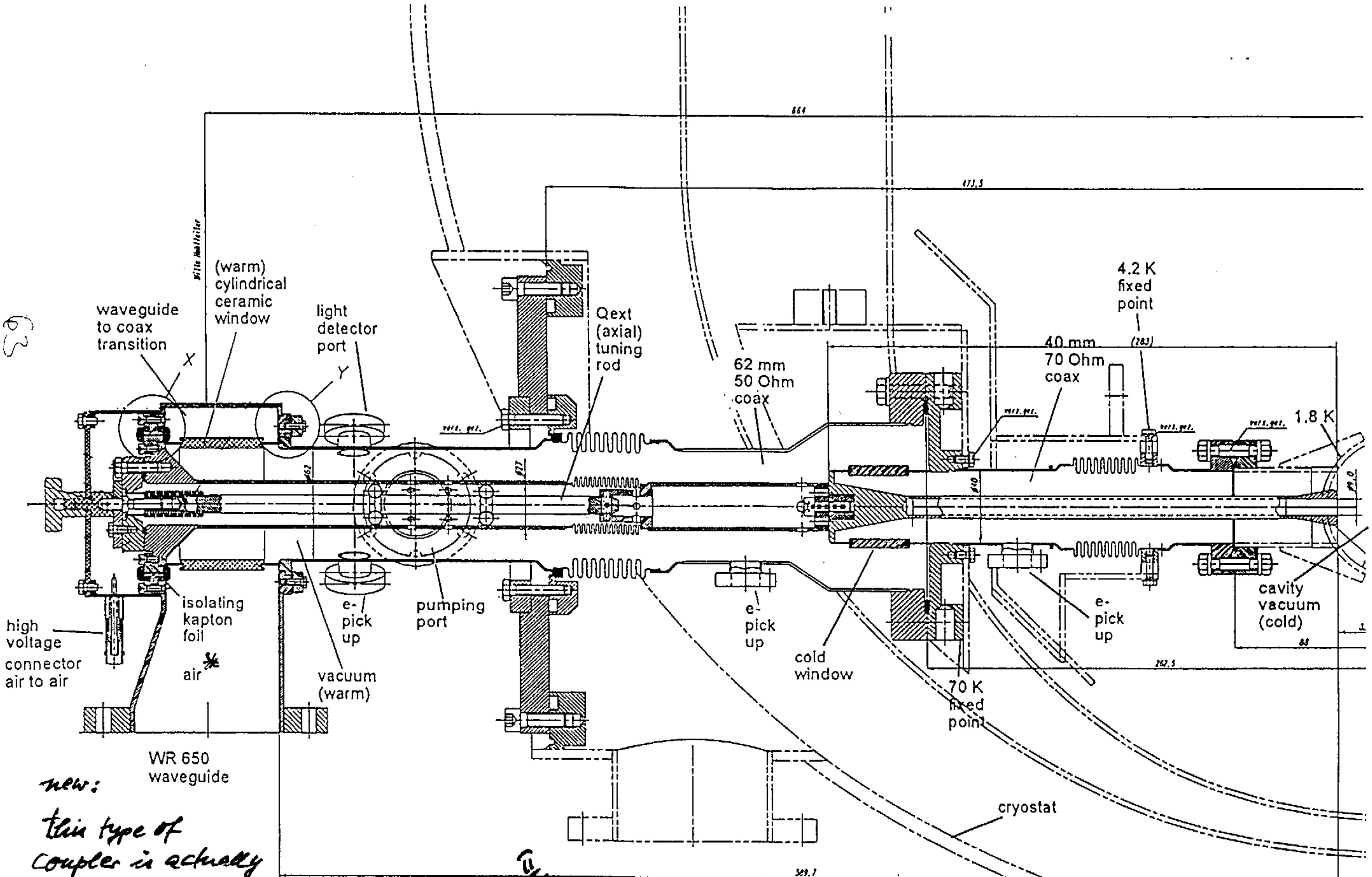

DESY TTF-Main Coupler , Version III

with inner conductor bias

new:
this type of
coupler is actually
(IP 99) being manufactured;
cold part identical with ver. II
expected to be clearly cheaper than Version II
* prepared for SF6 overpressure if necessary for power upgrade

63

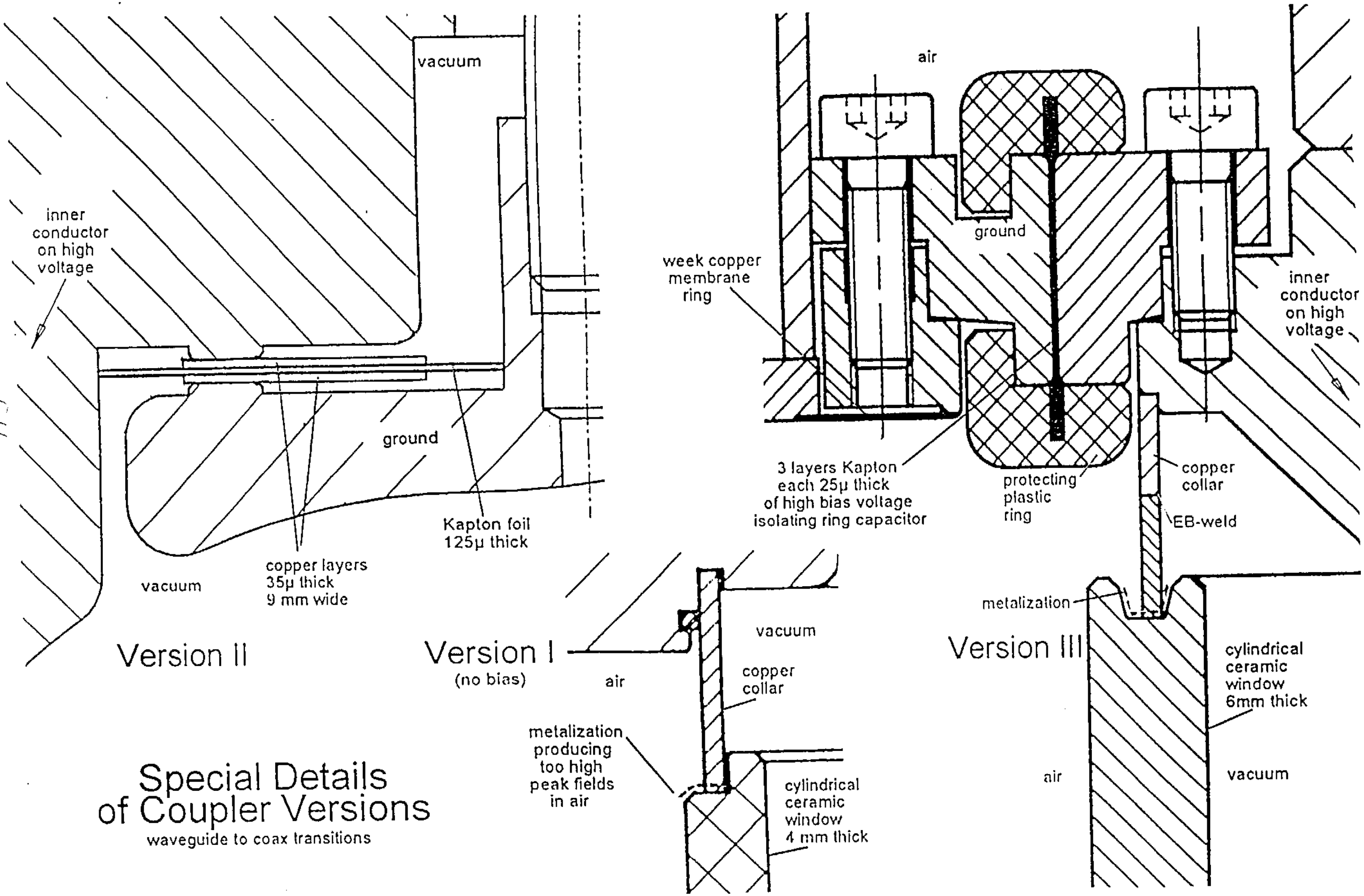

Special Details of Coupler Versions

waveguide to coax transitions

– Proper Position of Windows to escape MP at DESY TTF III Coupler

Dw Mon Feb 09 1998 Refldiag

■ **Transient reflection factor at 'Ref.-Plane' of Waveguide to coax transition , in resonance :**

'warm window'

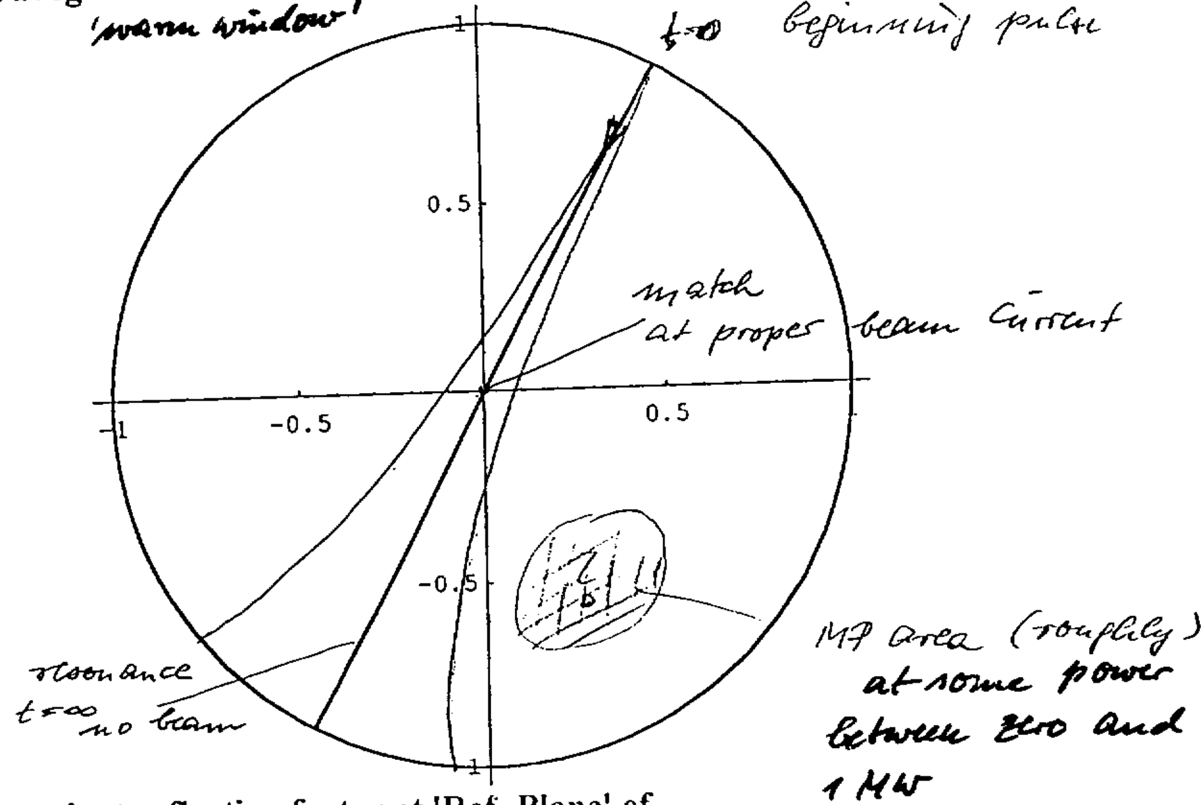

■ **Transient reflection factor at 'Ref.-Plane' of 'Cold window', at resonance :**

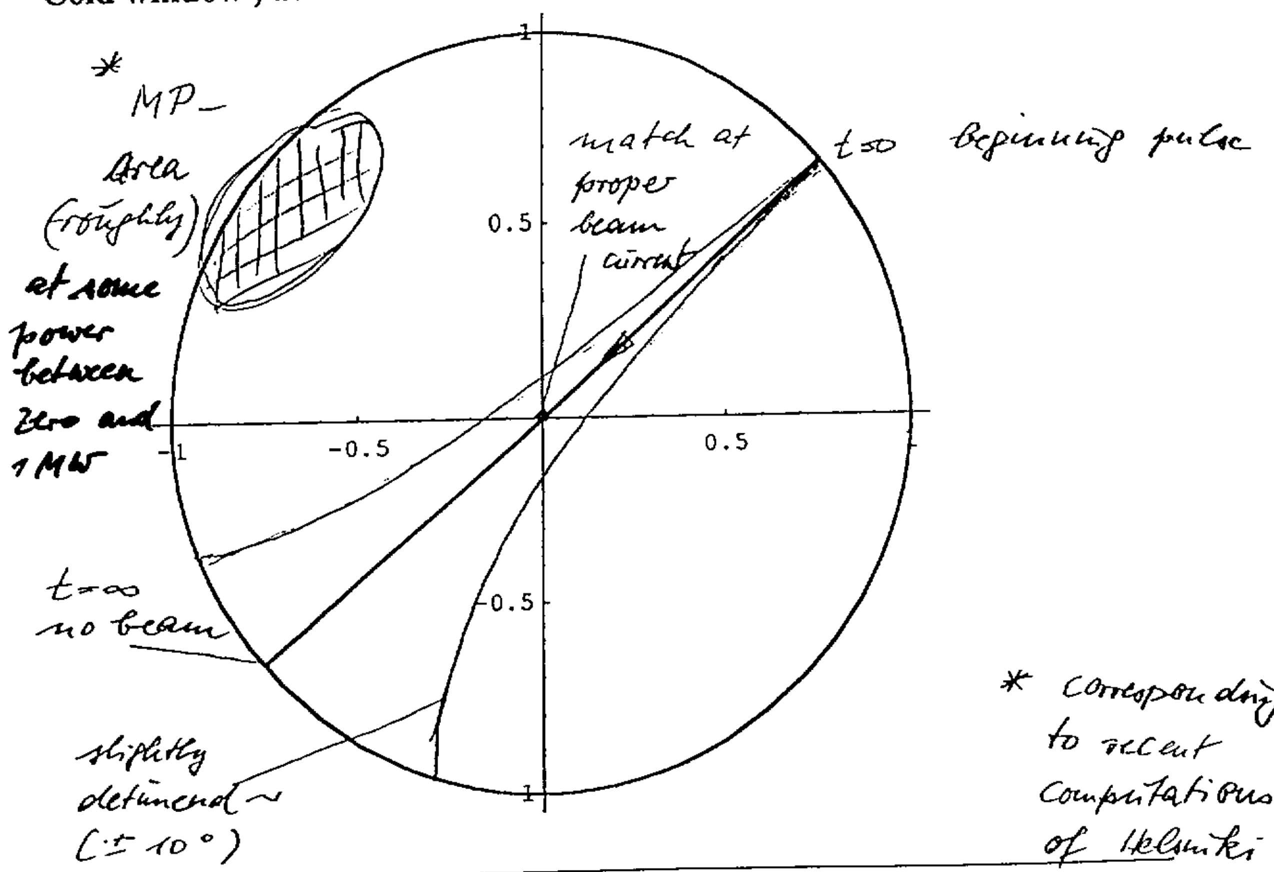

* corresponding to recent computations of Helsinki Institute

2

1- and 2-point multipacting in coaxial lines at full reflection

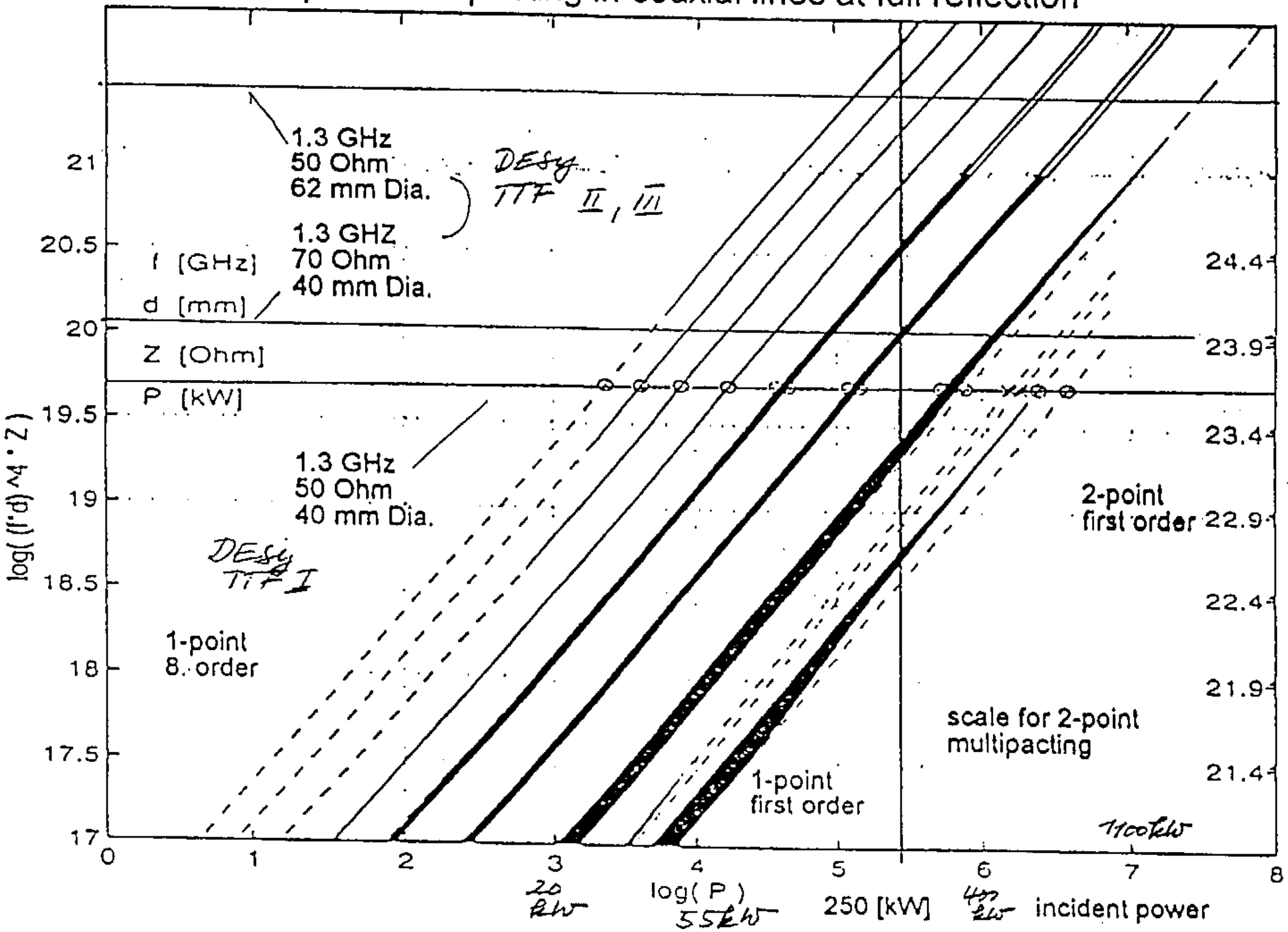

'Helsinki' - computations correspond to practically observed MP phenomena

Scaling law for R<=1 : Pinc(R) = P(R=1) * 4 / (1+R)^2 for same type of MP

Scaling with Frequency f , Coaxial Line Diameter d , Impedance Z

Pone-oint~(f*d)^4 * Z , Ptwo-point~(f*d)^4 * Z^2 ;

Example of found MP type on 'cold' side of 'cold window' DESY Version II/III TTF Coupler 9

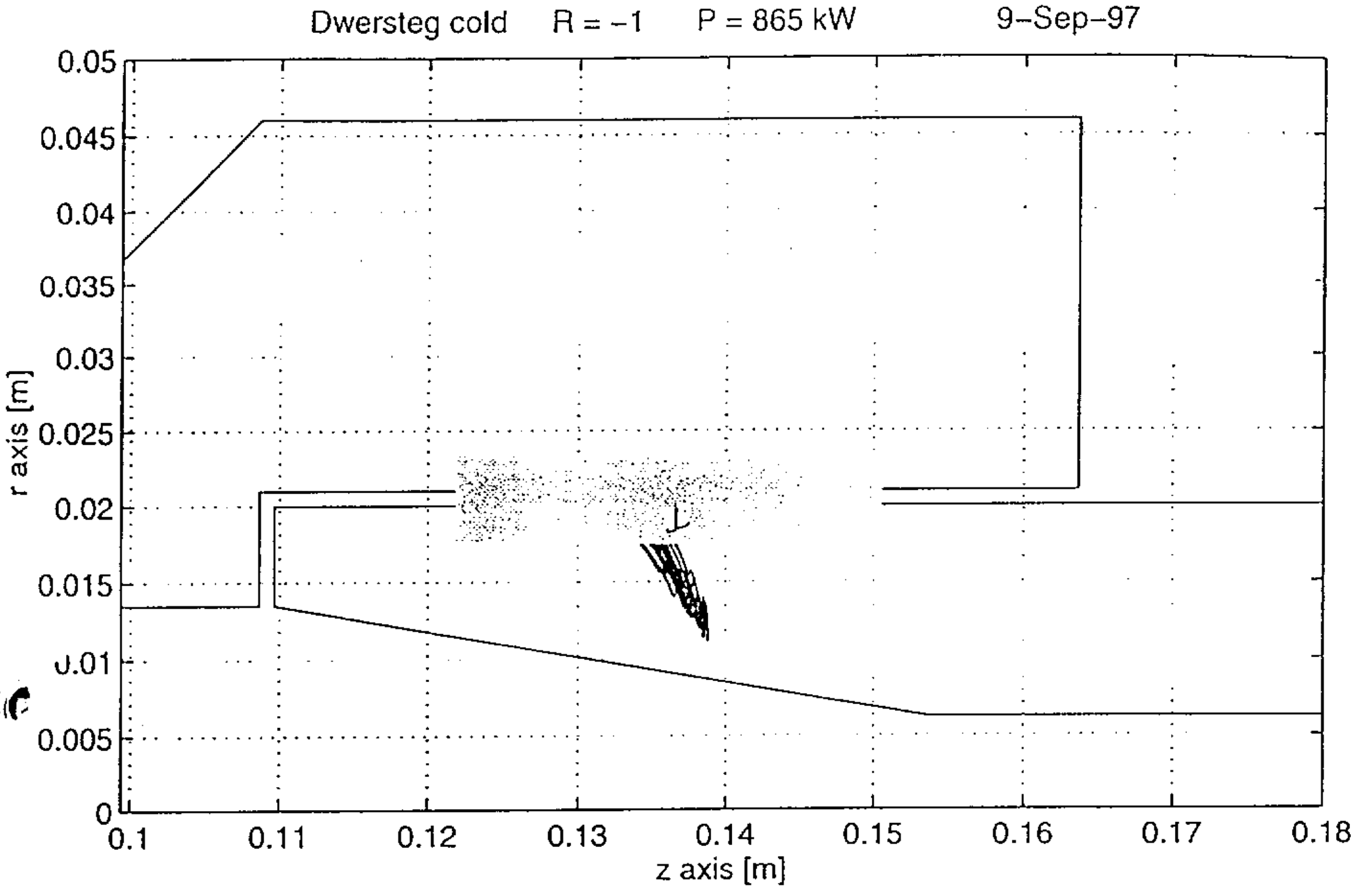

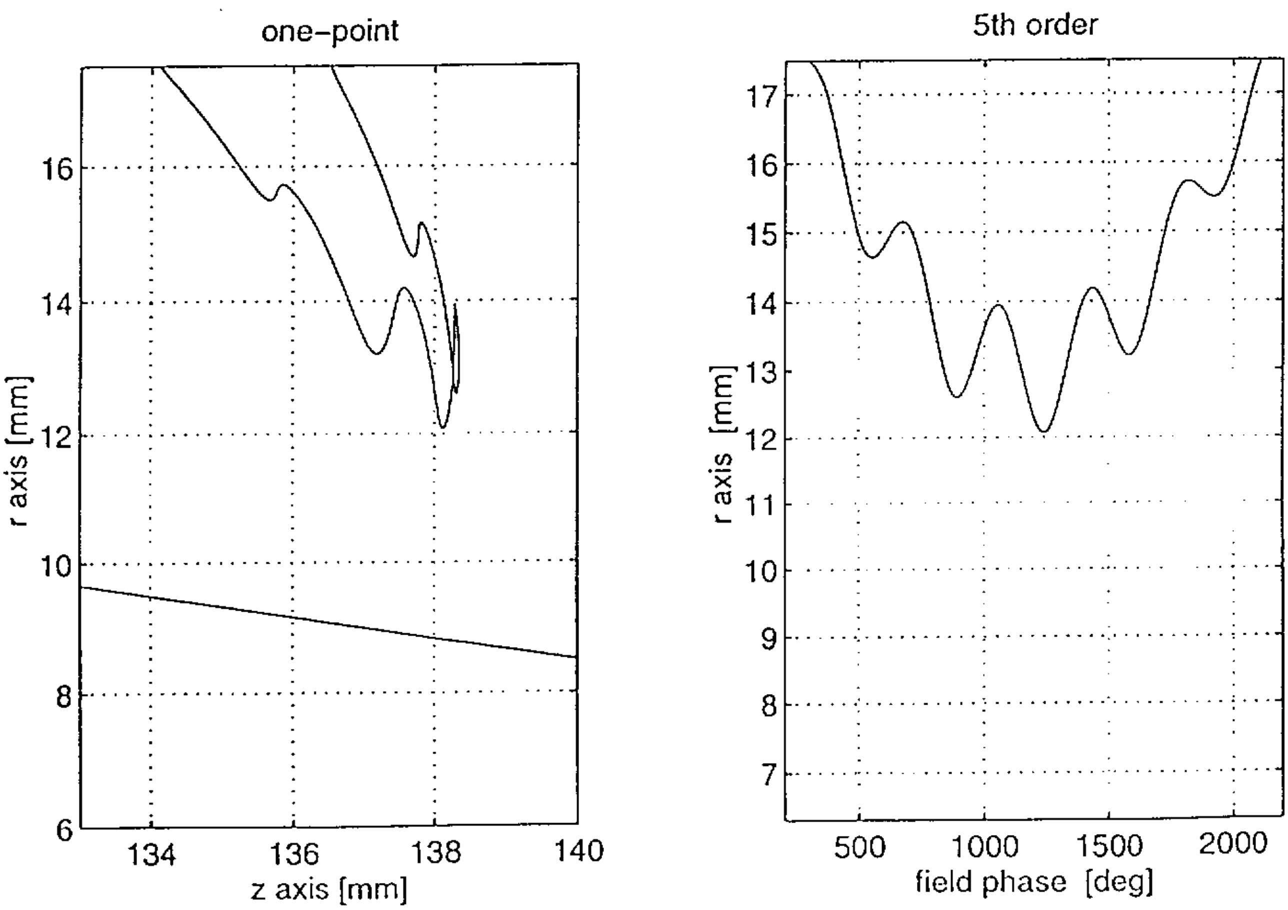

avoid conical gaps!

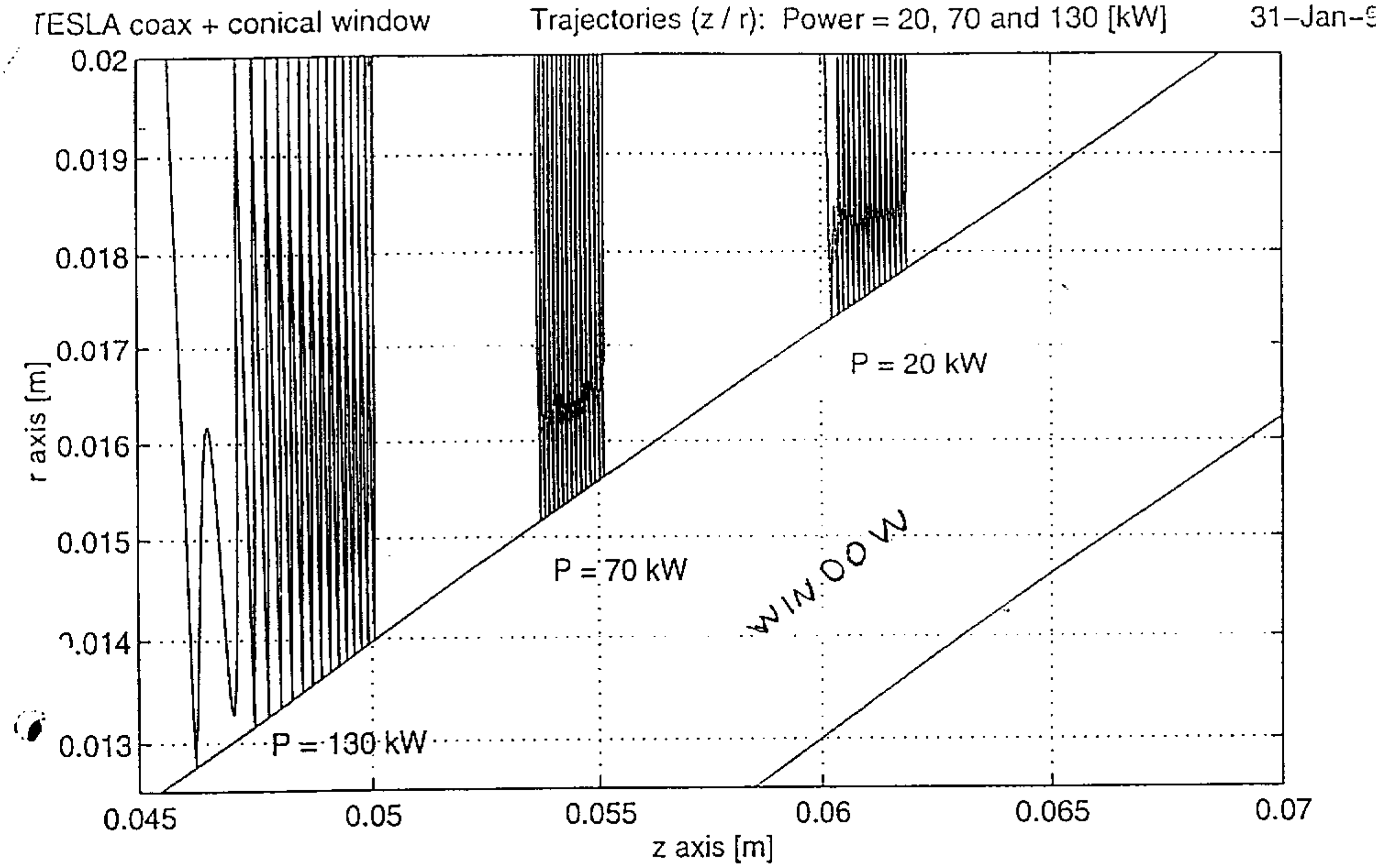

FIGURE 11A

broad band multipacting was also practically observed

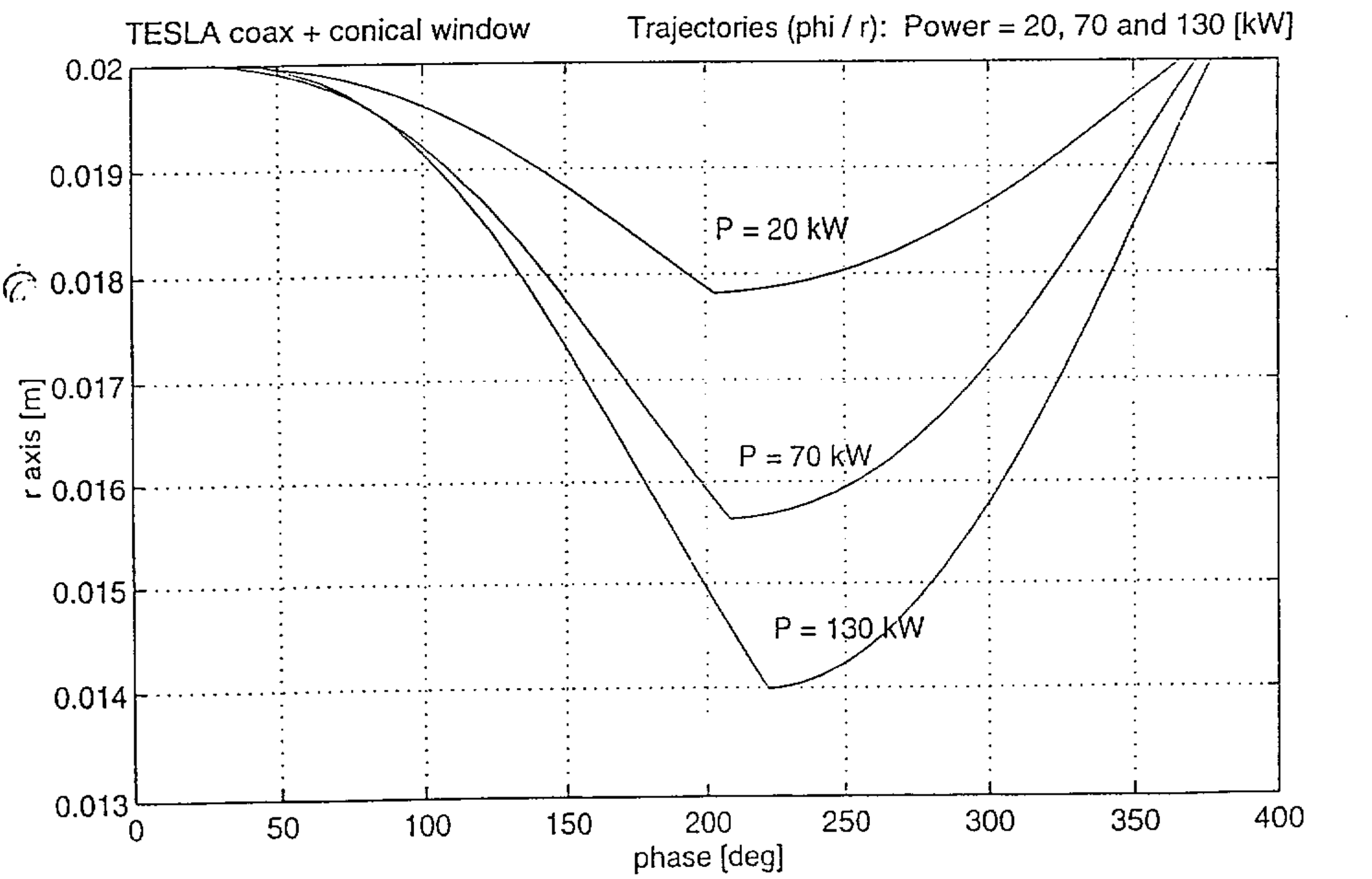

68

FIGURE 11B

Principal design of DESY TTF coupler Version IV

→ Coax-type actually under development as a possible coupler for the superstructure; similar to version III but with bigger coax diameter

the aim is to save the features of reduced price and - as expected - poor MP like Version III

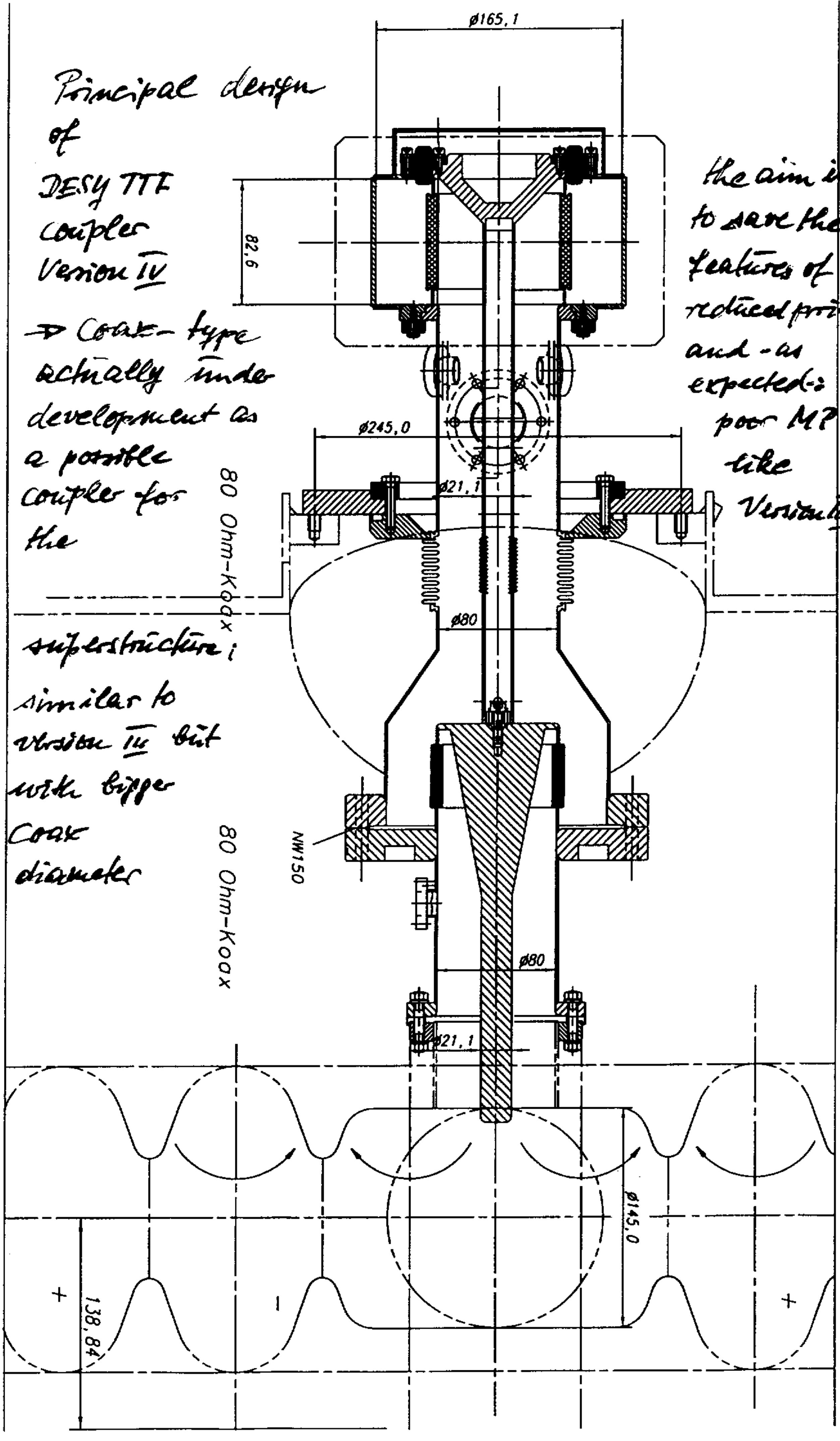

Decision for coaxial impedance at

80 mm outer coaxial diameter (1.3 GHz)

the onset of 8. th order multipacting (according to Helsinki computations is compared.

di (mm)	da (mm)	Z (Ω)	log [(f da)^4 Z]	log (P/kW)	P/kW	Coupler Type
34.8	80	50	22.5	5.47	~~397~~	
24.9	80	70	22.83	6.28	533	Choice for TTF(DESY) IV
21.9	80	80	23.95	6.393	597	
27.0	62	50	21.5	5.03	160	TTF (DESY) II
17.4	40	50	19.7	3.23	25.3	TTF (DESY) I

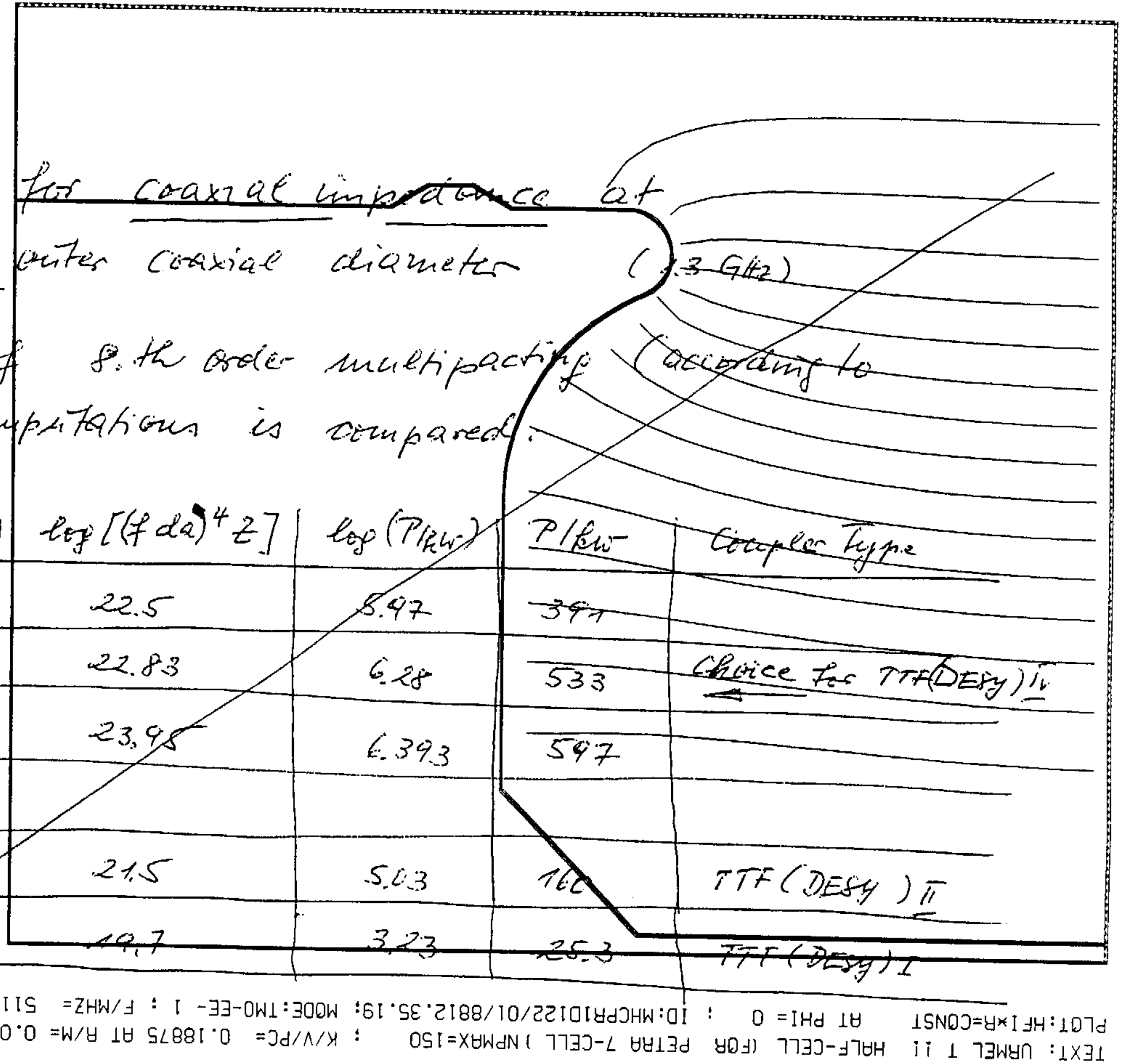

Version IV
Coupler:

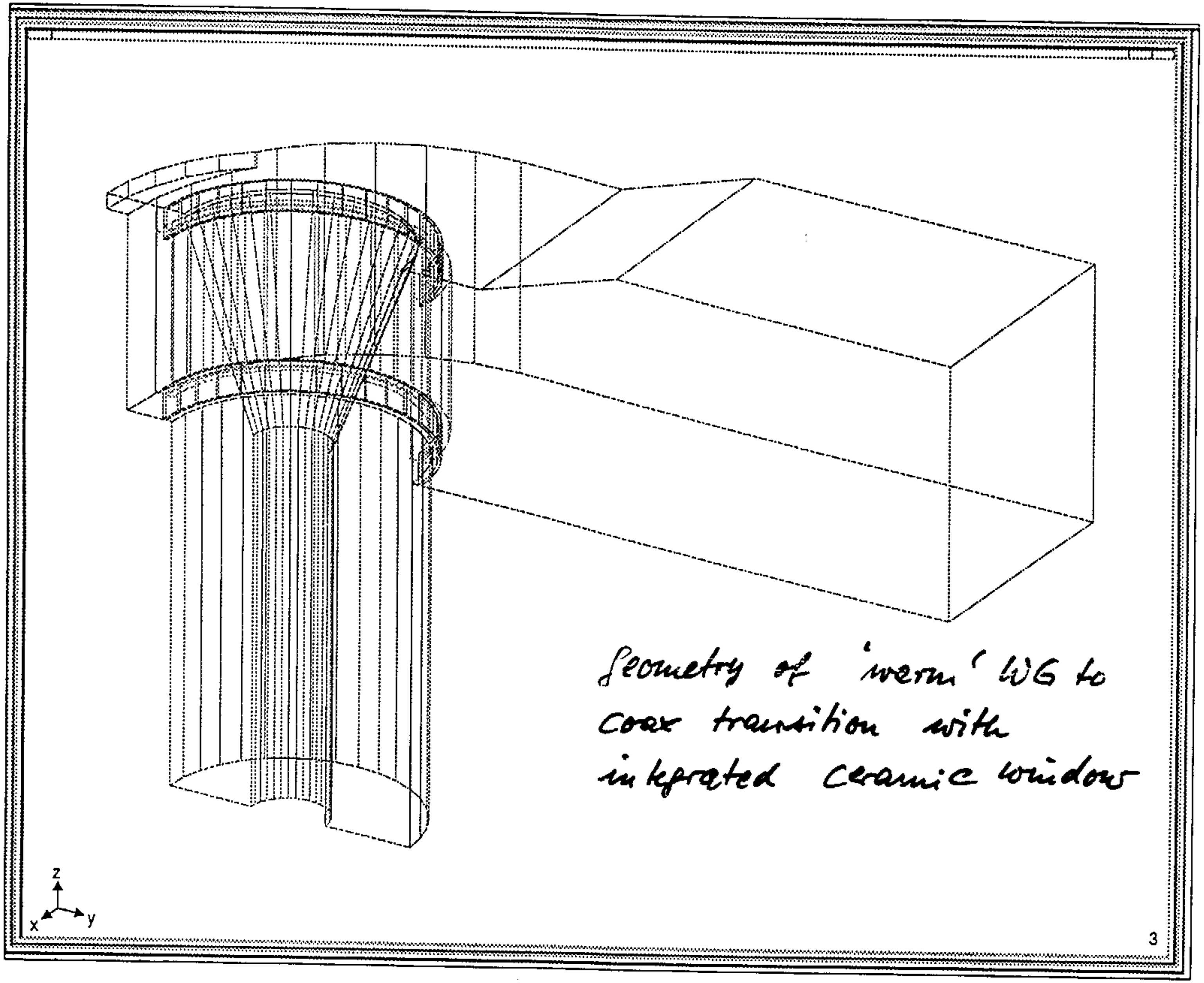

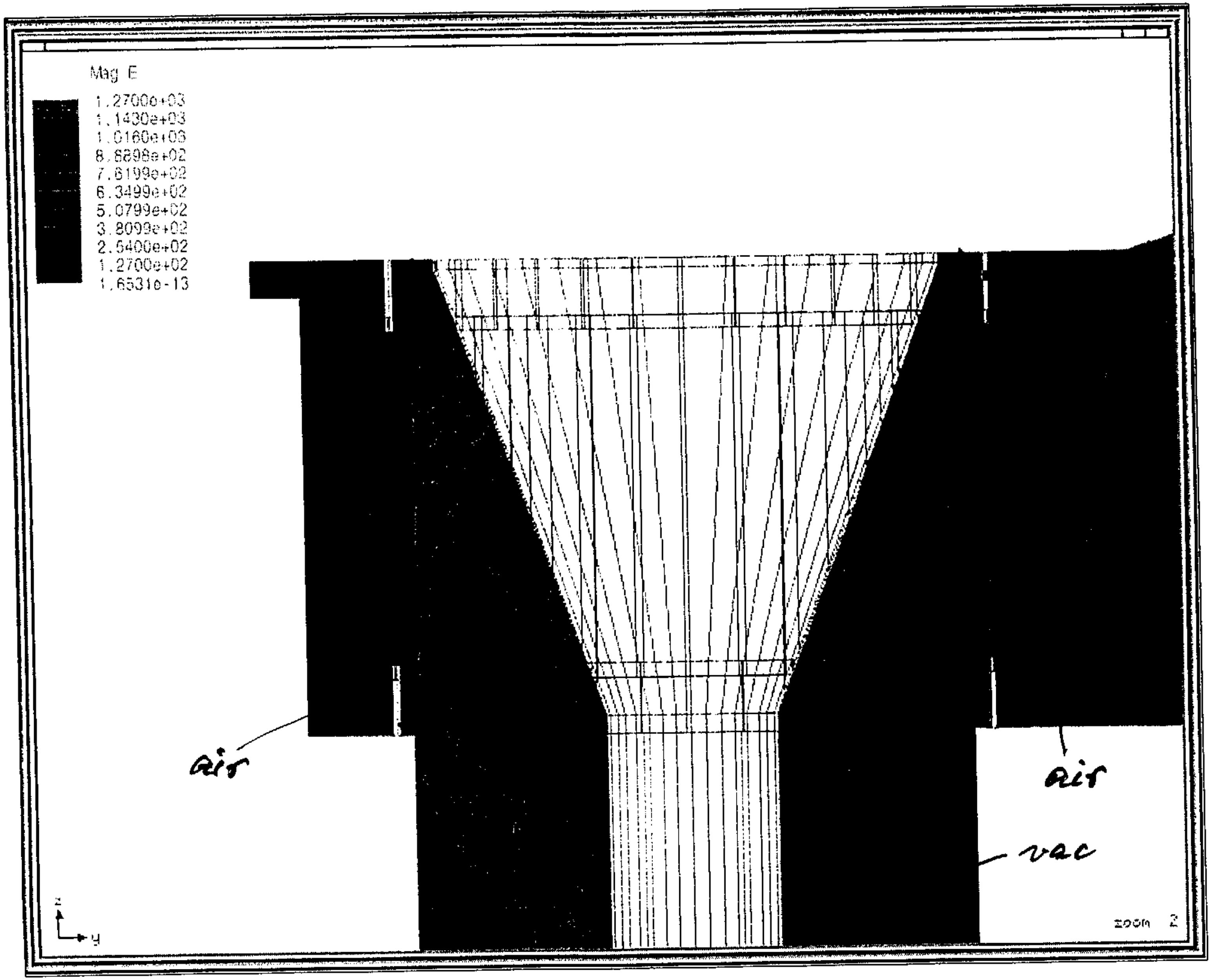

Version IV
coupler;
warm window;
electrical field
in air
roughly
1/2 of max
coax-field

72

73

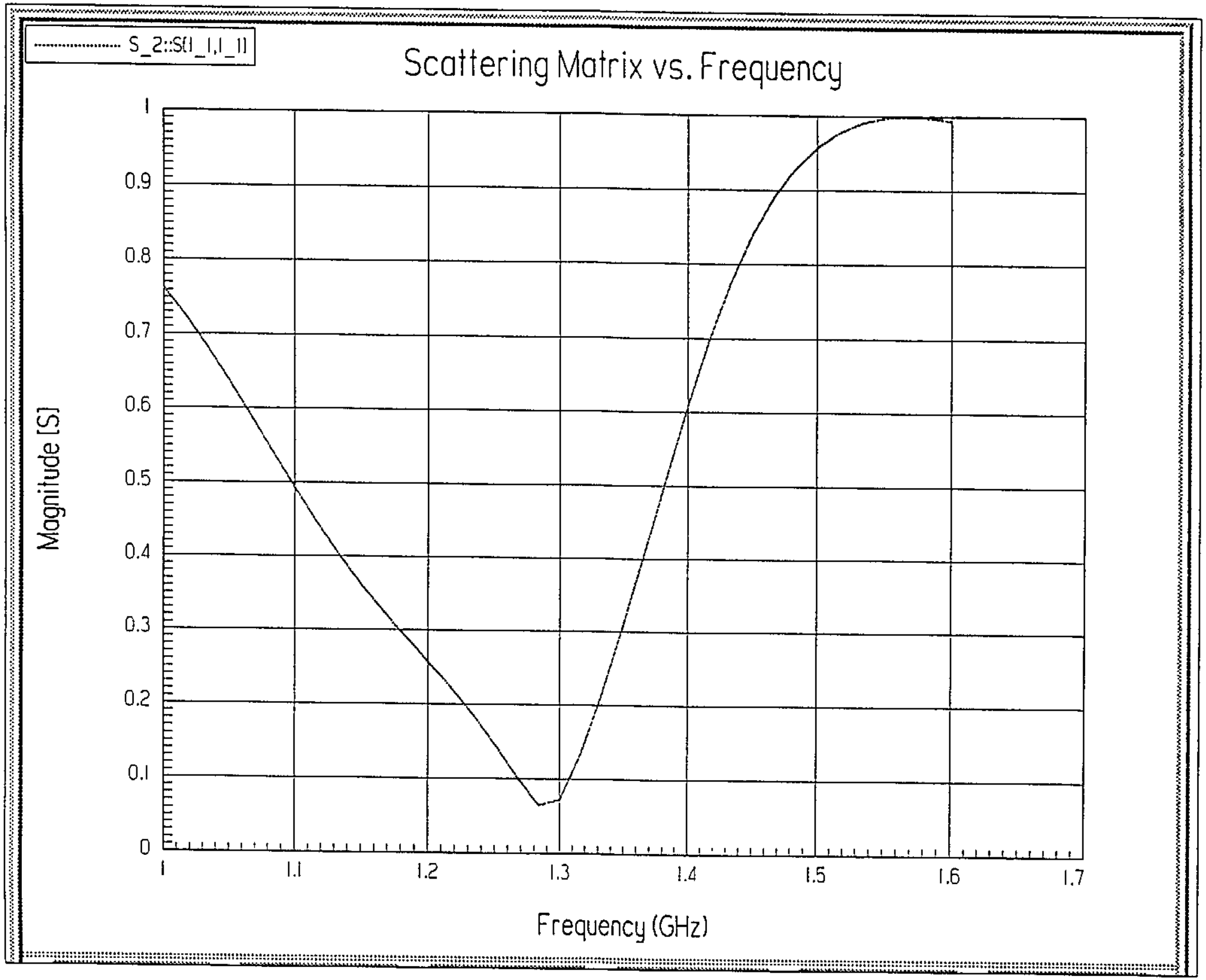

'warm window'

Version IV

Voltage reflection

TRS3

TEXT: URMEL T !! HALF-CELL (FOR PETRA 7-CELL) NPMAX=1500 ; K/V/PC= 0.03830 AT R/M= 0.0450 ; FRAME= 6
PLOT: E-FIELD AT PHI=0 ; ID: MHCPR1D123/01/8813.04.12; MODE: -EE- 1 ; F/MHZ= 874.00 ; F/FC= 0.4

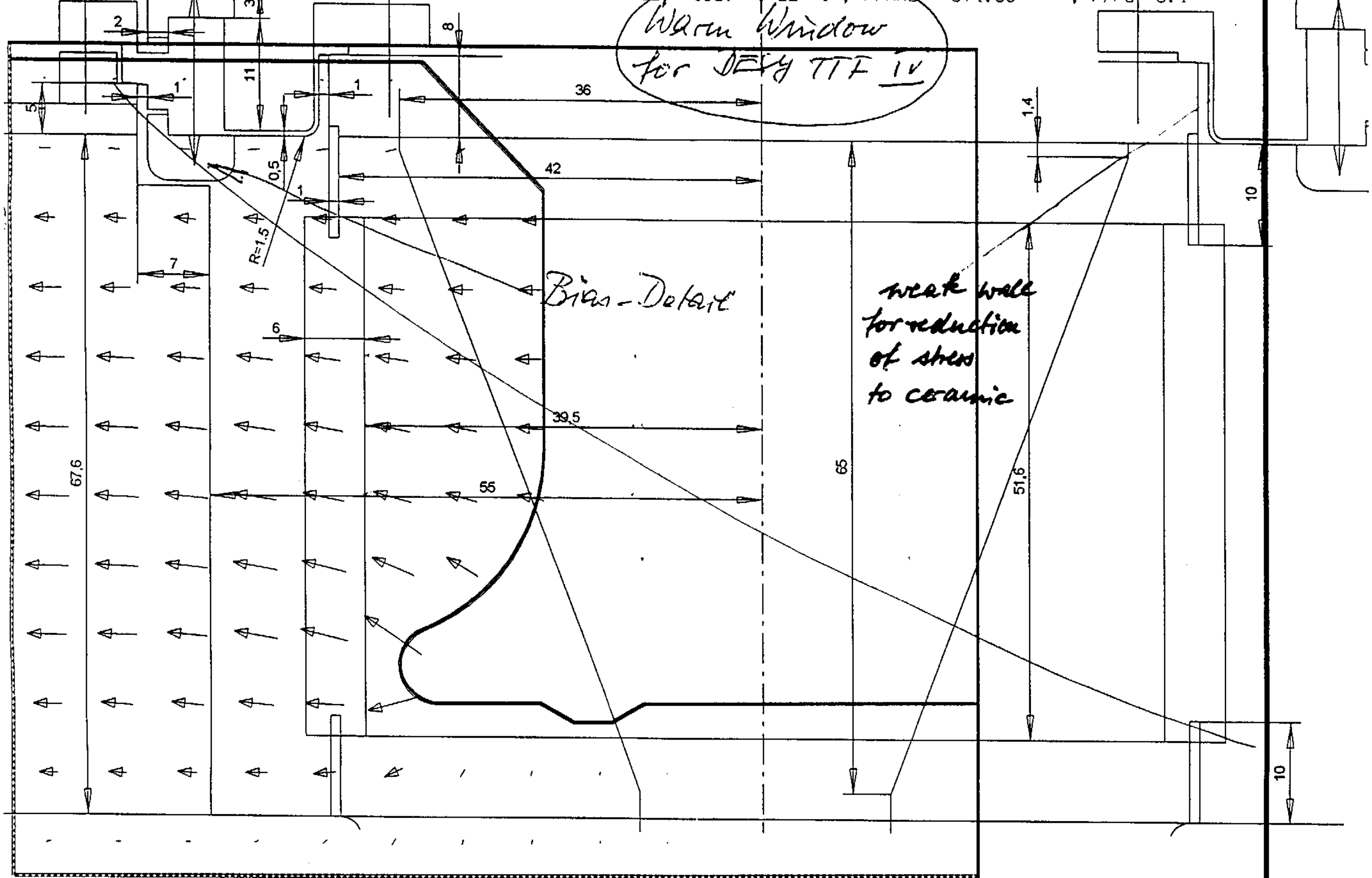

5

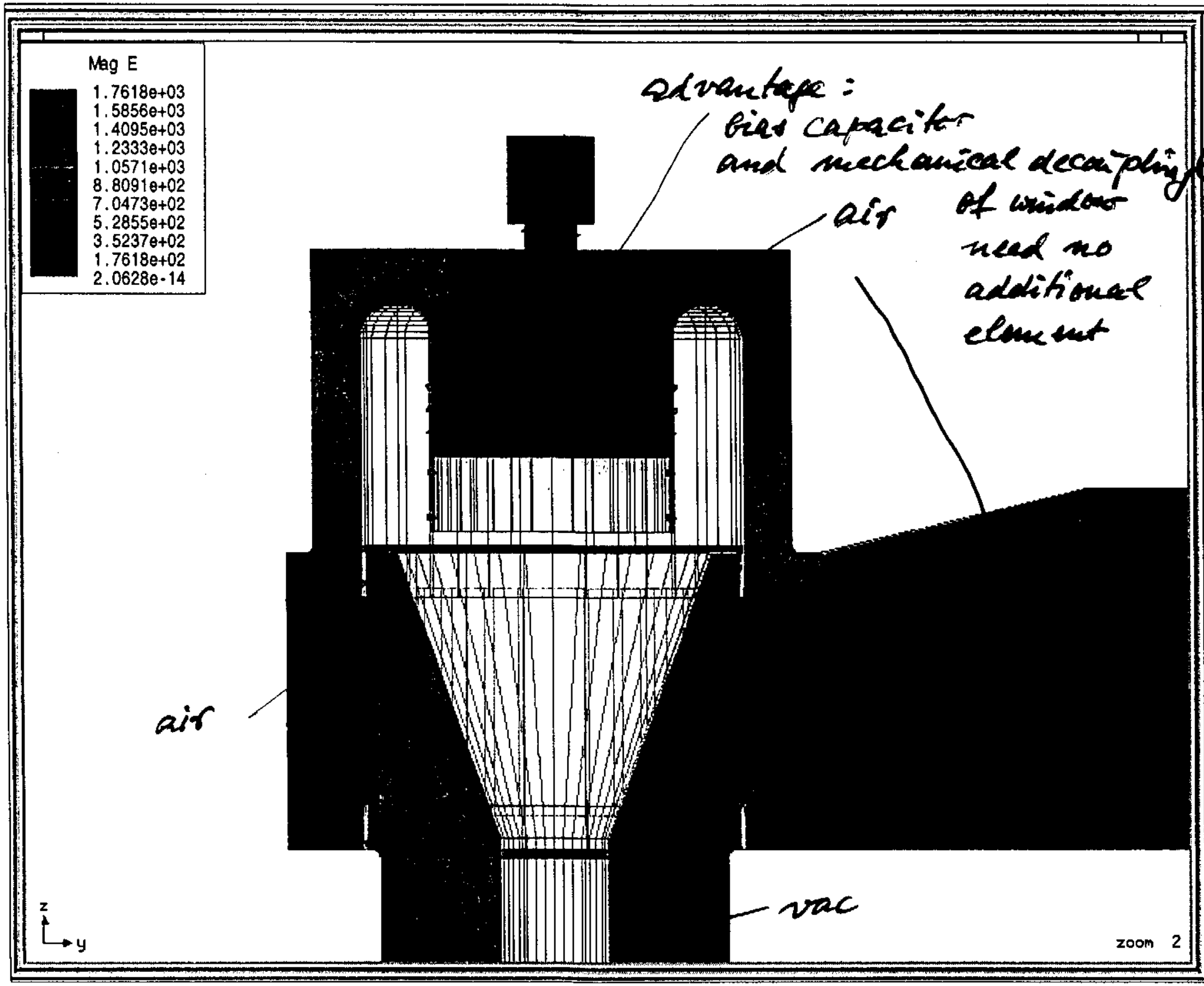

Version IV
warm window
alternative
design;
electric field
in air
equal or
higher than
coax field

TR58

75

6

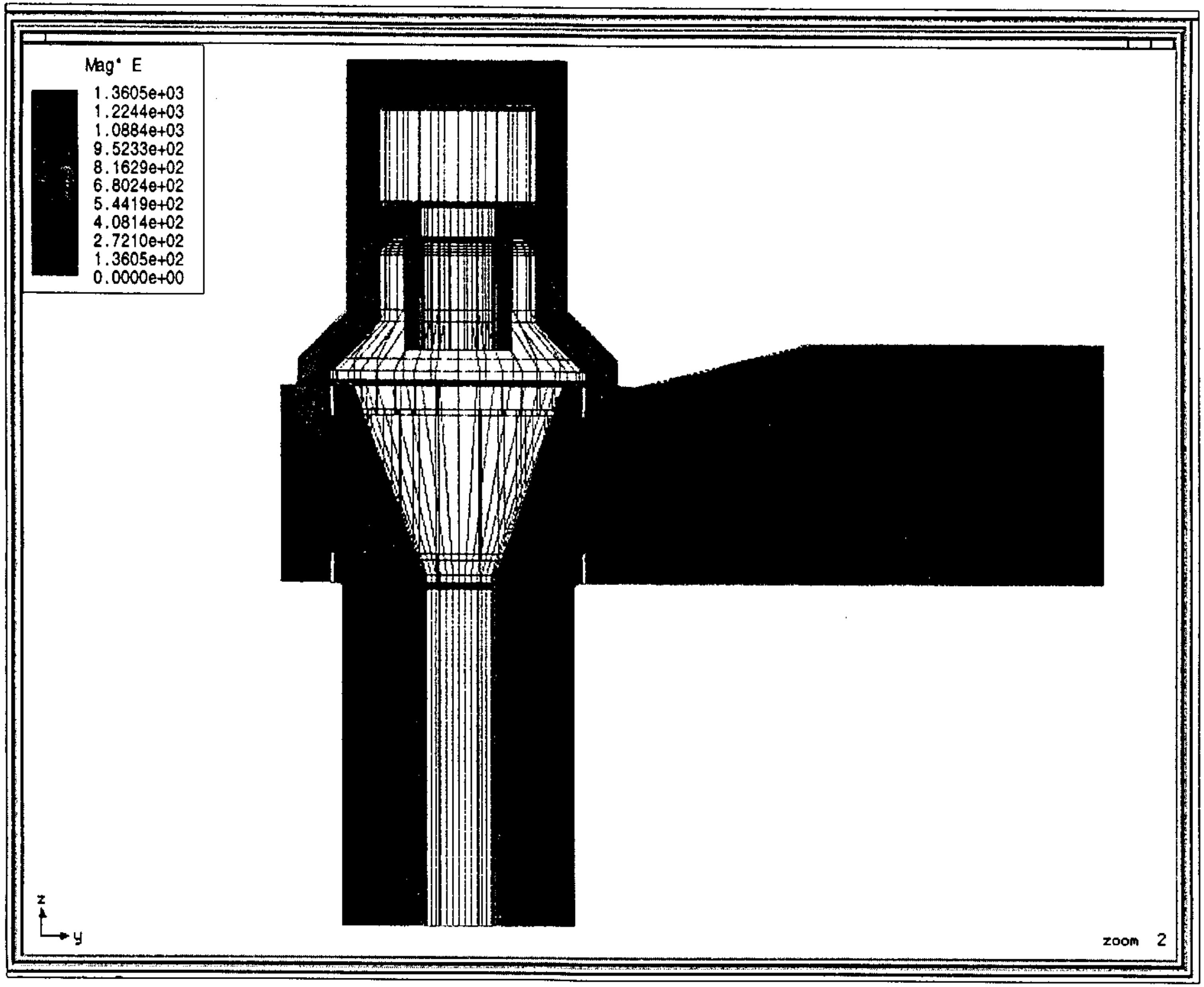

Version IV
warm window
modified
alternative
design

comments
like TR 58

TR57

76

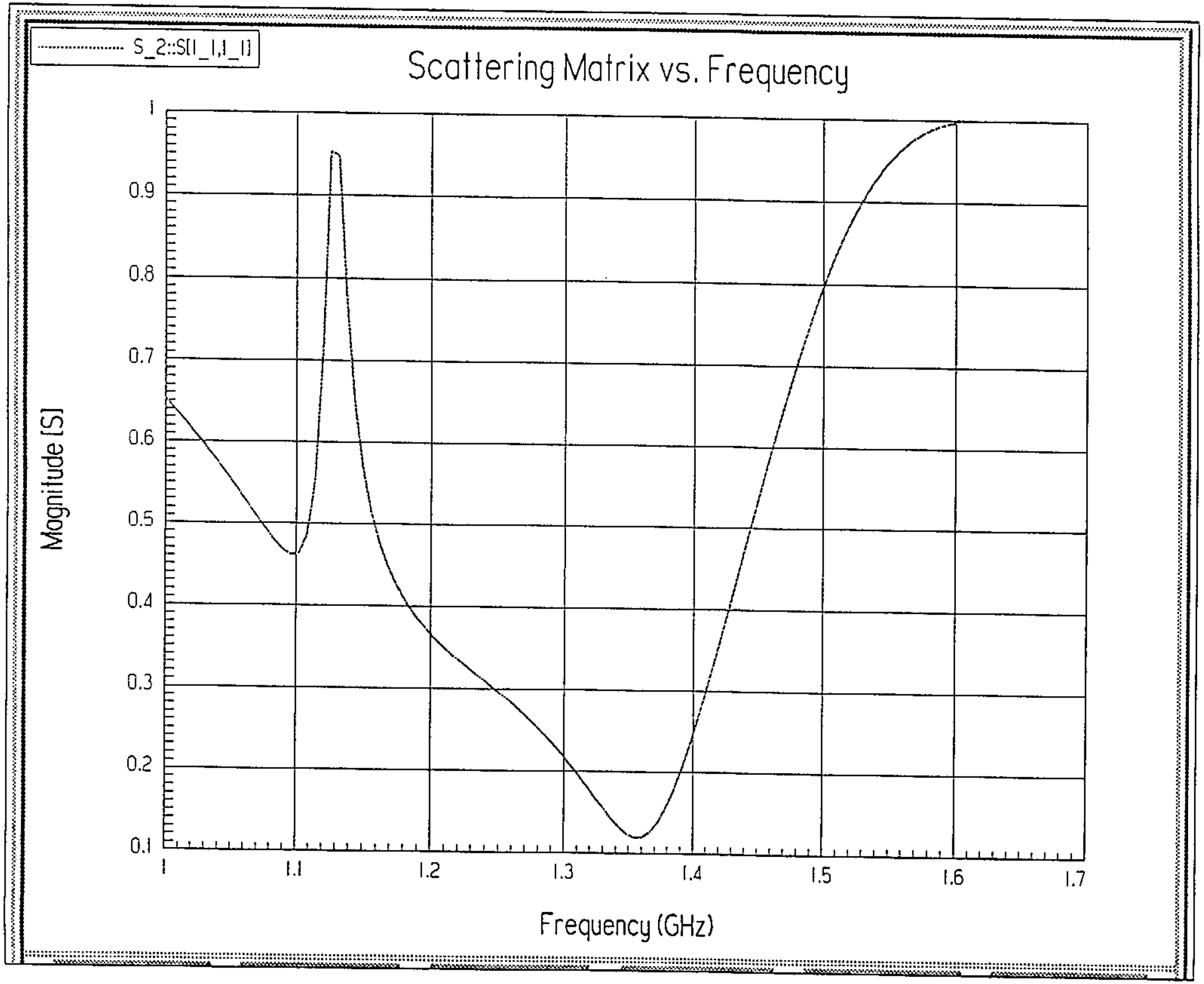

warm window version IV; reflection vs frequency of modified alternative design

Fig. 57

MAFIA	FRAME: 2	16/11/93 - 10:14:07	VERSION(V4.010)	DT21.DRC
	FREQUENCY	1.3000000000000E+09		R10=40.00, Z1_01=120, R1_56=1.0, R1_34=34.0, FA1_12=55.0;
	AZIMUTHAL ORDER	0.0000000000000E+00		R20=12.45, Z2_89=120, R3_23=6.0, R2_67=8.0 , FA2_37=60.0;
	SAMPLE TIME	7.4999997323744E-09		Z2_27=3.5, Z1_23=75, Z1_45=15, Z2_56=15, Z2_34=16, Z3_12=35.0;
				ELECTRIC FIELD IN V/M

P--:4010

#ARROW

COORDINATES/M
FULL RANGE / WINDOW
R[0.0000, 0.075000]
 [0.0000, 0.075000]
Z[0.0000, 0.28579]
 [0.0000, 0.28579]

SYMBOL = ECOMP
INTERPOLATE.= 0
LOGSCALE....= 2.0000
ITIME.......: 15015
TIME......: 7.50000E-09
MAX ARROW = 780.99

70 Ω cold window for
DESY Type TTF Coupler Version IV

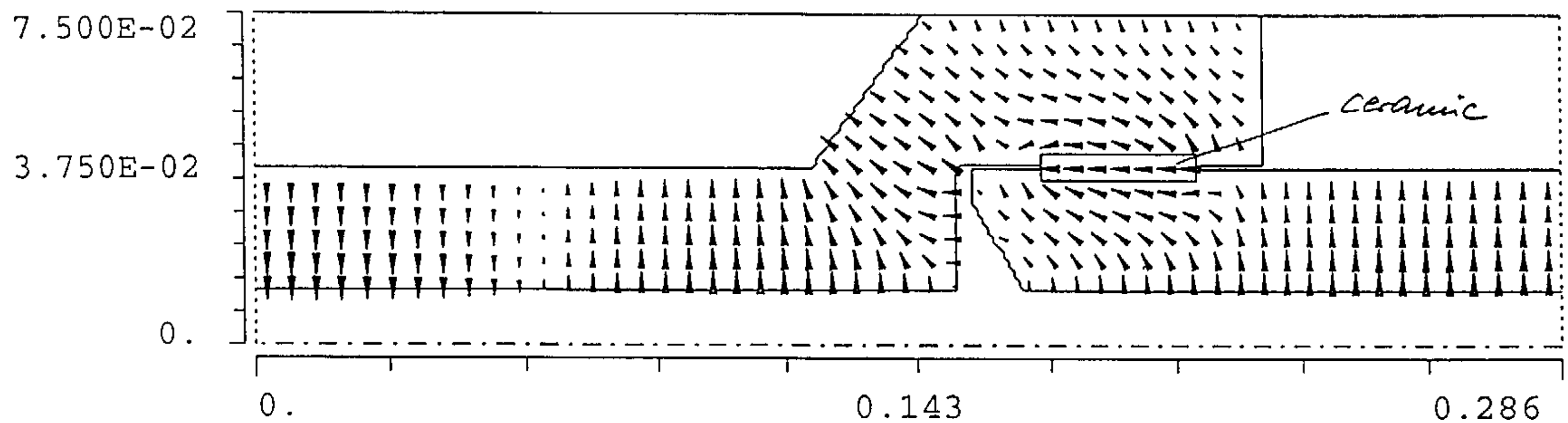

The electric field around and inside the ceramic is mainly axial. Its field strength is roughly 1/2 of the coaxial field.
→ parallel to the ceramic surface and thus will not support MP on the ceramic surface

MAFIA

FRAME: 1 16/11/93 - 10:17:13 VERSION(V4.010) DT21.DRC

R10=40.00, Z1_01=120, R1_56=1.0, R1_34=34.0, FA1_12=55.0;
R20=12.45, Z2_89=120, R3_23=6.0, R2_67=8.0 , FA1_37=60.0;
Z2_27=3.5, Z1_23=75, Z1_45=15, Z2_56=15, Z2_34=16, Z3_12=35.0;
(SREFLAM_F16*(AFACTOR))/(SINCAM_F16*(BFACTOR))

P--:4010

#1DGRAPH

ORDINATE: S11AM
COMPONENT: -

FIXED COORDINATES:
DIM..........MESHLINE
- 1
N 1

ABSCISSA: SCATTIME_F_16
(BASE OF S11AM)

REFERENCE COORDINATE: F
VARY..........MESHLINE
FROM 1
TO 65536

70 Ω cold window for DESY Type TTF Coupler version IV

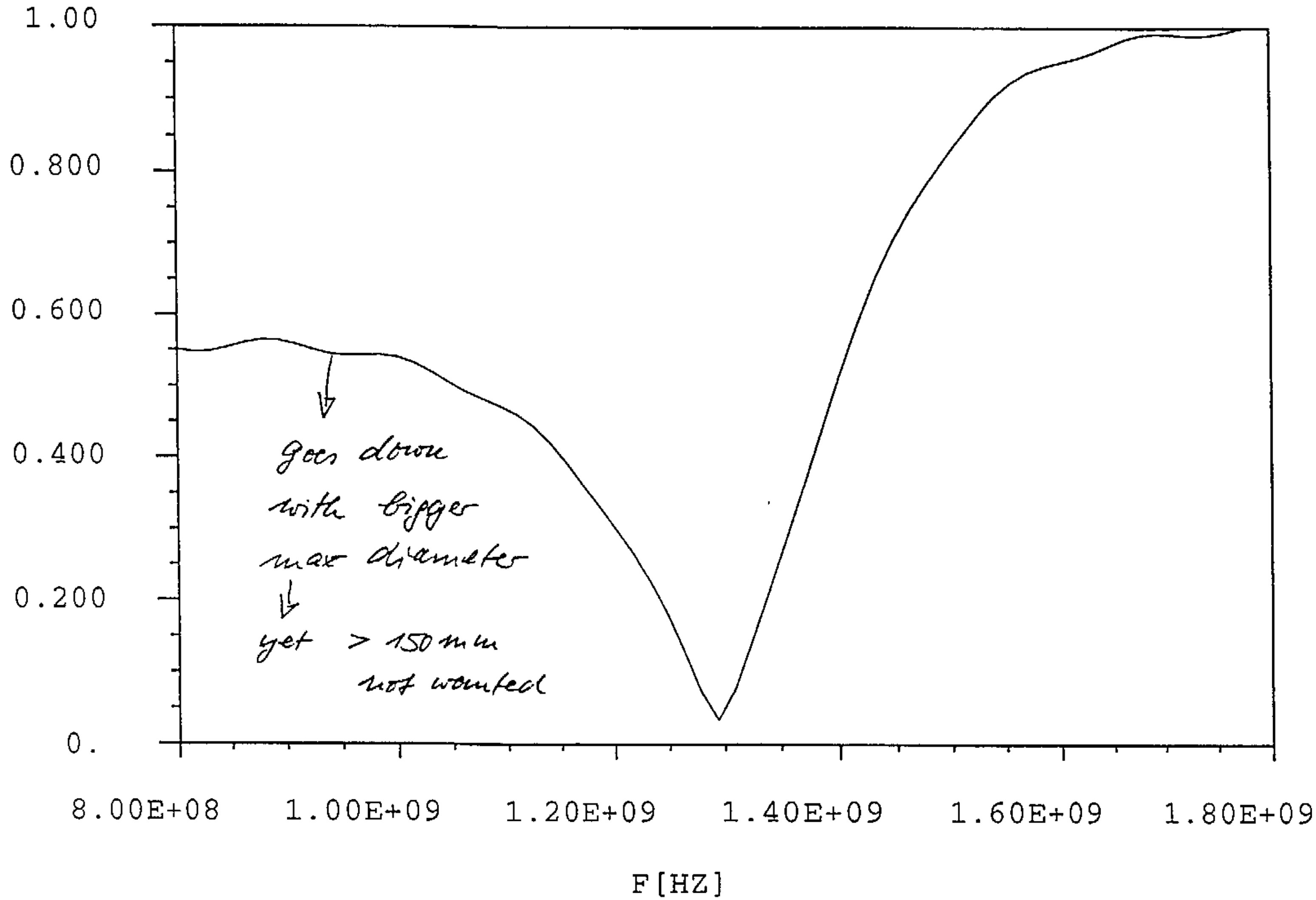

11

Rech 4

4

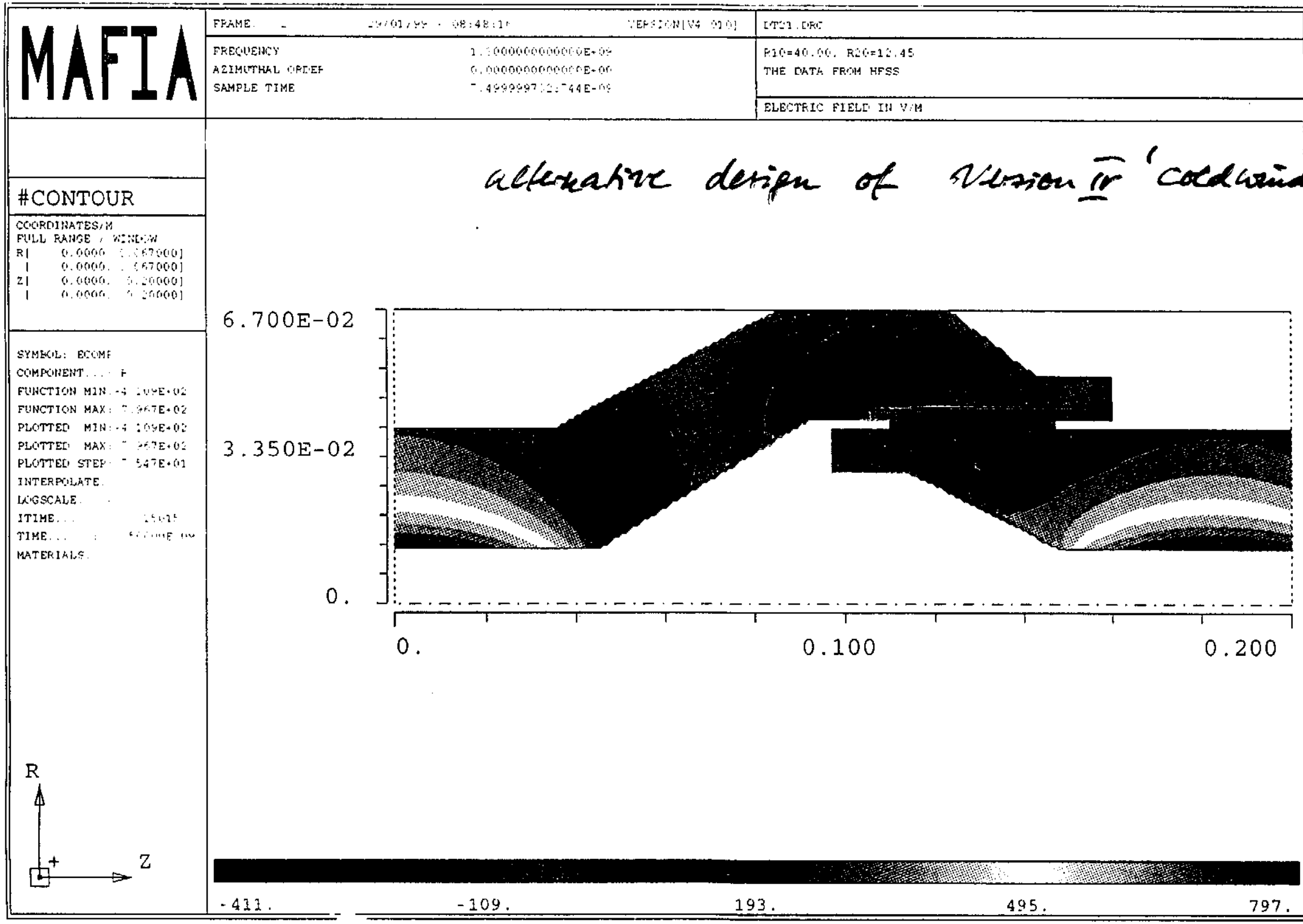

80

(19)

CHENHE & SOLAR03, JAN29/08:54

MAFIA

FRAME: 2 29/01/99 - 06:47:02 VERSION[V4.010] DT21.DRC

FREQUENCY	1.3000000000000E+09	R10=40.00, R20=12.45
AZIMUTHAL ORDER	0.0000000000000E+00	THE DATA FROM HFSS
SAMPLE TIME	7.4999997323744E-09	ELECTRIC FIELD IN V/M

P--:4010

#ARROW

COORDINATES/M
FULL RANGE / WINDOW
R[0.0000, 0.067000]
(0.0000, 0.067000]
Z[0.0000, 0.20000]
(0.0000, 0.20000]

SYMBOL = ECOMP
INTERPOLATE.= 0
LOGSCALE....= 2.0000
ITIME.......: 15015
TIME......: 7.50000E-09
MAX ARROW = 599.64

alternetive design of Version IV 'cold window';
advantages: no edges → smooth contour, low fields
outer diameter not so big

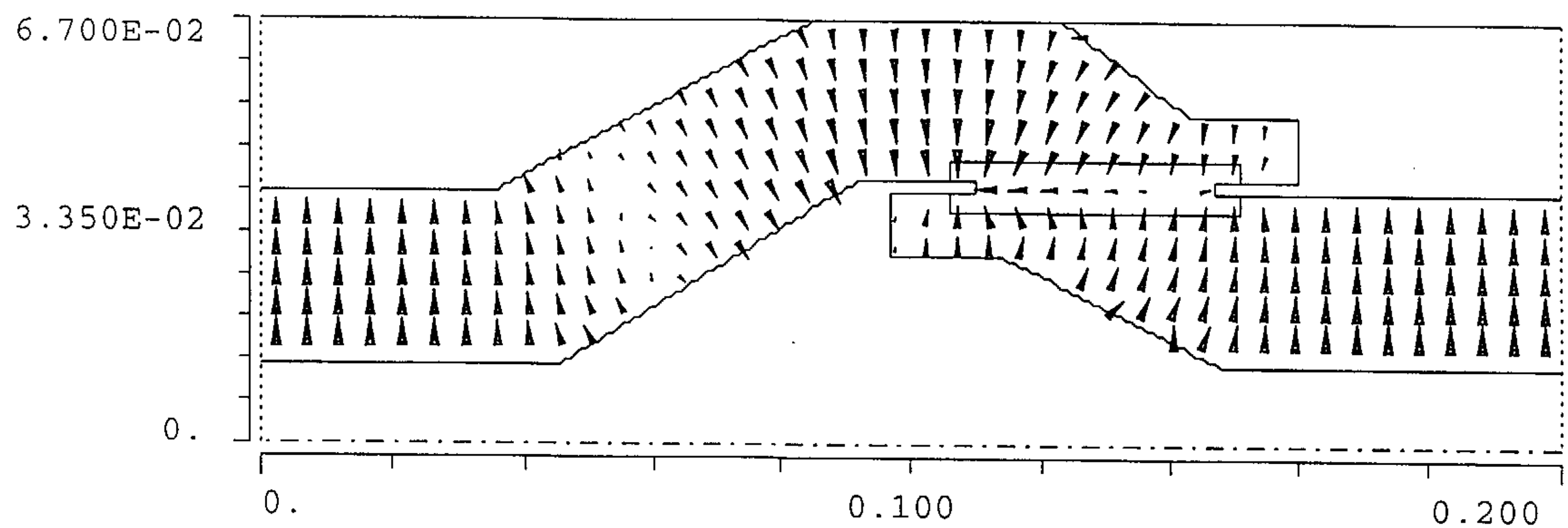

The electric field around and inside the ceramic is mainly radial and normal to the ceramic. It's field strength is roughly 50% of the coaxial field.

Smoothend edges reduce peak fields.

disadvantage: Conical areas lead to more multipacting (compare to Helsinki comp.) together with field direction normal to the ceramic

81

(20)

3

82

Calculation of Coupling Elements of Coaxial and Waveguide Input Couplers for Superstructure

A. Zavadtsev
DESY MHF-SL

Introduction

The input coupler consists of

- warm window disposed at 300 K temperature (it may be combined with waveguide-coaxial transition for coaxial coupler);
- cold window disposed at 70 K temperature;
- connecting transmission lines;
- coupling element.

The questions of the windows and the transmission lines are described in [1, 2 and others]. The windows for the coaxial coupler were calculated and the results will be presented at this meeting.

This report is devoted to the calculation of coupling elements for the coaxial and waveguide input couplers only.

1. Calculation Method

The input coupler is connected to one end of the accelerating cavity. It may be 9-cells TTF cavity or 4*7-cells Superstructure. The needed $Q_{ext}=3*10^6$ for TTF and $Q_{ext}=2.12*10^6$ for Superstructure. The own Q-factor $Q_0>5*10^9$.

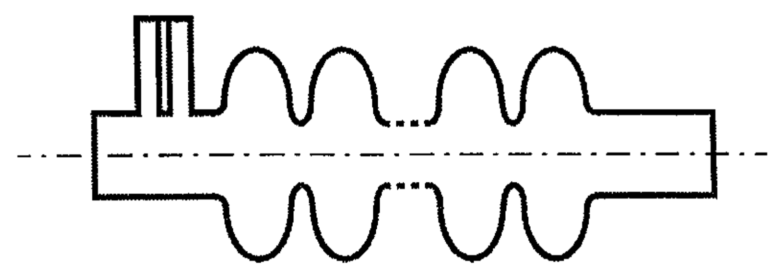

Let's assume that the second same coupler is installed at the second end of the cavity.

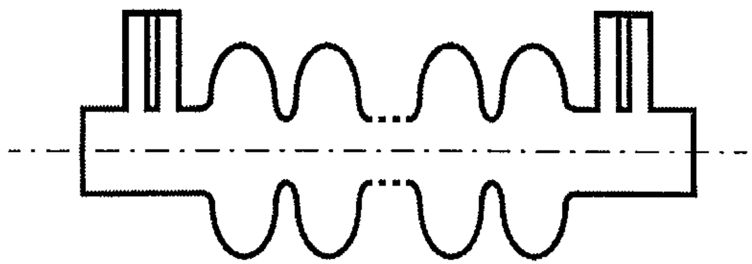

The loaded Q-factor of this cavity is

$$Q_L = \frac{1}{2} \cdot Q_{ext} \cdot \frac{1}{1 + \frac{Q_{ext}}{2 \cdot Q_0}} \approx \frac{1}{2} Q_{ext}$$

83

The power transition through the cavity is

$$S_{21}^2 = \frac{4Q_L^2}{Q_{ext}^2} \cdot \frac{1}{1 + \left(2Q_L \cdot \frac{f - f_0}{f_0}\right)^2} \approx \frac{1}{1 + \left(Q_{ext} \cdot \frac{f - f_0}{f_0}\right)^2}$$

We may calculate $S_{21}(f)$ for this model without losses in the walls in frequency range and find Q_{ext}.

This model has zero reflection, that corresponds to the beam acceleration case. Therefore we may calculate the electric and magnetic field and use them for the beam dynamic calculation.

There are two ways to speed up these calculations.

The first way is to calculate this model with one cell only.

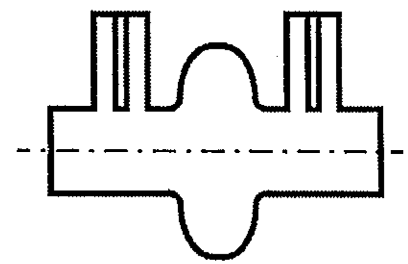

This cell consists of two end half-cells of the cavity. We may calculate external Q-factor Q_{ext1} of this cavity, which is coupled with Q_{ext} of the cavity by following formula:

$$Q_{ext} = Q_{ext1} \cdot \frac{W_{cav}}{W_1}$$

where W_{cav} and W_1 are the stored energies in the cavity and in one cell of this model. We should know W_{cav}/W_1 calculated by some method.

The second way is to calculate two models with two couplers. The first model consists of two end cells of the cavity.

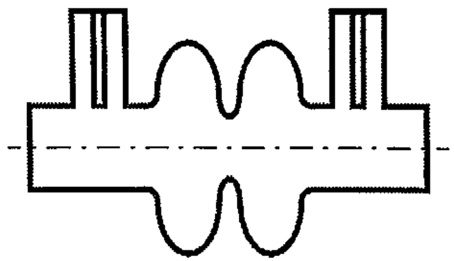

The second model consists of two end cells and one inner cell of the cavity.

84

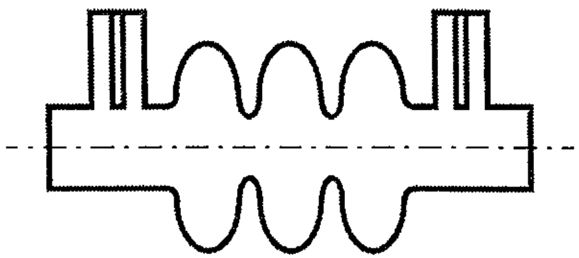

We may calculate external Q-factors of these models Q_{ext2} and Q_{ext3} by described method. The external Q-factors of 9-cells cavity and 4*7 cells Superstructure may be find by following formulas:

$$Q_{ext} = 7Q_{ext3} - 6Q_{ext2}$$

$$Q_{ext} = 20Q_{ext3} - 16Q_{ext2}$$

2. Calculation Results

The coupling elements for following input couplers were calculated:

1. TTF input coupler Version I (TTF-I).

2. TTF input coupler Version II (TTF-II).

3. Superstructure coaxial input coupler (SS-CC). 80 mm 70 Ohm coaxial transmission line. 4*7 cells Superstructure [2]. The sizes of Superstructure were got from [3].

4. Superstructure waveguide coupler (SS-WC). The distance from Superstructure axis to the waveguide short is equal to $\Lambda/4$.
5. Superstructure symmetrical waveguide coupler (SS-SWC). The coupling element consists of the rectangular waveguide with shorted end intersecting with the beam pipe of Superstructure and the wall in the centre of the waveguide. This wall

a) divides power flow and forces the power to come into Superstructure through two symmetrical holes and

b) close the waveguide cavity so that the cold ceramic window is not seen from the beam axis.

One of main parameters of the input coupler is the electromagnetic kick for the beam. Of course the correct conclusion about this kick may be done after beam dynamic calculation using calculated fields in the coupling element. The field axis transverse shift is considered in this paper only. The kick depends on the transverse electric and magnetic fields at the beam axis. These fields are equal to zero at the axis of the structure without the input coupler and increase linearly with transverse coordinate. Therefore the field axis shift in the input coupler region may be used for the comparison of different coupling elements.

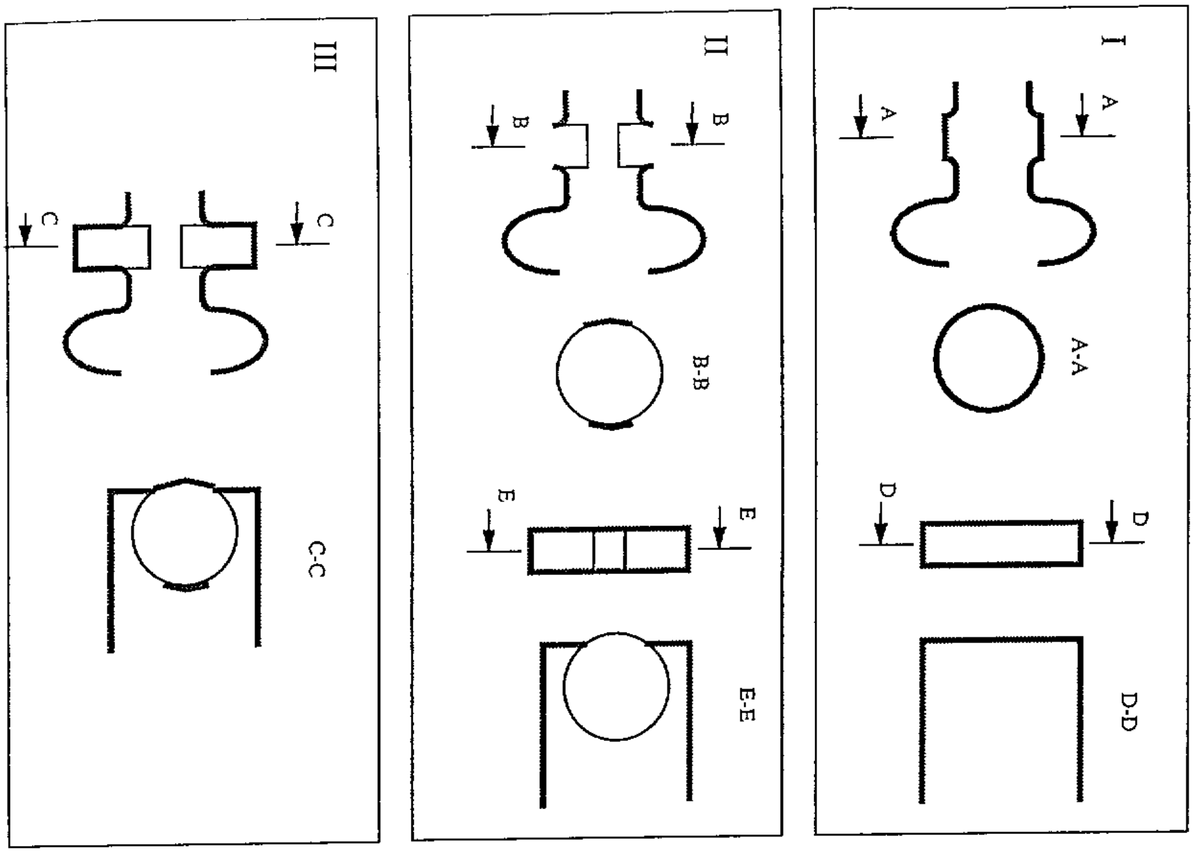

SS-SWC scheme forming.

Table 1: Calculated Input Couplers Parameters.

Parameter	TTF-I	TTF-II	SS-CC	SS-WC	SS-SWC
Transmission line	40 mm 50 Ohm	40 mm 70 Ohm	80 mm 70 Ohm	165x30 mm	165x30 mm
Distance between centre of 1-st cell and axis of line (y_0), mm	101	101	130	173	107
Electric field at structure axis in coupler plane related to cell field	0.063	0.063	0.076	0.018	0.100
Distance between structure axis and end of inner conductor (or short for SS-WC) (z_0), mm	34.2	33.8	54.7	80	-
Full width of wall (x_0), mm	-	-	-	-	40
$10^{-6}dQ_{ext}/dy_0$, mm^{-1}	0.78	0.78	0.10	0.18	0.18
$10^{-6}dQ_{ext}/dz_0$, mm^{-1}	0.67	0.40	-	0.021	-
$10^{-6}dQ_{ext}/dx_0$, mm^{-1}	-	-	-	-	0.29
Shift of field axis, mm	0.9	0.9	1.8	6	0.8

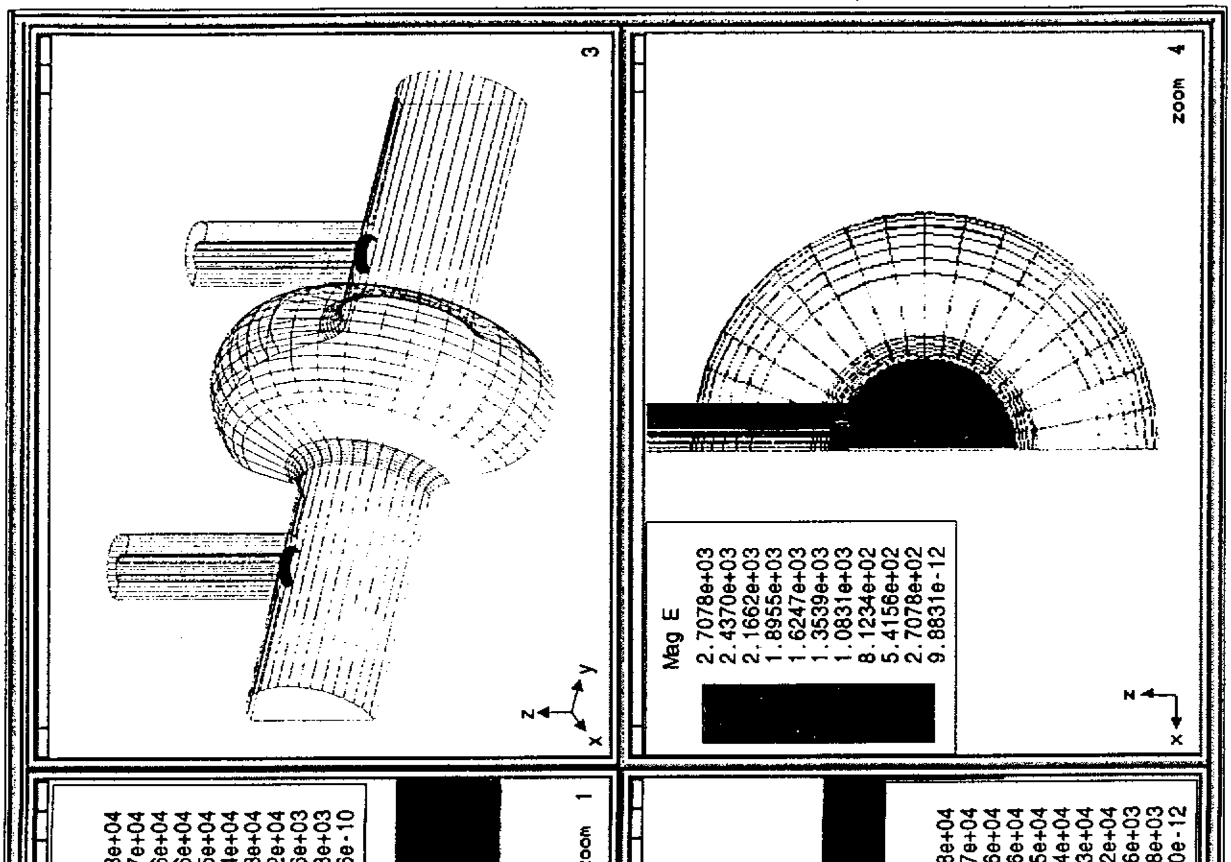
Mag E
3.4208e+04
3.0787e+04
2.7366e+04
2.3946e+04
2.0525e+04
1.7104e+04
1.3683e+04
1.0262e+04
6.8416e+03
3.4208e+03
4.3156e-10
zoom 1
y
x
3
z
y
x
Mag E
3.4208e+04
3.0787e+04
2.7366e+04
2.3946e+04
2.0525e+04
1.7104e+04
1.3683e+04
1.0262e+04
6.8416e+03
3.4208e+03
5.1640e-12
z
y
Mag E
2.7078e+03
2.4370e+03
2.1662e+03
1.8955e+03
1.6247e+03
1.3539e+03
1.0831e+03
8.1234e+02
5.4156e+02
2.7078e+02
9.8831e-12
zoom 4
z
x

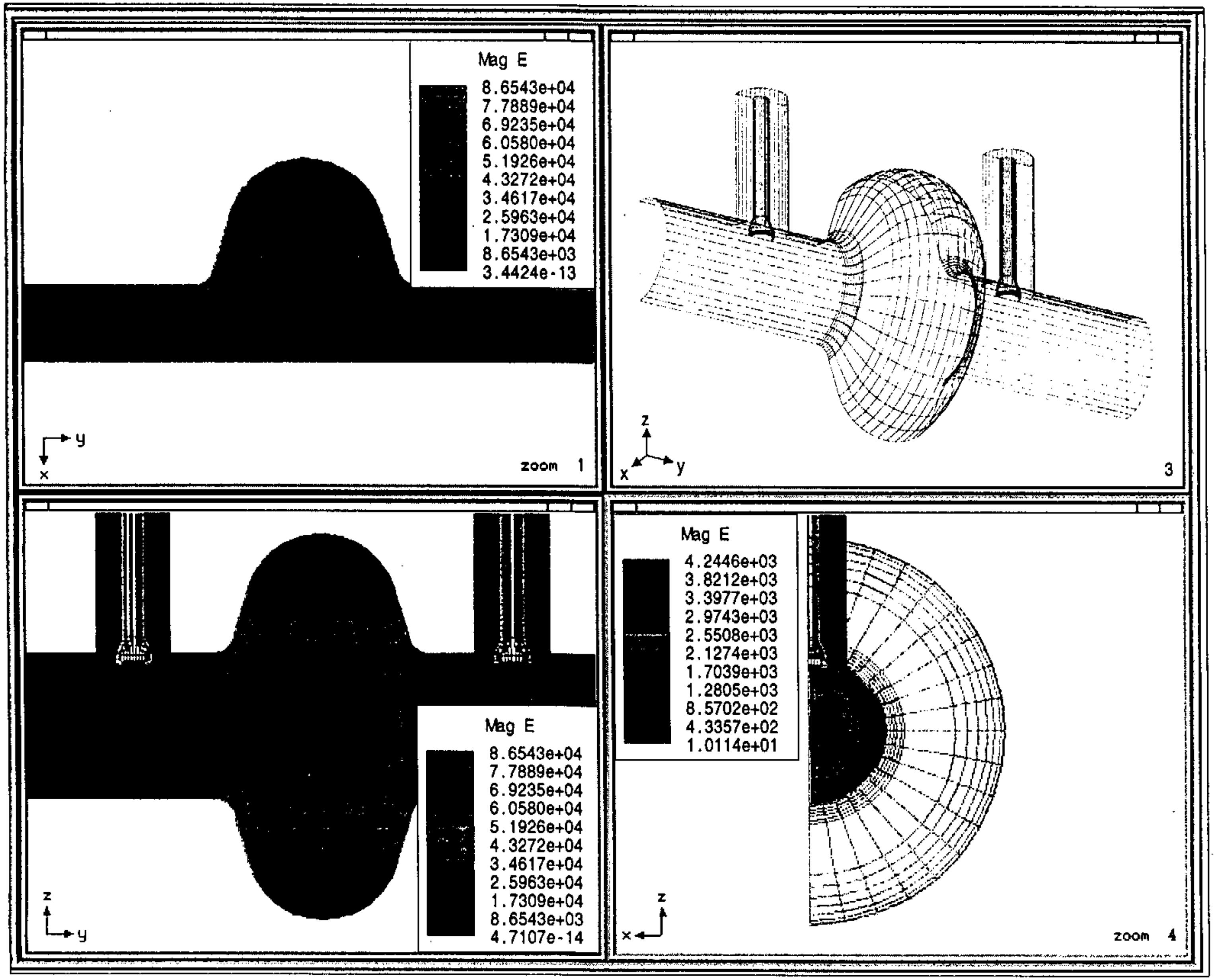
Mag E
8.6543e+04
7.7889e+04
6.9235e+04
6.0580e+04
5.1926e+04
4.3272e+04
3.4617e+04
2.5963e+04
1.7309e+04
8.6543e+03
3.4424e-13
y
x
zoom 1
z
x
y
3
z
y
Mag E
8.6543e+04
7.7889e+04
6.9235e+04
6.0580e+04
5.1926e+04
4.3272e+04
3.4617e+04
2.5963e+04
1.7309e+04
8.6543e+03
4.7107e-14
Mag E
4.2446e+03
3.8212e+03
3.3977e+03
2.9743e+03
2.5508e+03
2.1274e+03
1.7039e+03
1.2805e+03
8.5702e+02
4.3357e+02
1.0114e+01
z
x
zoom 4

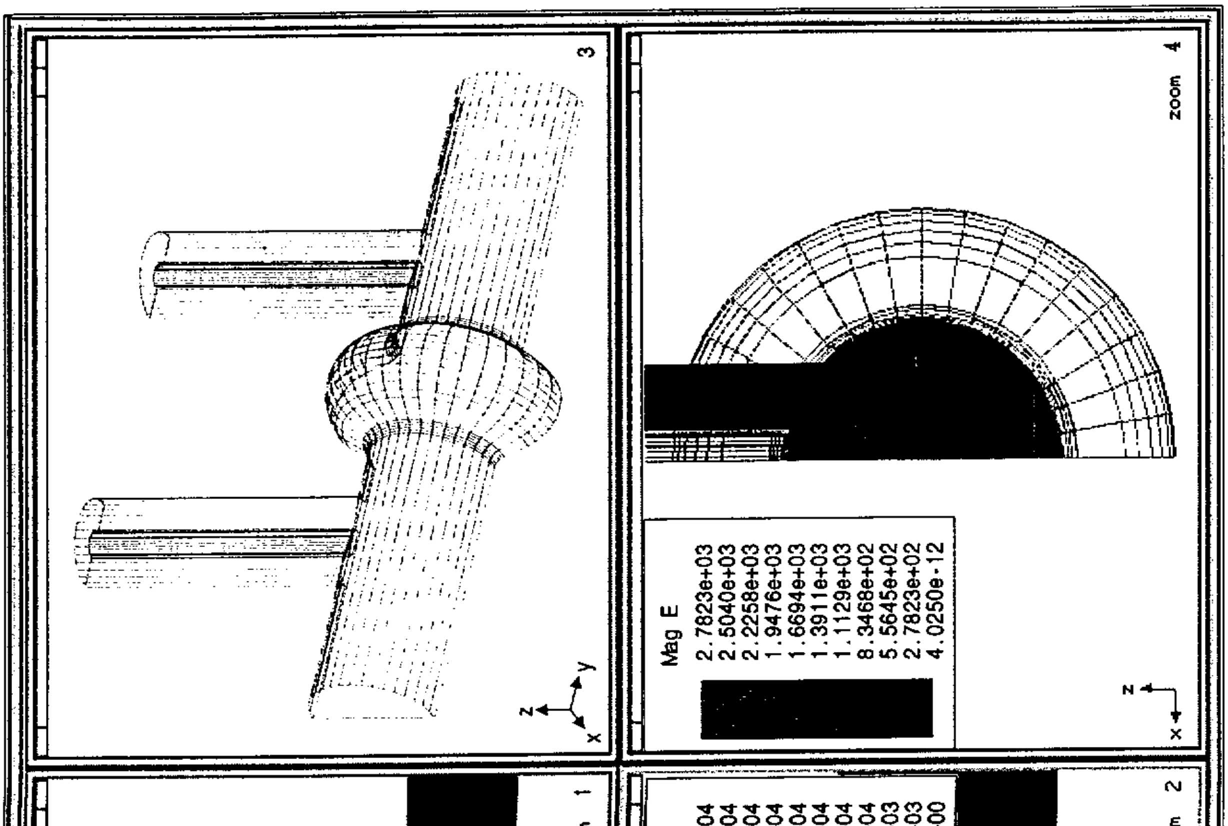
Mag E
3.8381e+04
3.4543e+04
3.0705e+04
2.6867e+04
2.3029e+04
1.9190e+04
1.5352e+04
1.1514e+04
7.6762e+03
3.8381e+03
5.1313e-13
zoom 1
Mag E
3.8381e+04
3.4543e+04
3.0705e+04
2.6867e+04
2.3029e+04
1.9191e+04
1.5353e+04
1.1515e+04
7.6774e+03
3.8395e+03
1.5726e+00
zoom 2
3
Mag E
2.7823e+03
2.5040e+03
2.2258e+03
1.9476e+03
1.6694e+03
1.3911e+03
1.1129e+03
8.3468e+02
5.5645e+02
2.7823e+02
4.0250e-12
zoom 4

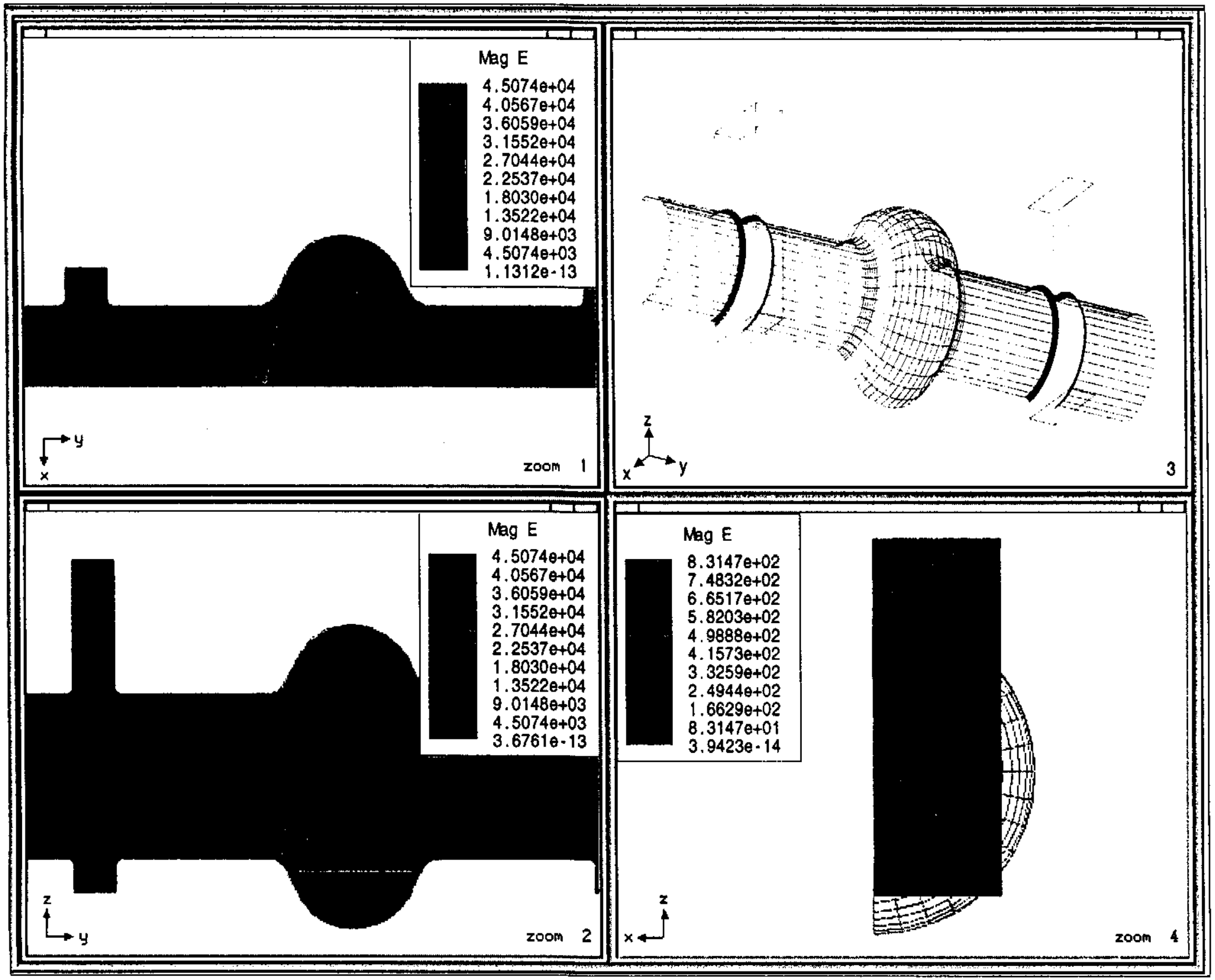
Mag E
4.5074e+04
4.0567e+04
3.6059e+04
3.1552e+04
2.7044e+04
2.2537e+04
1.8030e+04
1.3522e+04
9.0148e+03
4.5074e+03
1.1312e-13
y
x
zoom 1
z
x
y
3
Mag E
4.5074e+04
4.0567e+04
3.6059e+04
3.1552e+04
2.7044e+04
2.2537e+04
1.8030e+04
1.3522e+04
9.0148e+03
4.5074e+03
3.6761e-13
z
y
zoom 2
Mag E
8.3147e+02
7.4832e+02
6.6517e+02
5.8203e+02
4.9888e+02
4.1573e+02
3.3259e+02
2.4944e+02
1.6629e+02
8.3147e+01
3.9423e-14
z
x
zoom 4

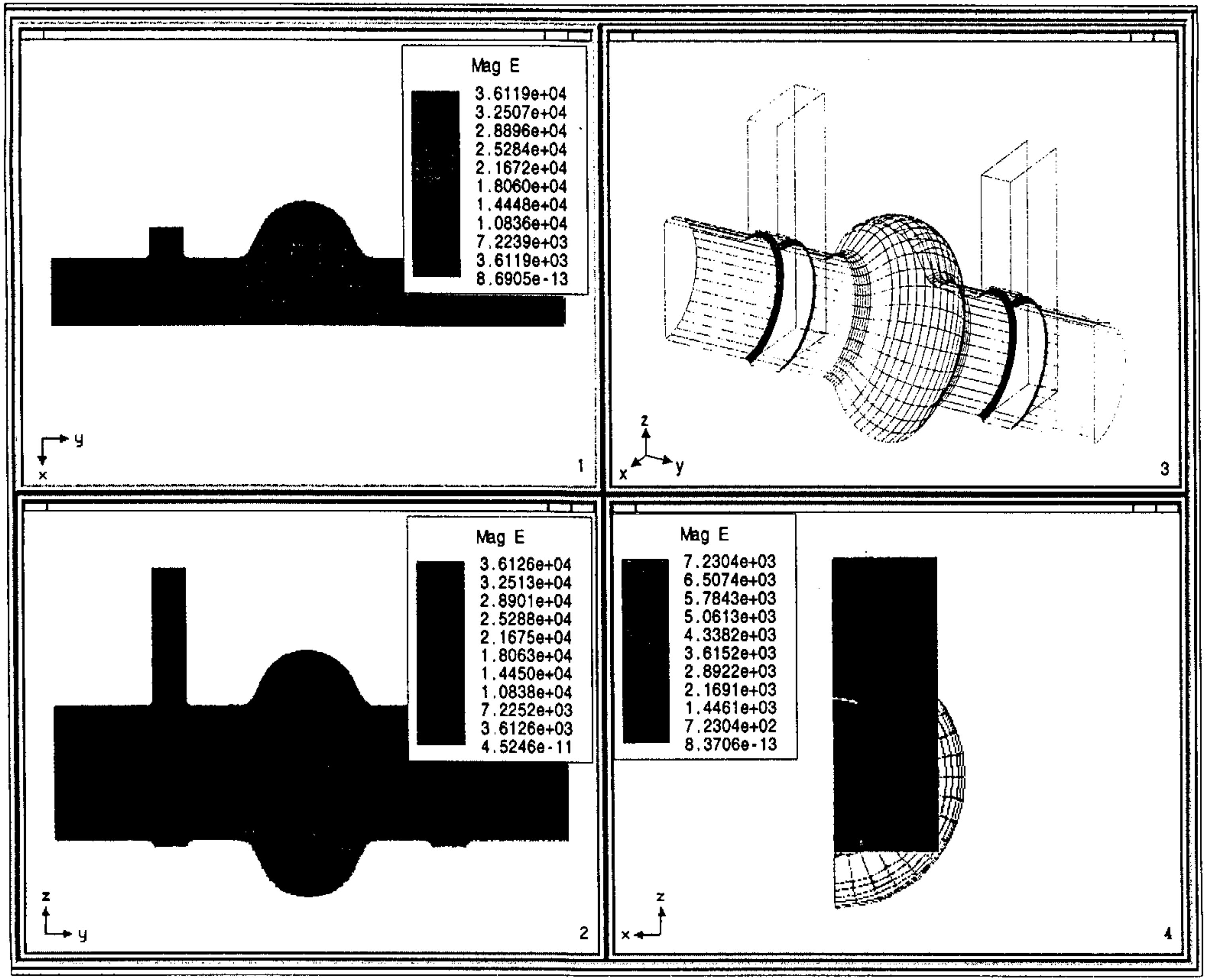
Mag E
3.6119e+04
3.2507e+04
2.8896e+04
2.5284e+04
2.1672e+04
1.8060e+04
1.4448e+04
1.0836e+04
7.2239e+03
3.6119e+03
8.6905e-13
y
x
1
z
x
y
3
Mag E
3.6126e+04
3.2513e+04
2.8901e+04
2.5288e+04
2.1675e+04
1.8063e+04
1.4450e+04
1.0838e+04
7.2252e+03
3.6126e+03
4.5246e-11
z
y
2
Mag E
7.2304e+03
6.5074e+03
5.7843e+03
5.0613e+03
4.3382e+03
3.6152e+03
2.8922e+03
2.1691e+03
1.4461e+03
7.2304e+02
8.3706e-13
z
x
4

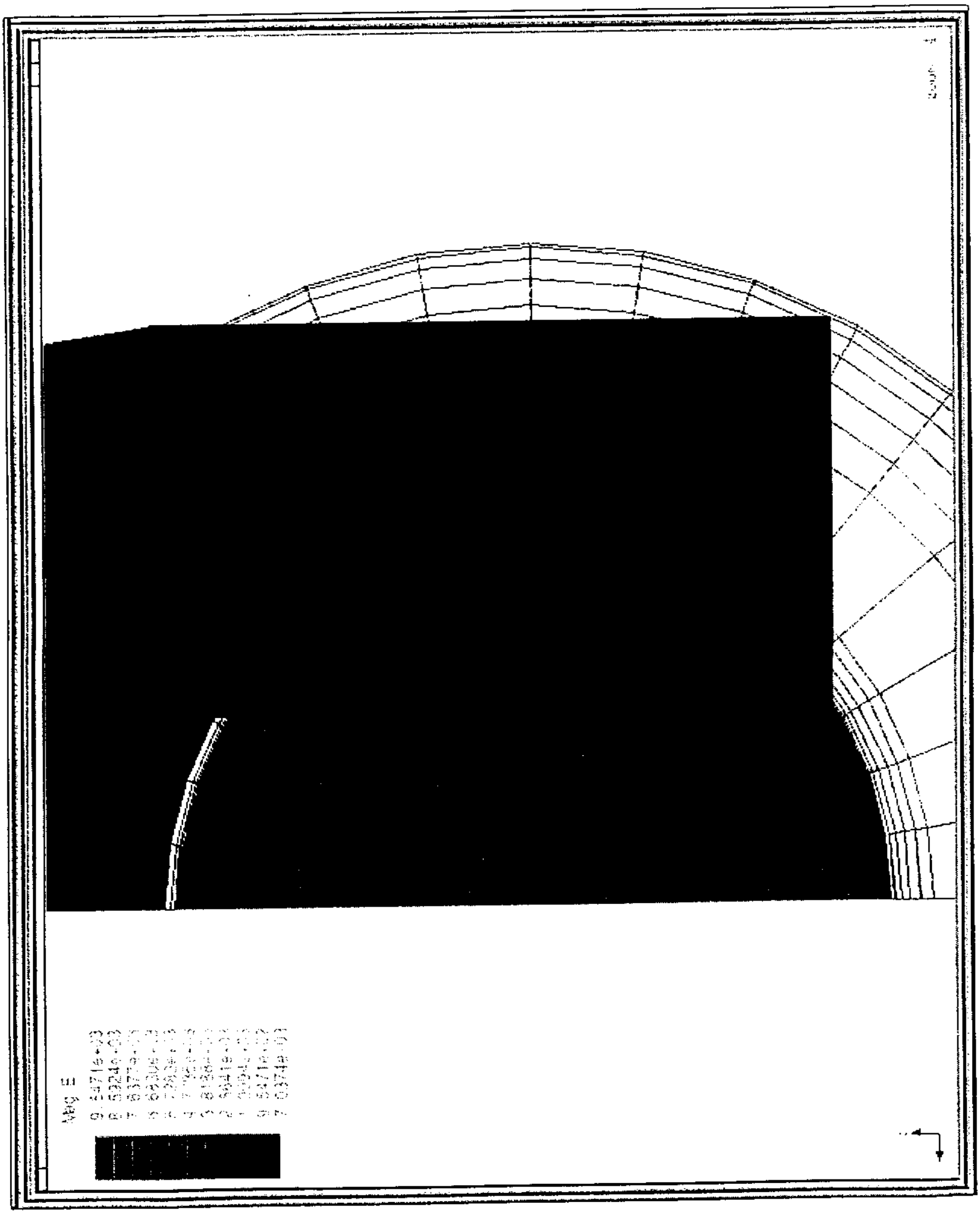
Mag E

3. Summary

3.1. Two-couplers method was used for the calculation. This method allows to find the form and the sizes of the coupling element corresponding to needed external Q-factor value Q_{ext} and to calculate the field distribution in the case of the beam acceleration (no reflection in the feeding line).

3.2. Three coupling elements for Superstructure were calculated. One of them may be chosen for Superstructure after the consideration of all elements of the input coupler (warm ceramic window, cold ceramic window, transmission line).

3.3. SS-CC is calculated for 80 mm 70 Ohm coaxial line.

3.4. SS-WC is interesting for future investigation of the kick, because the field in the coupler plane is 5-6 times less then in other couplers.

3.5. SS-SWC is proposed. It has following advantages:

- small kick for the beam (comparing with SS-CC);

- cold ceramic window is not seen from the beam axis;

- this coupling element can be used for the feeding of both one Superstructure and two Superstructures, as the wall may provide Q_{ext} up to needed value $2.12*10^6$ at $y_0=\lambda/2=115.3$ mm, comparing with SS-WC.

References.

1. D.Proch. Coaxial Coupler for Superstructures. - TTF coupler meeting, Saclay, October, 19-20, 1998.

2. A.Zavadtsev. Waveguide Input Coupler for Accelerating System. - TESLA meeting, March 1999.

3. J.Sekutowicz, M.Ferrario, C.Tang. Superconducting Superstructure. - LC98, Sept./Oct. 1997. Zvenigorod, Russia.

4. M. Dohlus, H.W.Glock, D.Hecht, U. van Rienen. Filling and Beam Loading in TESLA Superstructures. - TESLA-Report 98-14.

Coupler Workshop Community as of April 1999

Aune, B. - Saclay	aune@dapnia.cea.fr
Baboi, N. - DESY	nicoleta.baboi@desy.de,
Boachon, P. - Saclay	boachon@dapnia.cea.fr
Brinkmann, R. - DESY	reinhard.brinkmann@desy.de
Büttig, H. - FZ Rossendorf	h.buettig@fz-rossendorf.de
Chel, S. - Saclay	schel@cea.fr
Dohlus, M. - DESY	dohlus@desy.de
Dwersteg, B. - DESY	dwersteg@desy.de
Edwards, H. - FNAL	hedwards@adcalc.fnal.gov
Gamp, A. - DESY	alexander.gamp@desy.de
Garvey, T. - LAL Orsay	garvey@lal.in2p3.fr
Grandsir, L. - LAL Orsay	grandsir@lal.in2p3.fr
Haebel, E. - CERN	ernst.haebel@cern.ch
Janssen, D. - FZ Rossendorf	janssen@fz-rossendorf.de
Junquera, T. - IPN Orsay	junquera@ipno.in2p3.fr
Kang, Y.W. - Argonne Nat. Lab	ywkang@aps.anl.gov
Kindermann, H.P. - CERN	hans-peter.kindermann@cern.ch
Kopalko, K. - DESY	kopalko@mail.desy.de
Kreps, G. - DESY	guennadi.kreps@desy.de
Kuzminski, J. - Los Alamos	kuzmin@mail.sd.gat.com
LeDurff, J. - LAL Orsay	leduff@lal.in2p3.fr
Leenen, M. - DESY	martin.leenen@desy.de
Leqercq, P. - LAL Orsay	leqercq@lal.in2p3.fr
Lilje, L. - DESY	lilje@desy.de
Lorkeiwicz, J. - DESY	jerzy.lorkiewicz@desy.de
Marini, M. - LAL Orsay	marini@lal.in2p3.fr
Martens, C. - DESY	cornelius.martens@desy.de
Möller, W.-D. - DESY	wolf-dietrich.moeller@desy.de
Pagani, C. INFN Milano/DESY	pagani@mvlasa.mi.infn.it
Panvier - LAL Orsay	panvier@lal.in2p3.fr
Pekeler, M. - DESY	michael.pekeler@desy.de
Proch, D. - DESY	proch@proch.desy.de
Schmüser, P. - DESY	peter.schmueser@desy.de
Schnase, A. - FZ Jülich	a.schnase@fz-juelich.de
Schwettman, H.A. - HEPL	has@leland.stanford.edu
Sekutowicz, J. - DESY	jacek.sekutowicz@desy.de
Simrock, S. - DESY	stefan.simrock@desy.de
Song, J. - Argonne Nat. Lab.	jsong@aps.anl.gov
Travier, C. - Saclay	travier@dapnia.cea.fr
Trines, D. - DESY	dieter.trines@desy.de
White, M. - Argonne Nat. Lab.	mwhite@aps.anl.gov
Zaplatine, E. - FZ Jülich	e.zaplatine@fz-juelich.de